

OZONATION OF DYE WASTEWATER BY MEMBRANE CONTACTING PROCESS  
USING MODIFIED PVDF MEMBRANES

Mr. Sermpong Sairiam

A Dissertation Submitted in Partial Fulfillment of the Requirements  
for the Degree of Doctor of Philosophy Program in Environmental Management  
(Interdisciplinary Program)  
Graduate School  
Chulalongkorn University  
Academic Year 2013

บทคัดย่อและแฟ้มข้อมูลฉบับเต็มของวิทยานิพนธ์นี้สงวนลิขสิทธิ์ของมหาวิทยาลัยเทคโนโลยีพระจอมเกล้าธนบุรี (CUIR)  
เป็นแฟ้มข้อมูลของนิสิตเจ้าของวิทยานิพนธ์ที่ส่งผ่านทางบัณฑิตวิทยาลัย

The abstract and full text of theses from the academic year 2011 in Chulalongkorn University Intellectual Repository (CUIR)  
are the thesis authors' files submitted through the Graduate School.

การใช้ไอโซนบำบัดน้ำเสียด้วยระบบเมมเบรนคอนแทคเตอร์  
ด้วยการใช้ PVDF เมมเบรนที่มีการปรับสภาพ

นายเสริมพงศ์ สายรัมย์

วิทยานิพนธ์นี้เป็นส่วนหนึ่งของการศึกษาตามหลักสูตรปริญญาวิทยาศาสตรดุษฎีบัณฑิต  
สาขาวิชาการจัดการสิ่งแวดล้อม (สหสาขาวิชา)  
บัณฑิตวิทยาลัย จุฬาลงกรณ์มหาวิทยาลัย  
ปีการศึกษา 2556  
ลิขสิทธิ์ของจุฬาลงกรณ์มหาวิทยาลัย

Thesis Title OZONATION OF DYE WASTEWATER BY MEMBRANE  
CONTACTING PROCESS USING MODIFIED PVDF  
MEMBRANES

By Mr. Sermpong Sairiam

Field of Study Environmental Management

Thesis Advisor Professor Ratana Jiratananon, Ph.D.

Thesis Co-advisor Associate Professor Wang Rong, Ph.D.

---

Accepted by the Graduate School, Chulalongkorn University in Partial Fulfillment of the  
Requirements for the Doctoral Degree

.....Dean of the Graduate School  
(Associate Professor Amorn Petsom, Ph.D.)

#### THESIS COMMITTEE

.....Chairman  
(Assistant Professor Chantra Tongcumpou, Ph.D.)

.....Thesis Advisor  
(Professor Ratana Jiratananon, Ph.D.)

.....Thesis Co-advisor  
(Associate Professor Wang Rong, Ph.D.)

.....Examiner  
(Assistant Professor Patiparn Punyapalukul, Ph.D.)

.....Examiner  
(Associate Professor Pisut Painmanakul, Ph.D.)

.....Examiner  
(Assistant Professor Supatpong Mattaraj, Ph.D.)

.....External Examiner  
(Associate Professor Siriwan Srisorrachatr, Ph.D.)

เสริมพงศ์ สายเรียม : การใช้โอโซนบำบัดน้ำเสียสีย้อมด้วยระบบเมมเบรนคอนแทคเตอร์  
 ด้วยการใส่ PVDF เมมเบรนที่มีการปรับสภาพ. (OZONATION OF DYE  
 WASTEWATER BY MEMBRANE CONTACTING PROCESS USING MODIFIED  
 PVDF MEMBRANE) อ.ที่ปรึกษาวิทยานิพนธ์หลัก: ศ.ดร.รัตนา จิระรัตนานนท์, อ.ที่ปรึกษา  
 วิทยานิพนธ์ร่วม: ASSOC. PROF. WANG RONG, Ph.D., 147 หน้า.

วิทยานิพนธ์นี้เสนอการปรับสภาพผิวเมมเบรนเส้นใยกลาง PVDF และทดสอบเสถียรภาพของเมมเบรน  
 โดยการสัมผัสกับก๊าซโอโซนเพื่อประยุกต์ใช้ในกระบวนการเมมเบรนคอนแทคเตอร์ในการบำบัดน้ำเสียสีย้อม  
 ด้วยโอโซนเนชัน PVDF ผลการศึกษาพบว่าความไม่ชอบน้ำของเมมเบรนเดิมมีค่ามุมสัมผัส  $68^\circ$  ในขณะที่ค่ามุม  
 สัมผัสของเมมเบรนที่ถูกกระตุ้นด้วยสารละลาย 7.5M NaOH และสารละลาย 0.01M FAS-C8 เป็นเวลา 24 ชม. มี  
 ค่าเพิ่มขึ้นเป็น  $100^\circ$  และพบว่าขนาดรูพรุนและการกระจายตัวของรูพรุนไม่มีการเปลี่ยนแปลง ส่วนเมมเบรนที่ถูก  
 กระตุ้นด้วยอีเลียมพลาสมาและทำปฏิกิริยากับสารละลาย 0.01M FAS-C8 เป็นเวลา 24 ชม. พบว่ามุมสัมผัสและ  
 ความหยาบของผิวเมมเบรนมีค่ามากกว่าเมมเบรนที่ถูกกระตุ้นด้วยสารละลาย NaOH

การศึกษาค่าความเสถียรภาพของเมมเบรนต่อการสัมผัสกับก๊าซโอโซนของเมมเบรนทั้ง 4 ชนิด (PVDF เมม  
 เบรนที่ไม่มีการปรับสภาพ, PVDF เมมเบรนที่ถูกปรับสภาพด้วยสารละลาย NaOH (PVDF-CM2), เมมเบรนที่ถูก  
 ปรับสภาพด้วยพลาสมา (PVDF-PAM) และ เมมเบรนชนิด PTFE) ที่ความเข้มข้นและเวลาต่างๆกันพบว่า มุม  
 สัมผัสของเมมเบรนชนิด PVDF-PAM และ PVDF-CM2 ที่สัมผัสกับโอโซนมีค่าลดลงในขณะที่มุมสัมผัสของ  
 PVDF เมมเบรนที่ไม่มีการปรับสภาพมีค่าเพิ่มขึ้นและคงที่เมื่อความเข้มข้นและระยะเวลาสัมผัสกับโอโซนต่ำ  
 ขนาดรูพรุนและพารามิเตอร์ของเมมเบรนที่สัมผัสกับโอโซนไม่มีการเปลี่ยนแปลงในขณะที่คุณสมบัติเมมเบรนชนิด PTFE ที่  
 สัมผัสกับโอโซนไม่มีการเปลี่ยนแปลง

การศึกษากำหนดน้ำสีย้อมโดยใช้โอโซนด้วยระบบเมมเบรนคอนแทคเตอร์โดยเมมเบรน PVDF  
 ที่ไม่มีการปรับสภาพ, PVDF-PAM และ PTFE ของสารละลายสีย้อม พบว่าค่าโอโซนพลักซ์เมื่อใช้ PVDF-PAM  
 เมมเบรนมีค่าสูงและคงที่กว่า PVDF เมมเบรนที่ไม่มีการปรับสภาพ กระบวนการเมมเบรนคอนแทคเตอร์ด้วย  
 โอโซนสามารถลดความเข้มข้นสีได้อย่างสมบูรณ์และยังมีประสิทธิภาพในการย่อยสลายสารอะโรมาติกอีกด้วย  
 นอกจากนี้พบว่าซัลเฟต, ไนเตรต, กรดออกซาลิกและกรดอะซีติกเป็นผลิตภัณฑ์หลักของการเกิดออกซิเดชัน การ  
 ลดลงของ COD และ TOC แสดงให้เห็นว่าบางส่วนของสีย้อมทั้ง 2 ชนิดมีการย่อยสลายและการเปลี่ยนแปลง  
 แร่ธาตุ

สาขาวิชา การจัดการสิ่งแวดล้อม .....ลายมือชื่อนิติศ.....  
 ปีการศึกษา 2556 .....ลายมือชื่อ อ.ที่ปรึกษาวิทยานิพนธ์หลัก.....  
 .....ลายมือชื่อ อ.ที่ปรึกษาวิทยานิพนธ์ร่วม.....

## 5287839220 : MAJOR ENVIRONMENTAL MANAGEMENT

KEYWORDS : DYES / DECOLORIZATION / HYDROPHOBICITY / MEMBRANE CONTACTOR / MEMBRANE STABILITY / ORGANOSILANES / OZONATION / SURFACE MODIFICATION

SERMPONG SAIRIAM : OZONATION OF DYE WASTEWATER BY MEMBRANE CONTACTING PROCESS USING MODIFIED PVDF MEMBRANES. ADVISOR : PROF. RATANA JIRARATANANON, Ph.D., CO-ADVISOR: ASSOC.PROF. WANG RONG, Ph.D., 147 pp.

This thesis presented the study of the hydrophobic surface modification of PVDF hollow fiber membrane and membrane stability test of ozone exposure aiming for application as membrane contactor for dye wastewater treatment with ozonation process. For the 7.5M NaOH activation, the contact angle of original membranes ( $68^\circ$ ) was increased to  $100^\circ$  after modification with 0.01M FAS-C8 for 24h. There was no significant change in pore size and pore size distribution. The surface modified membranes under helium plasma activation followed by grafting with 0.01M FAS-C8 for 24h showed higher contact angle and surface roughness than that obtained by NaOH activation method.

In the study of membrane stability toward ozone, the four different hollow fiber membranes (original PVDF, modified PVDF by chemical activation/modification (PVDF-CM2) and plasma activation/modification (PVDF-PAM), and PTFE) were exposed to ozone at varied concentration and time. The contact angles of the PVDF-PAM and PVDF-CM2 membranes exposed to ozone decreased, whereas the contact angles of original PVDF membranes were increased at low concentration and duration, and remained constant. The pore size and outer surface of membranes exposed to ozone presented insignificant change. Meanwhile, the properties of PTFE membranes exposed to ozone did not changed.

For the study on the decolorization of dye solutions by membrane contactor with ozonation process, the long-term ozone fluxes by PVDF-PAM were higher and more stable than those of the original PVDF membrane. The use of the PVDF-PAM membrane as the membrane contactor with ozonation is very beneficial due to complete decolorization and high degradation efficiency of dye derivative aromatic fragments. Sulfate, nitrate, oxalic and acetic acids were identified as main oxidation products. The reduction of COD and TOC showed partial degradation and mineralization of these dyes.

Field of Study : Environmental Management Student's Signature .....

Academic Year : 2013 Advisor's Signature .....

Co-advisor's Signature .....

## ACKNOWLEDGEMENTS

I would like to express my sincere thanks to my advisor Prof. Dr. Ratana Jiraratananon and my Co-advisor Assoc. Prof. Dr. Wang Rong for their invaluable advice, guidance, support, and encouragement throughout the course of this study. Their comments and suggestions are very valuable and also broaden my perspective in the research quality. Special thanks go to the committee members, Asst. Prof. Dr. Chantra Tongcumpou, Asst. Prof. Dr. Patiparn Punyapalakul, Assoc. Prof. Dr. Pisut Painmanakul, Asst. Prof. Dr. Supatpong Mattaraj, and Assoc. Prof. Dr. Siriwan Srisorrachatr for their helpful and valuable comments. I would like to thank the Singapore Membrane Technology Centre (SMTC), School of Civil and Environmental Engineering, Nanyang Technological University (NTU), Singapore and the Department of Chemical engineering, King Mongkut's University of Technology Thonburi (KMUTT), Bangkok, Thailand for providing the worth opportunity for me to do my research. I would like to thank the Hazardous Substance Management program (HSM), Chulalongkorn University, the Commission on Higher Education, and Thailand Research Fund for financial support. I also thank wonderful friends, Thai and Singapore students, who took care and helped me while staying at SMTC and NTU and others who have shared experiences throughout my studying period and made my research much more enjoyable and my friends at HSM, Chulalongkorn University, Thailand.

Finally, I would also like to extend my very special thanks to my family for love and encouragement.

## CONTENTS

	Page
ABSTRACT (THAI).....	iv
ABSTRACT (ENGLISH).....	v
ACKNOWLEDGEMENTS.....	vi
CONTENTS.....	vii
LIST OF TABLES.....	xi
LIST OF FIGURES.....	xii
NOMENCLATURE.....	xv
CHAPTER I INTRODUCTION.....	1
1.1 Statements of problem.....	1
1.2 Objectives.....	5
1.3 Hypotheses.....	5
1.4 Scope of investigation.....	5
1.5 Expected results.....	6
1.6 Outline of thesis.....	6
CHAPTER II THEORETICAL BACKGROUND AND LITERATURE	
REVIEWS.....	8
2.1 Dyes and water pollution.....	8
2.2 Current dye wastewater treatment process.....	9
2.3 Principle of membrane contacting processes.....	13
2.3.1 Basic theory of the gas-liquid membrane contactor.....	14
2.3.2 Membrane wetting.....	17
2.3.3 Membrane material.....	17
2.3.4 Application of gas-liquid membrane contactors.....	20
2.3.5 Parameters affecting membrane contactor performance for ozonation process.....	22
2.4 Hydrophobic membrane modification .....	24

	Page
2.4.1 Alkaline treatment.....	25
2.4.2 Plasma activation.....	27
2.4.3 Grafting of membrane by organosilanes .....	28
2.4.4 Parameters affecting the membrane grafting.....	30
2.4.5 Application of modified membrane in gas-liquid membrane contactor.....	33
2.5 Ozone oxidation.....	33
2.6 Durability and stability of membranes when expose to oxidizing agent.....	37
2.7 Membrane characterization.....	38
2.7.1 Contact angle measurement.....	38
2.7.2 X-ray Photoelectron Spectroscopy (XPS).....	40
2.7.3 Fourier transform-infrared spectroscopy (FT-IR).....	40
2.7.4 Scanning Electron Microscopy (SEM) or FE-SEM.....	41
2.7.5 Pore size and pore size distribution.....	41
2.7.6 Surface roughness (Atomic Force Microscopy).....	42
2.7.7 Mechanical strength.....	42
<b>CHAPTER III HYDROPHOBIC MEMBRANE MODIFICATION OF PVDF HOLLOW FIBER MEMBRANE.....</b>	<b>43</b>
3.1 Introduction.....	43
3.2 Methodology.....	45
3.2.1 Materials and chemicals.....	45
3.2.2 Methods.....	46
– Chemical modification (CM).....	46
– Plasma-activated modification (PAM).....	47
3.2.3 Membrane characterizations.....	47
3.2.4 Long-term stability study of modified PVDF membranes for CO <sub>2</sub> absorption.....	49
3.3 Results and discussion.....	50



	Page
3.3.1 Effect of NaOH concentration and organosilanes.....	50
3.3.2 Comparison of chemical modification (CM) and plasma- activated modification (PAM).....	60
3.3.3 Stability test on modified membrane for CO <sub>2</sub> absorption.....	69
3.4 Conclusions.....	72
CHAPTER IV THE STABILITY OF MODIFIED MEMBRANES EXPOSED TO OZONE.....	73
4.1 Introduction.....	73
4.2 Methodology.....	74
4.2.1 Materials and chemicals .....	74
4.2.2 Methods.....	74
– The stability test of membranes exposed to ozone.....	74
4.3 Results and discussion .....	76
4.3.1 Change of membrane properties and structures.....	76
4.4 Conclusions.....	84
CHAPTER V APPLICATION OF MODIFIED MEMBRANE IN MEMBRANE CONTACTOR FOR DYE SOLUTION TREATMENT.....	86
5.1 Introduction.....	86
5.2 Methodology.....	88
5.2.1 Materials and chemicals.....	88
5.2.2 Methods .....	89
– The long-term ozone flux of PVDF and PTFE membranes...	89
– Decolorization performance of dye solution by ozonation using membrane contactor.....	90
5.3 Results and discussion.....	93
5.3.1 Long-term ozone flux of PVDF and PTFE membranes.....	93

	Page
5.3.2 Decolorization performance of dye solution using modified PVDF and PTFE membranes.....	95
5.3.3 Effect of dye solution types.....	97
5.3.4 Determination of by-products from ozonation of dye solutions.	101
5.3.5 Investigation on biodegradability.....	107
5.4 Conclusions.....	109
 CHAPTER VI CONCLUSIONS AND RECOMMENDATIONS.....	 110
6.1 Conclusions.....	110
6.2 Recommendations.....	112
 REFERENCES.....	 114
 APPENDICES.....	 132
APPENDIX A.....	133
APPENDIX B.....	140
 VITAE.....	 147

**LIST OF TABLES**

Table		Page
2.1	Lists polymers which are frequently fabricated for hydrophobic membranes .....	18
2.2	Contact angles between water and membranes.....	20
3.1	Specifications of the PVDF hollow fiber membrane.....	45
3.2	Description of organosilanes used.....	46
3.3	Changes of the chemical structure of membrane surface.....	59
3.4	Mechanical properties of original and modified PVDF membranes...	60
3.5	Contact angle and surface roughness of the original and the modified membranes by 0.01M FAS-C8 (24h) after chemical and plasma activations.....	61
3.6	Changes of the chemical structure of membrane surface.....	64
3.7	Comparison of various PVDF hydrophobic membrane modifications	70
4.1	Specifications of the hollow fiber membranes .....	75
5.1	Specifications of the hollow fiber membranes and modules.....	88
5.2	Dyes properties used in this study.....	89

## LIST OF FIGURES

Figure		Page
1.1	Flow diagram of investigation.....	7
2.1	Schematic drawing of gas-liquid membrane contactors .....	14
2.2	Concentration profile for the transfer in dry mode and wetted mode....	14
2.3	Mass transfer process in a hollow fiber membrane gas-liquid contactor for dry mode .....	16
2.4	Surface modification process using plasma activation.....	28
2.5	Schematic diagram showing monolayer deposition of a monofunctional hydrophobing agent .....	30
2.6	Surface structures of organosilanes grafted on hydroxyl-terminated surfaces.....	30
2.7	Illustration of organosilane on membrane surface.....	32
2.8	Proposed mechanism of ozone oxidation .....	35
2.9	The products of ozonation of purified, hydrolyzed RR 120 and its simplified reaction pathway .....	36
2.10	Tensiometer for the contact angle measurement .....	39
3.1	PVDF hollow fiber membranes.....	46
3.2	Hollow fiber membrane modules.....	49
3.3	Experimental setup of CO <sub>2</sub> absorption in a membrane contactor.....	50
3.4	Contact angle of treated membrane by NaOH under 60°C for 3h.....	51
3.5	Dehydrofluorination mechanisms of PVDF membrane.....	51
3.6	Influence of NaOH concentration (60°C for 3h) in 0.01M of organosilane modification for 24 h and Influence of grafting time and organosilane under 7.5MNaOH (60°C for 3h).....	53
3.7	Cross section morphology of PVDF membrane.....	57
3.8	Outer surface morphology of PVDF membrane.....	57
3.9	FT-IR spectra of PVDF membrane.....	58
3.10	FT-IR spectra of modified PVDF membrane by 7.5M NaOH.....	58

Figure	Page	
3.11	The hydrolysis reaction of the organosilane and the addition of the silanol groups onto the PVDF membrane surface.....	59
3.12	FT-IR spectra of the PVDF membrane.....	62
3.13	XPS spectra.....	64
3.14	Pore size and pore size distribution of the original and modified membranes.....	66
3.15	SEM images of the original membrane and modified membrane.....	67
3.16	AFM 3D images of membranes.....	68
3.17	Membrane performance for CO <sub>2</sub> absorption over 15 days of operation	71
4.1	Schematic diagram of the stability test of membranes exposed to ozone.....	75
4.2	Contact angles of PVDF membranes after exposing to ozone.....	78
4.3	FT-IR spectra of membranes before and after exposing to ozone, 60 ppm for 60h.....	80
4.4	Illustration of intra-chain energy of modified PVDF using FAS-C8 as modifying agent.....	81
4.5	Mean and max. pore size of PVDF membranes after exposing to ozone.....	82
4.6	FE-SEM images of membranes before and after exposing to ozone....	83
4.7	Tensile modulus of PVDF membranes after exposing to ozone.....	84
5.1	Schematic diagram of the membrane contactor for ozonation of dye solution.....	92
5.2	Long term performance of PVDF and PTFE membranes.....	94
5.3	Comparison of decolorization performance using different membranes.....	96
5.4	Comparison of Reactive black 5 and Basic yellow 28 removal using PVDF-PAM membrane.....	98
5.5	Illustration of Reactive Black 5 and Basic Yellow 28 with different ozonation time by PVDF-PAM membrane.....	98

Figure		Page
5.6	The performance of PVDF-PAM in membrane contactor for dye wastewater.....	99
5.7	Color removal and ozone consumption.....	100
5.8	UV-Vis spectra of RB5 solution at different ozonation time.....	103
5.9	Oxalic and acetic acids produced at different ozonation time.....	104
5.10	The conductivity of dye solution during the ozonation.....	105
5.11	Concentration profiles of ions during the ozonation.....	108

## NOMENCLATURE

$A$	effective area of membrane ( $m^2$ )
$C_G$	bulk concentration in gas phase ( $mol/m^3$ )
$C_L$	bulk concentration in liquid phase ( $mol/m^3$ )
$C_{O_3,in}$	ozone concentration of gas phase at inlet (ppm)
$C_{O_3,out}$	ozone concentration of gas phase at outlet (ppm)
$D_{g,eff}$	diffusivity of the absorbing gas in the gas phase ( $m^2/s$ )
$D_l$	diffusivity of the absorbing gas in the liquid phase ( $m^2/s$ )
$d_i$	inner diameter of membrane (m)
$d_{ln}$	logarithmic mean diameters of membrane (m)
$d_o$	outer diameter of membrane (m)
$E$	enhancement factor (dimensionless)
$H$	Henry's constant $(mg/l)_g/(mg/l)_l$ ,
$J_i$	experimental flux of species i ( $mol/m^2.s$ )
$K_L$	overall mass transfer coefficient based on liquid phase (m/s)
$k_g$	mass transfer coefficient of gas phase (m/s)
$k_m$	mass transfer coefficients of membrane (m/s)
$k_l$	mass transfer coefficients of liquid phase (m/s)
$K_L$	overall mass transfer coefficient based on liquid phase (m/s)
$\Delta P$	penetration pressure (Pa)
$Q_{O_3}$	ozone flow rate (mg/L)
$T$	temperature ( $^{\circ}C$ )
$T_g$	glass transition temperature ( $^{\circ}C$ )
$V_L$	liquid velocity (m/s)
$V_G$	gas velocity (m/s)

Greek letters

$\delta$	thicknesses of membrane (m)
$\epsilon_M$	membrane porosity (dimensionless)
$\tau_M$	tortuosity. (dimensionless)
$\sigma$	surface tension of the liquid
$\theta$	contact angle between membrane and liquid (degree)

Abbreviation

AOPs	advanced oxidation processes
AS-C16	hexadecyltrimethoxysilane
BOD	biochemical oxygen demand
BY28	basic yellow 28
CM	chemical modification
CO <sub>2</sub>	carbon dioxide
CO <sub>3</sub> <sup>2-</sup>	carbonate ion
COD	chemical oxygen demand
FAS	fluoroalkylsilanes
FAS-C6	1H, 1H, 2H, 2H-perfluorooctyltriethoxysilane
FAS-C8	1H, 1H, 2H, 2H-perfluorodecyltriethoxysilane
PDMS	polydimethylsiloxane
HS	humic substance
H <sub>2</sub> S	hydrogen sulfide
MEA	monoethanolamine
N <sub>2</sub>	nitrogen gas
NaCl	sodium chloride
NaNO <sub>2</sub>	sodium nitrite
NaOCl	sodium hypochlorite solution
NaOH	sodium hydroxide
Na <sub>2</sub> CO <sub>3</sub>	sodium bicarbonate
NF	nanofiltration
NH <sub>3</sub>	ammonia



$\text{NH}_4^+$	ammonium ion
$\text{NO}_3^-$	nitrate ion
NOM	natural organic matter
$\text{O}_3$	ozone
$\bullet\text{OH}$	hydroxyl radicals
PAI	polyamide-imide
PAM	plasma-activated modification
PE	polyethylene
PEI	polyetherimide
PP	polypropylene
PSf	polysulfone
PTFE	polytetrafluoroethylene
PVDF	polyvinylidene fluoride
RB5	reactive black 5
RO	reverse osmosis
$\text{SO}_2$	sulphur dioxide
SS	suspended solids
TOC	total organic carbon
UF	ultrafiltration
VOCs	volatile organic compounds

# CHAPTER I

## INTRODUCTION

### 1.1 Statements of problem

Textile industry is one of the most important export industries of Thailand. The industries use large amount of water and chemicals for finishing and dyeing processes [1]. Wastewater from dyeing and finishing factories is the significant source of environmental pollution. Color is usually the first contaminant to be recognized in these wastewaters. The high strength of colored effluents may become visual eyesores and causes aesthetic pollution, eutrophication and perturbations in aquatic life. In addition, color-containing dyestuffs have been found to be toxic and carcinogenic to aquatic environments [2]. Due to their toxicity and slow degradation, these dyes are classified as environmentally hazardous materials. The release of colored wastewater poses a major problem for the industry as well as a threat to the environment. Therefore, it is necessary to find an effective method for dye wastewater treatment in order to remove color from textile effluents. The ozonation process has been recommended in recent years as a potential alternative for decolorisation. Ozone specifically attacks the conjugated chains that impart color to the dye molecule. During the ozonation process, molecule is selective and attacks preferentially the unsaturated bonds of the chromophores; as a result, color is removed. The process of ozonation can take place in two ways: directly by ozone molecules, or induced by hydroxyl radicals formed as a result of ozone decomposition in water. However, the low solubility of ozone in water limits the mass transfer driving force of ozone gas into the aqueous phase [3, 4]. In addition, conventional methods of gas–liquid contact for the ozonation of wastewater, such as bubble columns and packed beds, are limited by low mass transfer of ozone into the aqueous phase and low specific area. The effectiveness of ozonation can be increased by the generation of smaller bubbles [5, 6]. However, the drawbacks of the bubble column are flooding, uploading, emulsion, and foaming [7]. These problems can be solved by using a gas–liquid membrane contactor [8], a method employing a combination of membrane with gas absorption

which has been developed for the effective absorption of CO<sub>2</sub> by liquid absorbents [8]. Membrane-based equipment for bringing gas and liquid phases into contact could be suitable for industrial wastewater ozonation. Membrane contactors are systems in which hydrophobic porous membranes are used to promote gas–liquid or liquid–liquid mass transfer without dispersion of one phase into the other [9]. The advantages of the membrane contactors over conventional contactors are high interfacial area, the hydrodynamic decoupling of the phases [10], thus the process is expected to be simplified and requires small areas [11]. Also, increasing mass transfer coefficients results in higher gas transfer rate and a smaller process volume for installation is one advantage of this process [12]. Several studies have been conducted to use membrane ozone contactors for oxidation of organic compounds such as humic substance, phenol, acrylonitrile, nitrobenzene, dyes [7, 10, 12, 13]. However, there has been a limited study on the application of membrane contacting process for treatment of dye wastewater.

The membrane is a major component in the membrane contactor system. However, the membrane adds additional resistance for mass transfer that can be compensated by the increase in interfacial mass transfer area, especially, when the hollow fiber membrane is employed. Efficient gas-liquid membrane contactor should be operated in the dry mode in which there is no membrane wetting, the intrusion of liquid into the pores. Membrane wetting is the problem for the membrane contactor operation because it will reduce separation performance. It depends on the structural characteristics of the porous material, especially hydrophobicity, porosity and thickness. The potential hydrophobic membrane materials are polyethylene (PE), polypropylene (PP), polyvinylidene fluoride (PVDF), and polytetrafluoroethylene (PTFE). Based on the contact angle data, the hydrophobicity of the membrane is in the order of PTFE > PE > PP > PVDF [14, 15].

In this work we would like to modify PVDF hollow fiber membrane to increase hydrophobicity. However, most previous works have reported surface modification of ceramic membrane to increase its hydrophobicity since ceramic membranes are hydrophilic and they cannot be directly applied as membrane contactors. The methods

used to modify ceramic membranes, in principle, can also be applied to modify PVDF membranes with some modification. Several types of surface modifying agents can be used for modification, e.g. choloalkylsilanes, fluoroalkylsilanes (FAS), alcohol, polydimethylsiloxane (PDMS) [16-24]. Surface modification is usually performed with silanes due to its high reactivity with hydroxyl groups on the surface. Organosilanes have been recently used to prepare hydrophobic ceramic membrane because they have hydrolysable groups and other hydrophobic ends in their structures. The hydrolysable groups are coupled with hydroxyl groups (-OH) on the ceramic surface, forming a chemically bound hydrophobic layer. Several factors including the surface modifying agent, the length of hydrophobic tails, grafting time, and the temperature play important roles in the surface grafting process [19, 20, 22, 23].

However, PVDF membranes have no hydroxyl groups. Therefore, hydroxyl groups must be introduced on the membrane surface. There are several methods to produce OH groups on the PVDF membrane surface. Examples are the chemical method (alkaline treatment), plasma treatment, and radiation. Basically, the alkaline treatment via NaOH is a simple method that has been investigated to introduce OH groups on the membranes. Nevertheless, it was reported in the literature that the properties of PVDF membrane were destroyed by NaOH solution because NaOH had chemically attacked PVDF membrane and caused the dehydrofluorination in the polymer chain [25, 26]. For example, the mechanical strength and crystallinity of PVDF membranes were decreased even at 4wt% NaOH solution at 70°C within 24 hours or in 10wt% NaOH solution within 8 hours [25]. The reduction in mechanical strength of membrane treated by NaOH was due to the degradation of membrane as a result of the chemical reaction between PVDF membrane and NaOH. Liu *et al.* [26] also reported the hydrophilic PVDF membrane modification by alkaline treatment. The results showed that the alkaline treatment changed the membrane surface structure based on the results of pore size distribution.

Plasma treatments can alter the surface energy of membranes and change the surface polarity which is the less damaging method of membrane modification. During the plasma treatment, the membranes were exposed to a reactive environment of excited

atomic, ionic, and free radical species by hydrogen abstraction and radical formation, which resulted in modification of only the top-most nanometers of the membrane structure being altered [27, 28]. Therefore, the surface can be selectively modified for a specific application while the bulk properties of membrane are unaffected [27, 29]. Surface modification of membrane by plasma treatment is mainly achieved by using different gases including oxygen, nitrogen, argon, helium, water vapor and air [27, 29-32]. The use of plasma to activate the surface to generate oxide or hydroxide groups can be used in surface modification [33].

When the membranes are subjected to oxidizing agents, the deteriorative reaction may occur during the operation, leading to deterioration of permeate water quality, flux reduction and shortening of membrane life. Mori *et al.* [11] reported that the ozone resistance of the polymeric membranes was in the following order PTFE > PVDF > PE. Bamperng *et al.* [34] showed that PTFE could maintain stable ozone flux while PVDF exhibited a lower flux in the long term operation indicating that PVDF membrane may be wetted and oxidized by ozone. However, PTFE is much more expensive than PVDF (10 times) and is limited in availability. After the membrane deterioration, the membrane has to be replaced, resulting in the increase of the operation cost. The degradation of polymeric membranes by sodium hypochlorite solution (NaOCl) as the cleaning solution and oxidizing agent has been widely studied in the literature [35-39]. However, little is known on the changes on chemical and physical properties of membranes by ozone. Kukuzaki *et al.* [40] reported that the modified Shirasu porous glass (SPG) membranes by an organosilane compound not only increased the hydrophobicity but also resisted the ozone oxidation. To the best of our knowledge, there is no research on the possible changes in morphology and properties of hydrophobic membranes due to ozone contact. Therefore, the main objective of this research is to modify the surface of PVDF membrane by organosilanes, test membrane stability after ozone contact, then apply the modified membrane for decolorization of dye solution by ozonation using membrane contacting process.

## 1.2 Objectives

The aims of this research are to modify PVDF hollow fiber membranes to increase hydrophobicity, ozone stability and apply the modified membranes for dye wastewater treatment by membrane contacting process. To achieve these goals, this thesis is divided into three specific aims:

- 1.2.1 To modify PVDF hollow fiber membranes with different membrane activations, organosilanes and grafting conditions to increase hydrophobicity.
- 1.2.2 To examine the stability and durability of modified PVDF membranes toward ozone, in comparison to PTFE membrane.
- 1.2.3 To determine the ozone flux and decolorization performance by ozonation with membrane contactor of dye solutions using unmodified, modified PVDF membranes, and PTFE membrane.

## 1.3 Hypotheses

The research is driven by the following hypotheses:

- 1.3.1 Hydrophobicity and stability of PVDF membrane toward ozone can be improved by membrane modification with organosilanes.
- 1.3.2 Ozonation by membrane contactor using modified PVDF membranes can increase the decolorization performance of dye solutions, in comparison to using unmodified PVDF membrane.

## 1.4 Scope of investigation

The schematic diagram of investigation is illustrated in Figure 1.1, which can be explained below:

- 1.4.1 Study the surface activations of PVDF hollow fiber membranes by chemical activation (NaOH) and helium plasma activation.
- 1.4.2 Study the surface modification of PVDF hollow fiber membranes with three different organoalkylsilanes i.e. Hexadecyltrimethoxysilane (AS-C16), 1H, 1H, 2H, 2H-perfluorodecyltriethoxysilane (FAS-C8), and 1H, 1H, 2H, 2H-Perfluorooctyltriethoxysilane (FAS-C6).

- 1.4.3 Characterize the modified membranes by various techniques to obtain important physical and chemical properties of grafted membranes compared with the original membrane.
- 1.4.4 Study the stability of the original and modified membranes towards ozone by examining the changes of physical and chemical properties of membranes after ozone contact at various durations and concentrations.
- 1.4.5 Study the decolorization performance by ozonation using the modified membranes for dye wastewater containing Reactive black 5 and Basic yellow 28, including COD and TOC removals, BOD<sub>5</sub>/COD and pH changes, and by-product generation.

## **1.5 Expected Results**

- 1.5.1 The modified PVDF hollow fiber membrane with improved hydrophobicity and ozone stability.
- 1.5.2 The efficient process for dye wastewater treatment.

## **1.6 Outline of thesis**

The dissertation is organized into six chapters. CHAPTER 1 presents the introduction, including the objectives, hypotheses, scope of investigation and expected results. CHAPTER 2 is reviews of the state-of-the-art focused in membrane contacting process, hydrophobic membrane modification, ozonation process, and also the membrane characterizations. In CHAPTER 3, the study on the hydrophobic membrane modification by two different membrane activation, chemical and helium plasma activations, followed by grafting with different organosilanes is presented. The stability test of the modified membrane towards ozone is studied in CHAPTER 4. CHAPTER 5 deals with application of modified membranes in ozonation process for dye wastewater containing Reactive Black 5 and Basic Yellow 28. In this chapter, the long-term ozone fluxes of membranes were investigated. The by-products of treated dye wastewater were also determined. Finally, in CHAPTER 6, the main conclusions are summarized and future research recommendations are proposed.

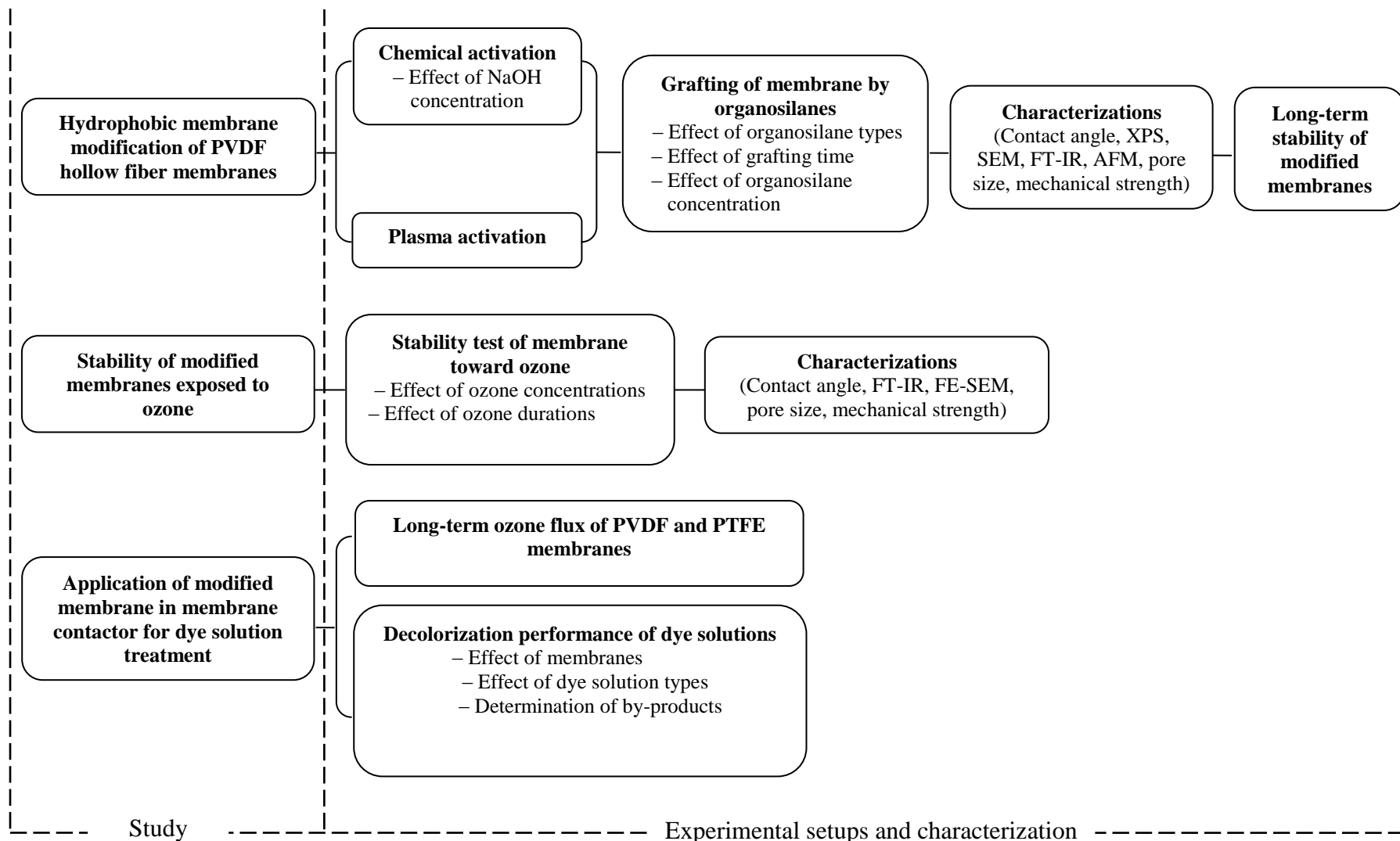


**Figure 1.1** Flow diagram of the investigation



## **CHAPTER II**

### **THEORETICAL BACKGROUND AND LITERATURE REVIEWS**

This chapter provides detailed information of dye wastewater from textile industries and the harmful effects on environment and human health. Furthermore, the currently available techniques for dye wastewater treatment are also reviewed. Membrane contactor with ozonation process as the alternative method for dye wastewater treatment, which is the research focus on this study, is presented. The hydrophobic membrane modification in order to enhance hydrophobicity, and membrane stability when exposed to oxidizing agents are also reviewed in detail. The membrane characterization methods, including qualitative and quantitative analyses for physical and chemical properties, are described.

#### **2.1 Dyes and water pollution**

By definition “Dyes” can be said to be coloured, ionizing and aromatic organic compounds which show an affinity toward the substrate to which it is being applied. It is generally applied in a solution that is aqueous. Both dyes and pigments appear to be colored because they absorb some wavelengths of light more than others. In contrast with a dye, a pigment generally is insoluble, and has no affinity for the substrate. Dyes have many different and complex chemical structures such as acid, basic, direct, reactive, disperse, azo dyes [41, 42].

Large amounts of dyes are annually produced and applied in many industries including the textile, cosmetic, paper, leather, pharmaceutical, and food industries. However, the textile industry consumes large quantities of water and chemicals, producing the large volumes of effluent causing intense water pollution. The textile wastewaters are highly colored by dye used which have attracted the most attention since color in the effluent not only causes the environmental concerns, but also creates a significance aesthetic problem in sewage treatment.

The main route of dye wastewater is from the textile industries which cause the serious impacts when encountering the natural area. The dye wastewater has an adverse effect on the flora and fauna biological cycles of ecosystem. The decrease of transparency in water can prevent the penetration of solar radiation, resulting in the decrease of photosynthetic activity and disruption of aquatic places [43-46]. Dyes can remain for decades on aquatic environments endangering the stability and lives of ecosystems. They are persistent and recalcitrant compounds to the microbial degradation and their accumulation in certain forms of aquatic life which may lead to toxic products and potentially carcinogenic compounds [46, 47]. The degradation products of the dyes may be more harmful than dyes themselves. This is due to the breaking of azo groups that could consist of aromatic amines potentially carcinogenic/mutagenic [48]. In addition, the characteristics of textile wastewater containing dye solution commonly present suspended solids (SS), high temperature, unstable pH, high Chemical Oxygen Demand (COD), and low Biochemical Oxygen demand (BOD) [45, 49-52].

## **2.2 Current dye wastewater treatment process**

During the past years, many studies have been performed on three conventional methods for dye wastewater treatment: biological, chemical, and physical methods. Biological treatment of wastewater is the most economical method for the removal of organic pollutant from wastewater. There are several microorganisms that are able to decolorize such as white-rot fungi, *Pseudomonas luteola*, *Bacillus gordonae*, *Saccharomyces cerevisiae* [53-55]. However, the long period needed for microorganisms to become acclimated and many of dyes are xenobiotic and non-biodegradable. Therefore, physical and chemical methods have been used as alternatives.

Physical methods such as coagulation, carbon adsorption have been used currently for the purification of textile dyeing wastewater. Coagulation is an economical method of dye removal. It involves the addition of ferrous sulphate or ferric chloride, allowing excellent removal of direct dyes from wastewaters. The optimum coagulant concentration is dependent on the static charge of the dye in solution and difficulty in

removing the sludge formed as part of the coagulation is a problem, results in high disposal costs [56]. Adsorption is relevant in environment pollution and protection with reference to water and wastewater treatment. Adsorption onto activated carbon has been proven to be one of the most effective and reliable physicochemical treatment techniques [57]. However, activated carbon adsorption has the associated cost and difficulty of the regeneration process and a high waste disposal cost [58, 59].

Membrane technology, with its unique separation performance holds great promise in the field of water reclamation. The recovery of the wastewaters to the degree of reuse quality is often achieved by nanofiltration (NF) and reverse osmosis (RO) [60]. NF membrane technology has been successfully used to obtain industrial water from textile effluents and is able to reject dyes and other organic molecules, while NaCl and other monovalent salts passed through the membrane [61]. NF is much more efficient than ultrafiltration (UF) in term of rejection and also, it faces lesser fouling problems than RO [62]. On the other hand, RO is not only suitable for ions removal and larger species from the dye effluents but RO also removes the color and helps in desalinating wastestream. The concentrated residue left after RO poses disposal problems. High capital cost, the problem of fouling, and membrane replacements are the disadvantages of most membrane processes. Membrane processes are suitable for water recycling within a textile dye plant if the effluent contains low concentration of dyes, but it is unable to reduce the dissolved solid content, which makes water reuse a difficult task [63].

Advanced oxidation processes (AOPs), as the chemical treatment, are the most commonly used methods for decolourisation by chemical means. This is mainly due to its simplicity of application. These technologies generate hydroxyl radical ( $\bullet\text{OH}$ ) which is a highly reactive oxidant. Chemical oxidation removes the dye from the dye-containing effluent by oxidation resulting in aromatic ring cleavage of the dye molecules. There are several works on dye removal by hydroxyl radical in different techniques involving  $\text{H}_2\text{O}_2/\text{Fe}^{2+}$  (Fenton's reagent), electro-Fenton, and  $\text{H}_2\text{O}_2/\text{O}_3$  as chemical processes [63, 64],  $\text{H}_2\text{O}_2/\text{Fe}^{3+}/\text{UV}$  as a photochemical treatment [65] and  $\text{TiO}_2/\text{UV}$ ,  $\text{TiO}_2/\text{UV}/\text{O}_3$  and  $\text{Fe}^{2+}/\text{UV}/\text{O}_3$  as photocatalytic methods [66, 67]. AOPs can

be effectively used to achieve complete color and partial COD removal from textile effluent and thus an attractive option to prepare recalcitrant process streams compared to conventional activated sludge treatment of the combined wastewater. However, advanced oxidation products might be more toxic and/or inhibitory on the biological treatment systems used for the post treatment than the original textile dyes. One major disadvantage of Fenton process is sludge generation through the flocculation of the reagent and the dye molecules. The sludge, which contains the concentrated impurities, still requires disposal.

The ozonation process has been recommended for decolorization in recent years as a potential alternative for the following reasons [68-70]: (1) no chemical sludge in the treated effluent, (2) ozone has high potential to remove color and reduce organic matter in one step, (3) it requires little space and easy for installation, (4) ozone is less harmful than other oxidizing agent, and (5) residual ozone can easily be decomposed to oxygen. Ozone specifically attacks the conjugated chains that impart color to the dye molecule. During the ozonation process, ozone molecule is selective and attacks preferentially the unsaturated bonds of the chromophores, as a result, color is removed. The process of ozonation can take place in two ways which are directly by ozone molecules, or induced by hydroxyl radicals formed as a result of ozone decomposition in water. In addition, the efficiency of ozone mass transfer depends on the hydrodynamic behavior of the fluid, solubility ratio, and mass transfer coefficient [71]. The major drawback with ozonation is cost; continuous ozonation is required due to its short half-life. In order to enhance the ozonation efficiency, the effectiveness of ozonation can be increased by a higher surface area of ozone through the generation of smaller bubbles [5, 6]. Koch *et al.* [72] studied the degradation of hydrolyzed azo dye reactive yellow 84 (CI) by bubbling the ozone/air mixture and found that the decolorization of hydrolyzed azo dye reactive yellow 84 (CI) was almost complete after 60 and 90 min of ozonation with starting ozone concentrations of 18.5 and 9.1 mg/l, respectively. Konsowa [73] studied the decolorization of wastewater containing direct dye by ozonation in a batch bubble column reactor. The results showed that the rate of dye removal increased with increasing ozone concentration. The decolorization time increased with increasing initial dye

concentration; in contrast, decreased with an increasing ozone concentration. Oguz, Keskinler, and Çelik [74] studied the removal of aqueous Bomaplex Red CR-L dye by ozonation in a semi-batch reactor. They studied the effect of initial dye concentration, temperature, ozone (air flow rate), pH, and ozone generation percentage. The results showed that the efficiency of dye removal increased with increasing pH, ozone generation rate, and decreased with increasing temperature, but did not change with increasing ozone (air) flow rate and initial dye concentration.

However, the drawbacks of the bubble column are flooding, uploading, emulsion, and foaming [7]. In addition, conventional methods of gas–liquid contact for the ozonation of wastewater, such as bubble columns and packed beds, are limited by low mass transfer of ozone into the aqueous phase. These problems can be solved by using a gas–liquid membrane contactor [8], a method employing a combination of membrane with the ozonation process which has been developed for the effective absorption of CO<sub>2</sub> by liquid absorbents [8]. Membrane-based equipment for bringing gas and liquid phases into contact could be suitable for industrial wastewater ozonation. Membrane contactors are systems in which hydrophobic porous membranes are used to promote gas–liquid or liquid–liquid mass transfer without dispersion of one phase into the other [9]. The advantages of the contacting membrane over conventional contactors are high interfacial area, the hydrodynamic decoupling of the phases [10], and the prevention of membrane fouling, thus the process is simple and requires small areas [11]. Also, increasing mass transfer coefficients results in higher gas transfer rate and a smaller process volume for installation is another advantage of this process [12].

Recently, Zhang *et al.*[3], Atchariyawut *et al.* [7], and Bamperng *et al.* [34] investigated the use of hollow fiber membrane contactor with ozonation process for decolorization. The influence of operating parameters on the decolorization of dye solutions was studied in detail. The results indicated that the decolorization performance increased with pH, temperature and liquid velocity, therefore, the main mass transfer resistance was the liquid phase [3, 7, 34]. However, the results indicated that the decolorization and the reduction of COD highly depended on the type of dye

and dye auxiliary reagents [34]. The COD removal efficiency was inhibited when the  $\text{Na}_2\text{CO}_3$  was added into the dye solution [7]. This is because ozone was scavenged with  $\text{CO}_3^{2-}$ , resulting in losing ozone oxidizing power with dye in the solution. The decolorization performance of Acid blue 113 was higher than that of Direct red 23 [34]. The reason is that the pH of Acid blue 113 solution was lower than that of Direct red 23, hence, ozone molecule was dominated, resulting in the preferential oxidation at the unsaturated bonds of chromophores.

### 2.3 Principle of membrane contacting processes

The applications of G-L contactors are gas streams purification (gas absorption), water ozonation, water deoxygenation, and so on. Both hydrophobic and hydrophilic microporous membranes can be used to provide contact of gas with a liquid. The membrane in this process acts as a barrier between two phases, for purpose of mass transfer between the phases, without dispersing one phase into the other [75, 76]. The concept of using membranes to bring two phases into contact with one another is not new. Membrane contactors have the following features and advantages [8, 76]

- *High surface area per volume.* Membrane contactors can supply 20-100 times more surface area per volume than conventional equipment.
- *No flooding.* Membrane contactors can reduce or avoid solvent and raffinate entrainment, which can inhibit both packed towers and mixer-settlers.
- *Direct scale up.* Membrane contactors can be modified and designed when an application requires several contactors in series or parallel.

There are two types of membrane contactor, gas-liquid (G-L), and liquid-liquid (L-L) contactors. In the G - L contactors one phase is a gas or a vapor and the other phase is a liquid while, the L - L contactors, both phases are liquids. Gas-liquid and liquid-gas are G-L contactors applied for as absorption and stripping, respectively. G - L contactors are shown in Figure 2.1.

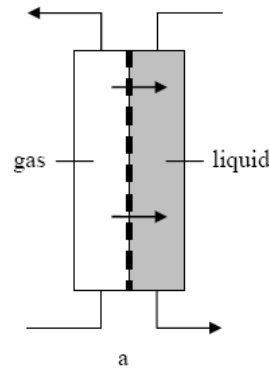


**Figure 2.1** Schematic drawing of gas-liquid membrane contactors

### 2.3.1 Basic theory of the gas-liquid membrane contactor

There are two possible characteristics in G-L membrane contactors, dry mode and wetted mode. For dry mode, the pores are filled with gas phase while in wetted mode, liquid phase fills the membrane pores. Then hydrophobic and hydrophilic membranes were used, respectively. Dry mode is usually preferred to take advantage of the higher diffusivity in the gas; however, wetted mode may be preferred if there is a fast or instantaneous liquid phase reaction, and as a result, the gas phase resistance controls the process. Figure 2.2 shows the concentration profile for the transfer in dry mode and wetted mode.

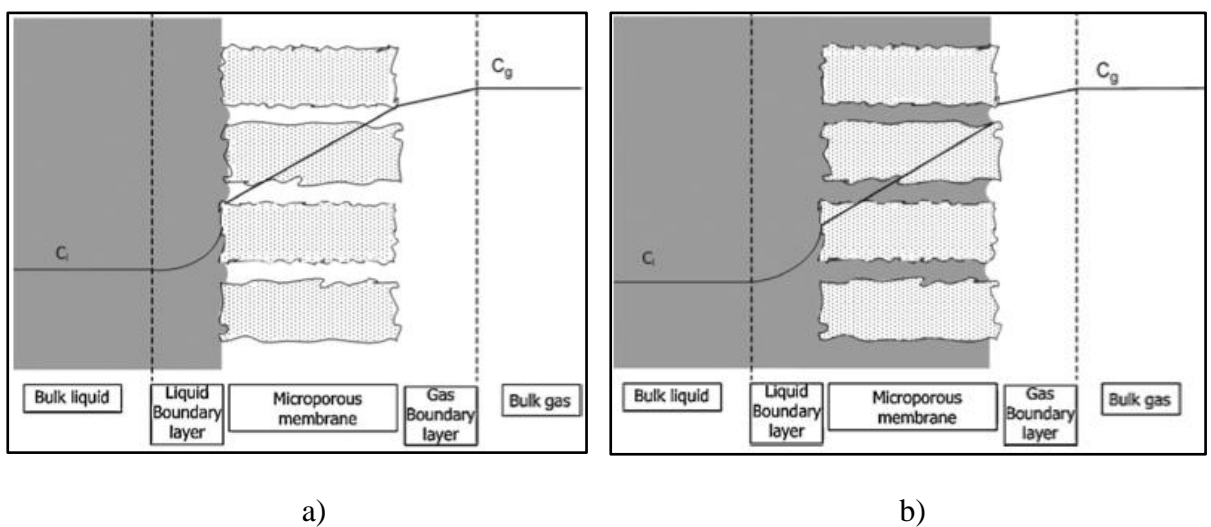


**Figure 2.2** Concentration profile for the transfer in dry mode (a) and wetted mode (b)

In a gas-liquid membrane contactor, the gas and liquid phases flow on the opposite sides of the hydrophobic membrane. The absorption occurs on the liquid side by physical absorption, chemical reaction or a combination of these two processes. It is advantageous to use the hollow fiber modules for this purpose. The direction of mass transfer of any molecular species depends on the concentration driving force maintained across the membrane for that species [75]. The overall process consists of three steps. First, the transfer of the solute gas from the bulk gas phase to the membrane surface. Second, transfer through the membrane pores and last, the transfer from the membrane-liquid interface into the bulk of the liquid. Figure 2.3 demonstrates the mass transport of gas in dry operating mode of hollow fiber gas-liquid membrane contactor, for the liquid flow in the lumen side and gas flow in the shell side (i.e., diffusion from the bulk gas through the membrane pores and dissolution in the liquid absorbent). The gas flux ( $J(\text{mol}\cdot\text{m}^{-2}\cdot\text{s}^{-1})$ ) can be calculated from the following equation:

$$J = K_L (C_G - C_L) \quad 2.1$$

where  $K_L$  is the overall mass transfer coefficient based on liquid phase (m/s)

$C_G$  is bulk concentration in gas phase ( $\text{mol}/\text{m}^3$ )

$C_L$  is bulk concentration in liquid phase ( $\text{mol}/\text{m}^3$ )

In addition, resistance in series model can be applied to analyze the overall mass transfer resistance ( $\frac{1}{K_L}$ ) of the process in terms of individual resistance by using equation 2.2 [7, 34, 75, 76], when the hollow fiber membrane is used.

$$\frac{1}{K_L d_i} = \frac{1}{E k_l d_i} + \frac{1}{H k_m d_{lm}} + \frac{1}{H k_g d_o} \quad 2.2$$

where  $k_g$ ,  $k_m$  and  $k_l$  are the individual mass transfer coefficients (m/s) of gas phase, membrane and liquid phase, respectively,

$d_o$ ,  $d_i$  and  $d_{lm}$  are the outer, inner and log mean diameters of hollow fiber membrane (m),

$H$  is the Henry's constant ( $\text{mg}/\text{l})_g/(\text{mg}/\text{l})_l$ ,



$E$  is the enhancement factor which accounts for the effect of reaction

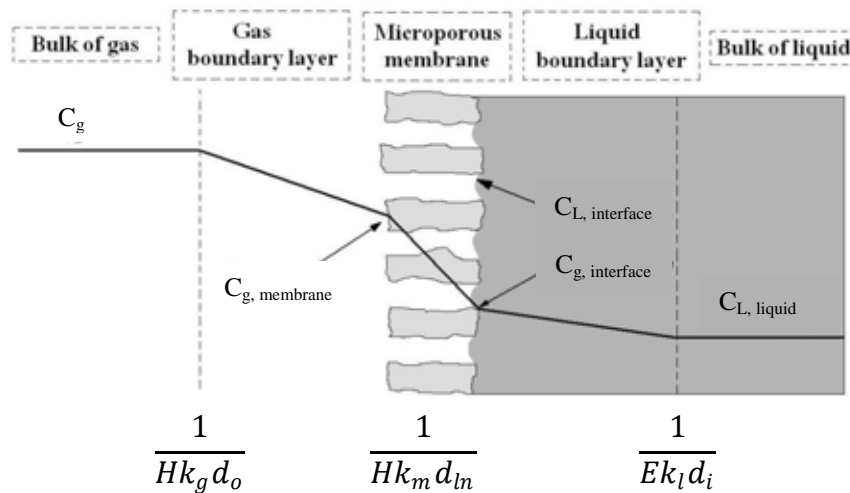


**Figure 2.3** Mass transfer process in a hollow fiber membrane gas-liquid contactor for dry mode [7, 34]

In the operation of a membrane contactor, either the gas phase or liquid phase can be fed through the shell side or tube side of the hollow fiber membrane module. In this work, liquid is fed through the tube side while gas is fed into the shell side.

The membrane resistance ( $\frac{1}{k_m}$ ) depends on membrane mode of operation, i.e. non-wetted, wetted or partially wetted mode. For totally gas-filled pores or totally liquid-filled pores, the membrane resistance depends on the diffusivity of the absorbing gas in the gas phase and liquid phase,  $D_{g,eff}$ ,  $D_l$ , respectively, and on the geometrical characteristics of the membrane, i.e. its thickness,  $l_m$ , porosity,  $\epsilon_m$  and tortuosity,  $\tau_m$ . For the non-wetted mode (gas filled pore), the membrane mass transfer coefficient is given by the equation 2.3.

$$k_m = \frac{D_{g,eff} \cdot \mathcal{E}_m}{\tau_m \cdot l_m} \quad 2.3$$

Non wetted mode is the superior mode of operation for gas absorption in the membrane contactor that can minimize the membrane resistance. In order to prevent

wetting, some criteria such as balanced gas-liquid operating pressure, using highly hydrophobic membrane materials, high surface tension liquid absorbent and optimized membrane structure with small pore size can be taken into consideration.

### 2.3.2 Membrane wetting

Membrane wetting is the significant problem for mass transfer in gas-liquid membrane contacting process. The operation in dry mode (gas-filled membrane pore) is more advantageous than that in the wet mode (liquid-filled membrane pore) because of the higher diffusivity of the gas. The liquid absorbents will not wet the membrane when the pressure difference between liquid stream and the gas stream is lower than the penetration pressure defined as the following equation 2.4:

$$\Delta P = \frac{-2\sigma \cos\theta}{r_p} \quad 2.4$$

where  $\Delta P$  = the penetration pressure or wetting pressure,  
 $\sigma$  = the surface tension of the liquid,  
 $r_p$  = the membrane pore radius,  
 $\theta$  = the contact angle between membrane and liquid

The wetting pressure depends on the properties of both the membrane and the liquid absorbent used. Normally, highly hydrophobic membranes are favorably selected to be used in membrane contacting process since they can provide the large contact angle between the membrane and the aqueous absorbent solution (in excess of 90°) keeping the membrane contactor operated in dry mode.

### 2.3.3 Membrane materials

Typical membranes for contactors are prepared from hydrophobic polymer materials possessing a high porosity, a membrane thickness of 10-300  $\mu\text{m}$  and providing microfiltration properties with pore size of 0.1-1 $\mu\text{m}$ . The choice of membrane material affects phenomena such as absorption and chemical stability under condition of actual application. This implies that the requirements for the polymeric material are

not primarily determined by the permeability and hydrophobicity but also by the chemical and thermal properties of the material.

Among various hydrophobic polymers, PE, PP, PVDF and PTFE are the most popular membrane materials. Chemical structures of the polymers are shown in Table 2.1, and properties for these polymers are as follows:

**Table 2.1** Lists polymers which are frequently fabricated for hydrophobic membranes.

Membrane	Chemical structure
Polyethylene (PE)	$\left[ \begin{array}{cc} \text{H} & \text{H} \\   &   \\ -\text{C} & -\text{C}- \\   &   \\ \text{H} & \text{H} \end{array} \right]_n$
Polypropylene (PP)	$\left[ \begin{array}{cc} \text{H} & \text{CH}_3 \\   &   \\ -\text{C} & -\text{C}- \\   &   \\ \text{H} & \text{H} \end{array} \right]_n$
Polyvinylidene fluoride (PVDF)	$\left[ \begin{array}{cc} \text{F} & \text{H} \\   &   \\ -\text{C} & -\text{C}- \\   &   \\ \text{F} & \text{H} \end{array} \right]_n$
Polytetrafluoroethylene (PTFE)	$\left[ \begin{array}{cc} \text{F} & \text{F} \\   &   \\ -\text{C} & -\text{C}- \\   &   \\ \text{F} & \text{F} \end{array} \right]_n$

**(a) Polyethylene: PE**

Polyethylene or polythene is a thermoplastic commodity heavily used in consumer products with the formula  $(\text{C}_2\text{H}_4)_n$ . PE has a glass transition temperature ( $T_g$ ) of about  $-120^\circ\text{C}$ , and a melting point of about  $100^\circ\text{C}$ . In its liquid state, polyethylene serves as a material that can be molded, injected, and cast in varying thicknesses and shapes to create many different usable products.

**(b) Polypropylene: PP**

Polypropylene or polypropene is a thermoplastic polymer with the formula  $(C_3H_6)_n$ . It is rugged and unusually resistant to many chemical solvents, bases and acids. PP has good resistance to fatigue and naturally hydrophobic. PP has a  $T_g$  of about  $-15^\circ C$ , while melting point of about  $160^\circ C$ .

**(c) Polyvinylidene fluoride: PVDF**

Polyvinylidene fluoride is a highly nonreactive and pure thermoplastic fluoropolymer. PVDF formula is  $(CH_2CF_2)_n$ . PVDF is a specialty plastic material in the fluoropolymer family; it is used generally in applications requiring the highest purity, strength, and resistance to solvents, acids, bases, and heat and low smoke generation during a fire event. Compared to other fluoropolymers, it has an easier melt process because of its relatively low melting point of around  $177^\circ C$ . It has a low cost compared to the other fluoropolymers. PVDF has a  $T_g$  of about  $-40^\circ C$  and is typically 50-60% crystalline.

**(d) Polytetrafluoroethylene: PTFE**

Polytetrafluoroethylene is a synthetic fluoropolymer of tetrafluoroethylene which finds numerous applications. Its molecular formula is  $C_nF_{2n+2}$ . PTFE is most well known as Teflon. PTFE is a fluorocarbon solid, as it is a high molecular weight compound consisting wholly of carbon and fluorine. Neither water and water-containing substances nor oil and oil-containing substances are wetted by PTFE, as fluorocarbons demonstrate mitigated London dispersion forces due to the high electronegativity of fluorine. PTFE has a high melting point and  $T_g$  of about  $327^\circ C$  and  $126^\circ C$ , respectively.

Table 2.2 shown below compares the hydrophobicity or water contact angle of major polymers used for fabrication of porous hydrophobic membranes. However, PTFE is much more expensive than PVDF due to the use of thermal method for fabrication. On the contrary, PVDF has received much attention as a membrane material due to its high mechanical strength, thermal stability and chemical resistance [77]. Fabrication of PVDF membrane by phase inversion method is also much more simpler.

**Table 2.2** Contact angles between water and membranes

PP	PE	PVDF	PTFE	Reference
102.5±1.5°				[78]
94±2°				[78]
100°				[14]
104°				[14]
118°				[14]
	127±6°			[15]
	103.5±1°			[78]
	105±2°			[78]
		97±3.6°		[15]
		86.5±1.5°		[78]
		92±2.5°		[78]
		100°		[14]
		92°		[14]
			124±3.4°	[15]
			113°	[14]
			127°	[14]
			133.5°	[14]

### 2.3.4 Application of gas-liquid membrane contactors

#### (a) Wastewater treatment

Gas-liquid membrane contactors have been used for several wastewater treatments. PVDF and PTFE membranes were selected as the membrane materials for the applications due to the highly hydrophobic membranes. Humic substance (HS) and natural organic matter (NOM) are a problem in drinking water production. Jansen *et al.* [10] applied the PVDF hollow fiber membrane contactor to produce drinking water from HS contaminated water. The decolorization of Norwegian natural organic matter in water source was also studied by Leiknes *et al.* [79]. The results showed that the decolorization of NOM decreased by membrane contactor with ozonation process. The decolorization rate constants obtained from the concentration-time ( $C-\tau$ ) model

for the ozonation membrane contactor were found to be in the range of 139.44–298.81M<sup>-1</sup> s<sup>-1</sup>.

Dye wastewater treatment by membrane contacting process using ozonation was also studied by Atchariyawut *et al.* [7] for C.I. reactive red 120 wastewater. The results showed that using water and 300 mg/l dye solution as liquid phase, the ozone fluxes increased with increasing liquid velocity. In contrast, increasing the gas flow rate did not affect ozone flux. Therefore, it was concluded that the main mass transfer resistance was in the liquid phase. In addition, the effect of auxiliary reagent was also studied. The result showed that ozone flux increased when Na<sub>2</sub>CO<sub>3</sub> was added into the dye solution due to the increase of pH solution, therefore, the •OH radical was generated by the decomposition of ozone molecule. In contrast, ozone flux decreased with added NaCl due to the salting out effect. The COD removals were 32% and 23% with Na<sub>2</sub>CO<sub>3</sub> and without Na<sub>2</sub>CO<sub>3</sub>, respectively, because of CO<sub>3</sub><sup>2-</sup> scavenging. Bamperng *et al.* [34] studied the treatment of Direct red 23, Acid blue 113 and Reactive red 120 solutions by ozone using hollow fiber membrane contactor of PVDF and PTFE membranes. The results showed that PVDF membrane provided higher ozone flux than PTFE, but PTFE membrane gave more stable and higher flux than PVDF for a long operation period. The ozone flux of different types of dye was in the following order: Direct red 23 > Reactive red 120 > Acid blue 113. While, the decolorization performance of Acid blue 113 was higher than those of Direct red 23 and Reactive red 120. The treatment of Acid orange 52 was also studied by membrane contacting process with ozonation using PVDF hollow fiber membrane [3]. The results showed that the decolorization efficiency increased with the increase of liquid velocity.

Zhang *et al.* [3] studied the decomposition of 4-nitrophenol by ozonation in a hollow fiber membrane. In this study, PVDF membrane was used, claiming to be ozone resistant. The results showed that increasing initial pH of 4-nitrophenol, liquid flow rate, gas flow rate, and ozone concentration, 4-nitrophenol removal was increased. Moreover, ozone effectiveness, which defines as the ratio of 4-nitrophenol removal to

ozone consumption, decreased with the increase of gas flow rate as well as ozone concentration. However, 4-nitrophenol removal did not change when initial pH was higher than 9.5.

### **(b) Gas absorption**

Gas–liquid membrane contactors have been widely studied for absorption of CO<sub>2</sub>, SO<sub>2</sub>, H<sub>2</sub>S, etc into aqueous or solutions. These acid gases are impurities which lower the quality of the gas and cause corrosive problems. The membrane gas absorption technology is not only technically feasible, but also an economical method for capturing gas on a large scale [80]. Lv *et al.* [80] investigated simultaneous absorption of SO<sub>2</sub> and CO<sub>2</sub> from coal-flue gas by monoethanolamine solution (MEA) in PP hollow fiber membrane. Hedayat *et al.* [81] studied the absorption of H<sub>2</sub>S and CO<sub>2</sub> gases from a gas mixture using PVDF and polysulfone (PSf) hollow fiber membrane and used the alkanolamines as the liquid absorbents. Mavroudi *et al.* [82] reported that the CO<sub>2</sub> removal by membrane contacting process using amine as the absorbent was nearly complete (99%). Park *et al.* [83] eliminated SO<sub>2</sub> from the flue gas using multi stage PVDF hollow fiber membrane contactor. The results showed that the SO<sub>2</sub> removal efficiency of 85% was achieved with 2M NaOH solution.

## **2.3.5 Parameters affecting membrane contactor performance for ozonation process**

### **(a) Membrane material and properties**

The membrane is the major component in the membrane contacting process. The membrane should be produced from the hydrophobic materials such as PVDF or PTFE in order to provide a wetting pressure high enough to prevent the water from the wetting or entering the pores which would decrease ozone diffusion substantially. According to Table 2.2, the hydrophobicity of major polymers for fabrication of porous hydrophobic membranes is compared. It can be seen that PTFE has the highest contact angle, 133.5°. The study of Pine *et al.* [13] showed that the mass transfer coefficient ( $k_m$ ) increased with increasing pore size and pore volume and decreasing thickness for the teflon membranes. The mass transfer coefficient for the PTFE membranes increased with decreasing membrane thickness. Comparison of the Pall

membranes indicated that membrane material (porous PTFE, nonporous PTFE, and porous PVDF) had limited effect on the ozone mass transfer [13]. In principle, ozone is an oxidizing agent which does not only react with the pollutants or foulants, some evidence has indicated the participation in the degradation of membrane material (discussed in section 2.6). Mori *et al.* [11] reported that the ozone resistance of the polymeric membranes was in the following order PTFE > PVDF > PE. Bamperng *et al.* [34] showed that PTFE could maintain stable ozone flux while PVDF exhibited a lower flux in the long term operation indicating that PVDF membrane may be wetted and oxidized by ozone. Therefore, it is important that the membranes should be both hydrophobic and ozone resistant.

#### **(b) Liquid and gas velocities**

The liquid velocity has a significant effect on the membrane contacting process which is expressed by Reynolds number. Increasing liquid velocity would lead to the increase of  $Re$ . The overall mass transfer coefficient ( $K_L$ ) would increase, meaning more ozone molecules would transfer into the aqueous phase. The ozone flux increased with increasing liquid velocity for physical and chemical experiments since the liquid phase mass transfer coefficient ( $k_l$ ) was enhanced with the liquid velocity. For the mass transfer system with the presence of chemical reaction, the mass transfer rate can be improved as the liquid mass transfer coefficient was increased. The study of Pine *et al.* [13] showed that increasing the Reynolds number from 60 to 2000 increased the mass transfer coefficient by about an order of magnitude. In contrast, the ozone flux did not change with the gas phase velocity for both water and dye solution used as the liquid phase [7, 34]. Therefore, it is likely that ozone mass transfer is liquid phase controlled with the membrane's properties having a secondary effect.

#### **(c) pH**

Generally, ozone reacts with organic pollutants via either direct ozone attack or indirect free radical attack. At lower pH, the direct reaction is dominant and depends strongly on the nature of organic molecules. When pH exceeds 9.5, the free radical reaction would become dominant since hydroxyl radicals are generated from ozone



decomposition catalyzed by hydroxide ion. The study of Zhang *et al.* [4] showed that the increase of pH, the degree of dissociation of 4-nitrophenol was higher, and the removal rate increased. On the contrary, the study of Zhang *et al.* [3] found that pH (5.6-8.6) had little effect on the decolorization efficiency.

#### **(d) Temperature**

The increase of chemical reaction rate between ozone and dye is due to the increase of temperature. Conversely, in case of using water as liquid phase, the ozone flux decreases as the operating temperature was increased owing to the decrease of gas solubility in the water [34]. Leiknes *et al.* [79] studied the Norwegian natural organic matter (NOM) decolorization in tubular membrane contactor. The results showed that the increase in liquid temperature reduced ozone fluxes into pure water, but raised the ozone fluxes into NaNO<sub>2</sub> solutions. In addition, the increase of the ozone flux with temperature was observed until approximately 40°C.

#### **(e) Ozone concentration**

The mass transfer rate of ozone from the gas phase to the liquid phase is directly dependent on mass transfer driving force. The mass transfer driving force is the difference between the equilibrium concentration and bulk concentration of ozone in the liquid phase. Increasing gaseous ozone concentration would increase the equilibrium concentration of ozone based on Henry's law, and the mass transfer driving force would increase accordingly. This would result in the increase of mass transfer rate of ozone, and more ozone is available in the liquid [4].

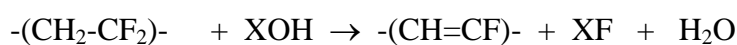
### **2.4 Hydrophobic membrane modification**

Recently, several studies have shown success in ceramic membrane modification to improve hydrophobicity since ceramic membranes are hydrophilic and are not suitable for use as membrane contactor. The methods used for modification of ceramic membranes were applied to modified PVDF membranes. According to the study of Bamperng *et al.* [34], the result showed that PTFE could maintain stable O<sub>3</sub> flux. In contrast, PVDF exhibited a lower flux in long term operation indicating that PVDF has lower ozone resistance than PTFE. Nevertheless, the application of PTFE is

limited for its high cost and availability. So, in this work we would like to modify PVDF hollow fiber membrane to increase the hydrophobicity. However, PVDF membranes have no hydroxyl groups. Therefore, hydroxyl groups must be introduced on the membrane surface. There are several methods to produce OH groups on the PVDF membrane surface. Examples are the chemical method (alkaline treatment) and plasma treatment as described below.

### 2.4.1 Alkaline treatment

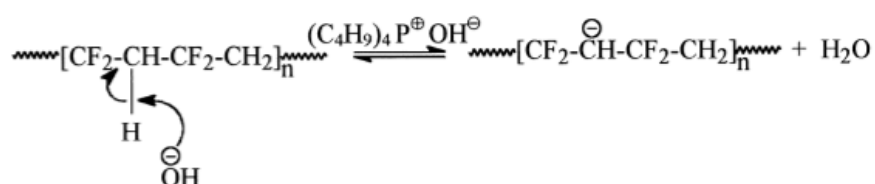
Chemical grafting between organosilanes and membranes requires that there are hydroxyl groups on the membrane surface. Hydroxyl groups can be introduced into the PVDF membranes by alkaline treatment. Although PVDF membrane is highly chemically resistant, it is susceptible to be attacked by concentrated sodium hydroxide. Previous investigations of the composition of such surface layers formed as a result of alkaline degradation of PVDF, all concluded that the following reaction occurs [84-86]:



Where X = Li or Na.

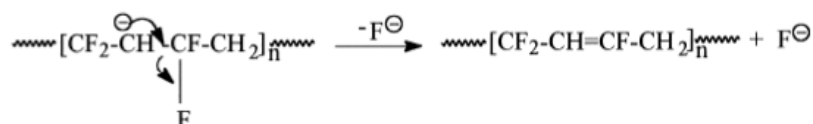
This mechanism is generally accepted, but has been generated on the basis of the experimental data. There were studies that expanded this mechanism to include the formation of hydroxide and carbonyl groups on the polyene chain. The possible mechanism of defluorination and oxygenation of PVDF in an aqueous solution is shown by deprotonation, elimination, hydroxylation and carbonyl formation reactions, respectively [84-89].

#### (a) Deprotonation

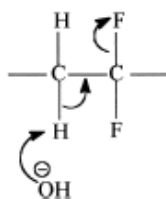


As a result of the high alkalinity of the aqueous solution and high temperature, deprotonation of CH<sub>2</sub> group in the chain will occur quite readily to achieve the above equilibrium.

### (b) Elimination

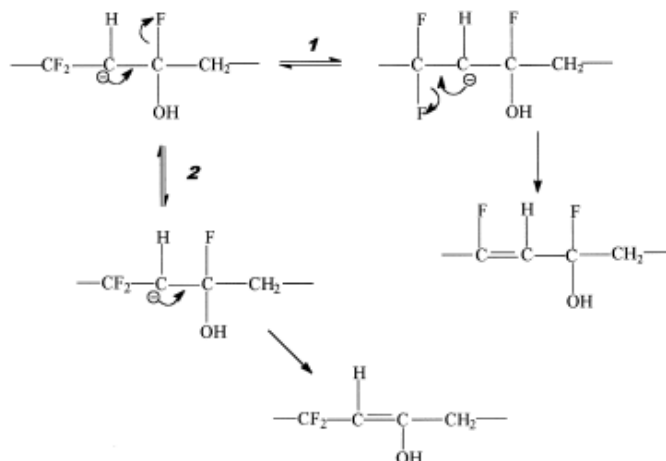


The above chain fragment can rearrange to yield in the chain C=C double bond, this is known as elimination reaction. The F<sup>-</sup> ion is stable as the reaction occurs in aqueous solution and the driving force is the formation of a carbon–carbon double bond. This process then, continues to yield a conjugated structure containing up to nine carbon double bonds. Step (a) and (b) may also occur simultaneously via an E2 (elimination and bimolecular) in the chain reaction.



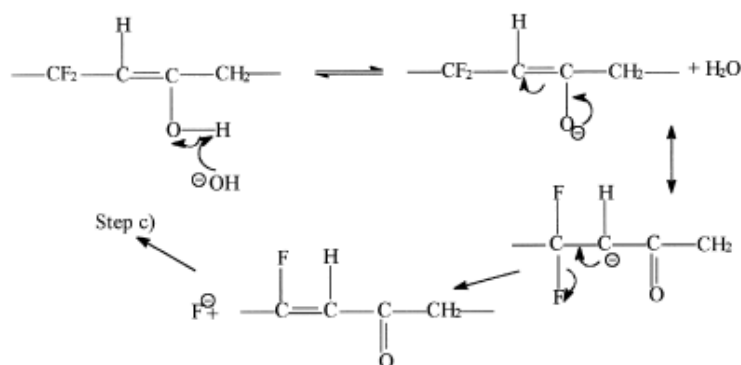
However, this is unlikely as it is part of a long polymer chain, then again in this case the hydroxide ion is associated with the phosphonium ion or ammonium ion in question.

### (c) Hydroxylation



In this step, there are two ways to generate HO–C–F in the treated PVDF surface, however there is no CF<sub>2</sub> remaining. It is concluded that all the CF<sub>2</sub> was removed but HO–C–F remains, as shown above. The attacking hydroxide is associated with a quaternary onium cation. The HO–C–F group can also be an intermediate group leading to the formation of hydroxide groups as shown above.

#### (d) Carbonyl formation



In the presence of an alkaline environment, deprotonisation of the incorporated hydroxide will occur to generate carbonyl group. The resultant structure is resonance stabilized as shown, and will lose fluoride, which is stable in aqueous solutions. Again, the driving force is the formation of a carbon–carbon double bond.

#### 2.4.2 Plasma activation

Plasma treatments can alter the surface energy of membranes and change the surface polarity which is the less damaging method of membrane modification. Plasma treatment of membranes was used in order to increase hydrophilicity by the reaction between hydrophilic monomers and membrane [28, 33, 90]. During the plasma treatment, the surface energy and polarity of membrane surface are changed by exposing to the reactive environment of excited atomic, ionic, and free radical species by hydrogen abstraction and radical formation, which resulted in modification of only the top-most nanometers of the membrane structure being altered [27, 28] as illustrated in Figure 2.4.

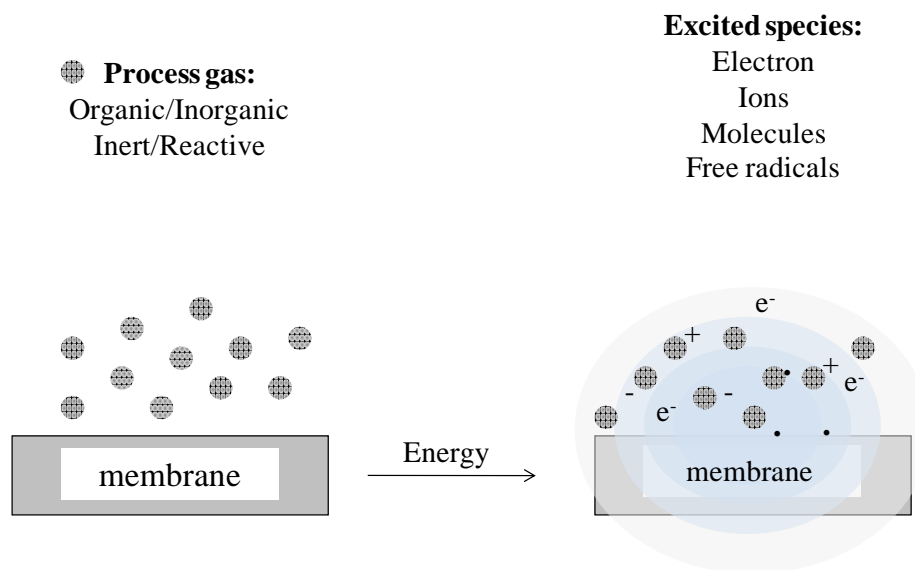


**Figure 2.4** Surface modification process using plasma activation

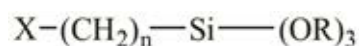
The excited species are also uniformly created on the membrane surface since the surface is bombarded by energetic particles and high energy radiation [91]. Therefore, the surface can be selectively modified for a specific application while the bulk properties of membrane are unaffected [27, 29]. Usually, surface modification of membrane by plasma treatment is mainly achieved by using different gases including oxygen, nitrogen, argon, helium, water vapor and air [27, 29-32]. The use of plasma to activate the surface to generate oxide or hydroxide groups can be used in surface modification [33]. Modification of membrane surfaces can be rapidly and cleanly achieved by plasma treatment due to the possibility of formation various actives on the surface.

### 2.4.3 Grafting of membrane by organosilanes

The modification of hydrophobic membranes was mostly developed for ceramic membranes because conventional ceramic microporous and mesoporous membranes are hydrophilic by nature. The hydroxyl groups present in the structure and on the pore surface are the main sources of hydrophilicity, which can link very easily to water molecules. This may lead to pore blocking at ambient conditions and will in any

case have a major effect on the separation properties of the membranes. The originally hydrophilic character of ceramic membrane can be changed by grafting process, leading to the increase of the hydrophobic properties that can be performed by reaction between OH<sup>-</sup> surface groups of the ceramic membranes and ethoxy groups (O-Et) present in organosilane compounds [22, 23].

Organosilanes have the ability to form a durable bond between organic and inorganic materials. A general structure of organosilane typically presents the two classes of functionality as below:



where X is an organofunctional group such as amino, methacryloxy, epoxy

RO is a hydrolysable group such as methoxy, ethoxy, or acetoxy, etc.

CH<sub>2</sub> is a linker

Si is silicon atom

There are two general strategies that can be pursued to bring about a hydrophobic modification of hydrophilic membranes as follows:

- **First strategy:** is to make a hydrophobic layer by hydrolysis and condensation of alkoxide precursors with hydrophobic side groups, such as organosilanes. The silane coupling treatment method is based on the derivatization of surface of UF and MF membranes with an organosilane in order to modify hydrophobic character.
- **Second strategy:** is to post-modify a mesoporous inorganic membrane by grafting both surface and the internal pore surface with organosilanes. This process is illustrated in Figure 2.5 and 2.6. A hydrolysable group of the organosilane undergoes coupling with the hydroxyl groups of the mesoporous layer, forming a chemically bound monolayer initially, which imparts the desired hydrophobicity as shown in Figure 2.5. Organosilanes with two or more hydrolysable groups can undergo further coupling with other organosilanes, forming a polymeric layer as shown in Figure 2.6 that case 1 is

monofunctional precursor anchoring to a hydroxyl site, case 2a and 2b are difunctional precursor anchoring to a hydroxyl site and forming a polymerized chain, respectively, and case 3 is trifunctional precursor forming a polymerized layer on a hydroxyl-terminated surface [19, 24].

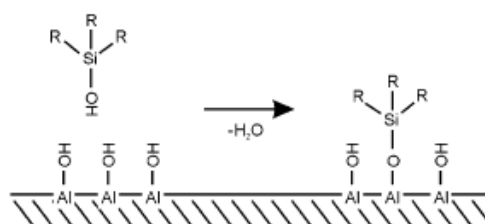


**Figure 2.5** Schematic diagram showing monolayer deposition of a monofunctional hydrophobic agent.

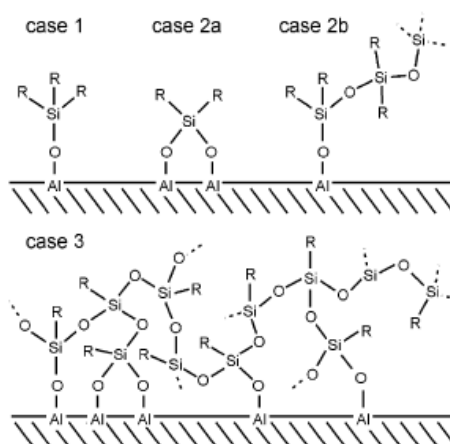


**Figure 2.6** Surface structures of organosilanes grafted on hydroxyl-terminated surfaces

#### 2.4.4 Parameters affecting membrane grafting

##### (a) The length of hydrophobic tail and type of functional group of organosilanes

The high hydrophobicity can be achieved by using agents with long organic tails. The use of organosilanes with two or more reactive groups can give rise to effective

membrane hydrophobicity. As these agents may couple with two adjacent OH groups, they may be more effectively reduce the number of vicinal OH groups that are responsible for the strongest hydrophilic interaction. Values of contact angle increase with increasing length of fluorinated chains. The study of Picard *et al.* [23] showed that increasing the length of fluorinated chains from C10Me ((3,3,3-trifluoropropyl)trimethoxysilane) to C6OEt (1H, 1H, 2H, 2H-perfluorooctyltriethoxysilane) or C8 (1H, 1H, 2H, 2H-perfluorodecyltriethoxysilane), the contact angles were increased. The solvent permeability coefficients of hexane for C8F (fluoroalkylsilane)-modified membrane were greater than C8H (alkylsilane)-modified membrane which is more hydrophobic membrane. In contrast, water permeability coefficient for C8F)-modified membrane was lower than C8H)-modified membrane [16].

#### **(b) Grafting time and number of soakings**

Multiplication of soakings results in an increase in fluorine concentration on the samples as and consequently an increase in the number of grafted molecules. Fluorine concentration appears to be very high when compared with carbon concentration and, especially with the concentration of carbon atoms bonded to fluorine. Picard *et al.* [22] confirmed that grafting time was important to reach a highest hydrophobicity of the material. The highest contact angle was 149° by 13 soakings with a grafting time between 6 and 20 hours [22]. Zhang *et al.* [92, 93] found that the contact angles were increased by a longer modification time of modifying agent for PAI and PEI membranes. This was because more reaction sites (hydroxyl groups) were generated on the membrane surface, and hence more molecules of modifying agents were able to graft and crosslink, leading to a higher hydrophobicity. Increasing number of soakings and sufficient grafting time, water permeability was decreased [22, 23]. Additionally, the decrease of permeability confirmed the importance of grafting time to improve the hydrophobicity.

#### **(c) Number of hydroxyl groups or active groups**

Factors that contribute to the ability of an organosilane to generate a hydrophobic surface are its organic substitution, the extent of surface coverage, residual unreacted





#### 2.4.5 Application of modified membrane in gas-liquid membrane contactor

Rahbari-Sisakht *et al.* [94, 95] studied the CO<sub>2</sub> absorption by membrane contactor using modified PVDF and polysulfone (PSf) membranes with surface modified macromolecule (SMM). The results showed that the performance of modified membrane was higher compared to the unmodified membranes which were the increase of CO<sub>2</sub> flux. The initial flux reduction of modified membranes was lower than that of unmodified membranes. The surface modified polyamide-imide (PAI) and polyetherimide (PEI) membranes also had higher CO<sub>2</sub> absorption flux than the unmodified membranes due to the increase hydrophobicity, larger pore size and reduction of thickness [92, 93, 96]. The modified PVDF-HFP membranes also presented the higher CO<sub>2</sub> absorption flux and membrane mass transfer coefficient than the unmodified membranes [97]. The study of Lv *et al.* [98] found that the modified polypropylene membranes (PP) in the long-term operation, the modified membrane in membrane contactor exhibited more stable and efficient performance than the unmodified PP membranes.

#### 2.5 Ozone oxidation

Ozone is an allotropic of oxygen which can be generated from air or pure oxygen when a high voltage is applied across the gap of a narrowly-spaced electrode. The high energy corona dissociates one oxygen molecule into two atomic oxygen which then combines with two other oxygen molecules to form two ozone molecules as shown in reaction 2.1 and 2.2.



Ozone is highly unstable and must be generated on site. Its oxidation potential (-2.07V) is greater than that of hypochlorite acid (-1.49V) or chlorine (-1.36V). The ozone is widely used in water treatment. Ozone molecule breaks down to oxygen molecules and oxygen atoms which have high oxidation potential. The oxidation power of ozone by measuring the REDOX potential is about 5 times higher than oxygen and about 2 times higher than chlorine. These higher potential increases its

reactivity with other elements and compounds which is about 20 to 50 times more reactive than chlorine and permanganates as it is well documented in the case of the high death rate of microorganism. Ozone is generated as a gas, therefore, treatment of aqueous contaminants requires the transfer from the gas to liquid phase.

The process of ozonation in aqueous solution takes place by two possible mechanisms [52, 99-101]:

- **Direct reaction** (important at low pH), where the oxidizing agent is the molecular ozone, in a slow and highly selective attack to organic matter, especially in the case of unsaturated organic compounds.
- **Indirect reaction pathways**, initiated by the ozone decomposition, in which free radicals, primary hydroxyl radicals ( $\text{OH}\cdot$ ) or hydroperoxide radicals ( $\text{OH}_2\cdot$ ). In this manner, the indirect mechanism can be significantly promoted in basic media, where hydroxide ions would initiate ozone decomposition entailing the following free radical mechanism.

It is now widely assumed that ozone reacts in aqueous solution with various organic and inorganic compounds, either a direct reaction or through a radical type reaction as shown in Figure 2.8.

Consequently, most ozone reactions involve a chain involving  $\text{OH}\cdot$  or  $\text{OH}_2\cdot$ , the reaction rate constant for the destruction of organics by  $\text{OH}\cdot$  is typically several orders of magnitude greater than for  $\text{O}_3$  alone. Ozone decomposition proceeds with chain reactions including initiation steps, propagation steps and chain breakdown. The fundamental role played by the hydroxide ions ( $\text{OH}^-$ ) in initiating the ozone decomposition process in water is well known [101]. In fact, for a typical aqueous solution, there are:

- **Initiators:** promote decomposition of ozone to form radicals (i.e. hydrogen peroxide ( $\text{H}_2\text{O}_2$ ), humics, reduced metals, formate).

- **Promoters:** react with  $\text{OH}\cdot$  to form radical species, resulting in propagation of reactions (i.e. primary and secondary alcohols, humics, ozone itself).
- **Scavenger:** react with  $\text{OH}\cdot$  to form secondary radicals which do not promote reaction but rather quench the chain reaction (i.e. tertiary alcohols, carbonate).

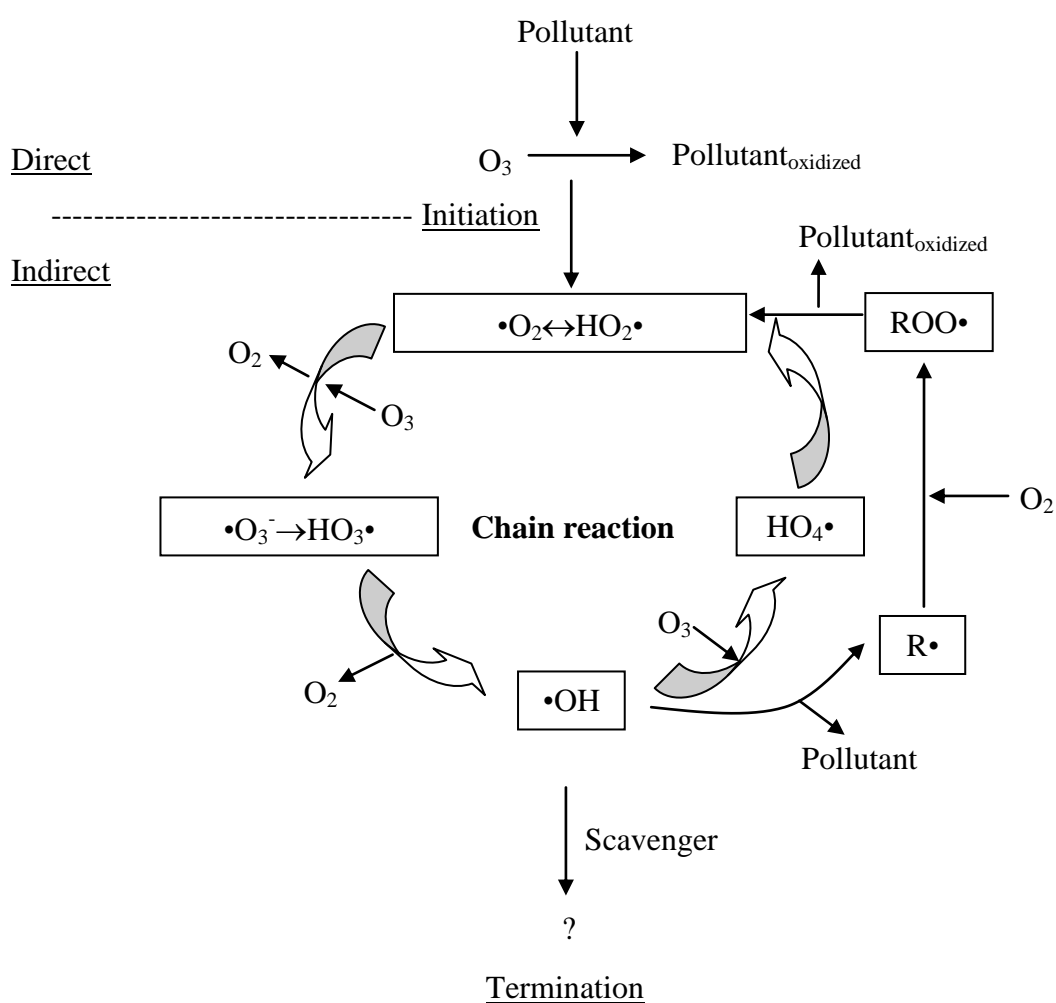


**Figure 2.8** Proposed mechanism of ozone oxidation [102]

The ozonation of azo reactive dyes is known to create mainly two types of by-products such as aldehydes and carboxylic acids with hydroxyl functional groups. For example, Zhang *et al.* [103] studied the decomposition pathways and reaction intermediate formation of azo reactive dye C.I. Reactive Red 120 by ozonation. It is believed that the azo-linkage of purified, hydrolyzed RR 120 during ozonation was reduced to a hydrogenated azo-linkage, resulting in the production of substituted benzene and naphthalene as shown in Figure 2.9. These substituted products can be further oxidized and finally mineralized to produce carbon dioxide. There are six sulfonic, four amino, two triazine and two azo groups in purified, hydrolyzed RR 120. The azo group was decomposed due to the elimination of molecular nitrogen such as ammonia and nitrate. After the electrophilic attack of ozone, a 1,3-dipolar cyclo addition of ozone proceeds to open the aromatic ring and ozonation intermediates with carbon-carbon double bonds are formed. These intermediates are assumed to be alcohols, aldehydes or ketones and carboxylic acid.

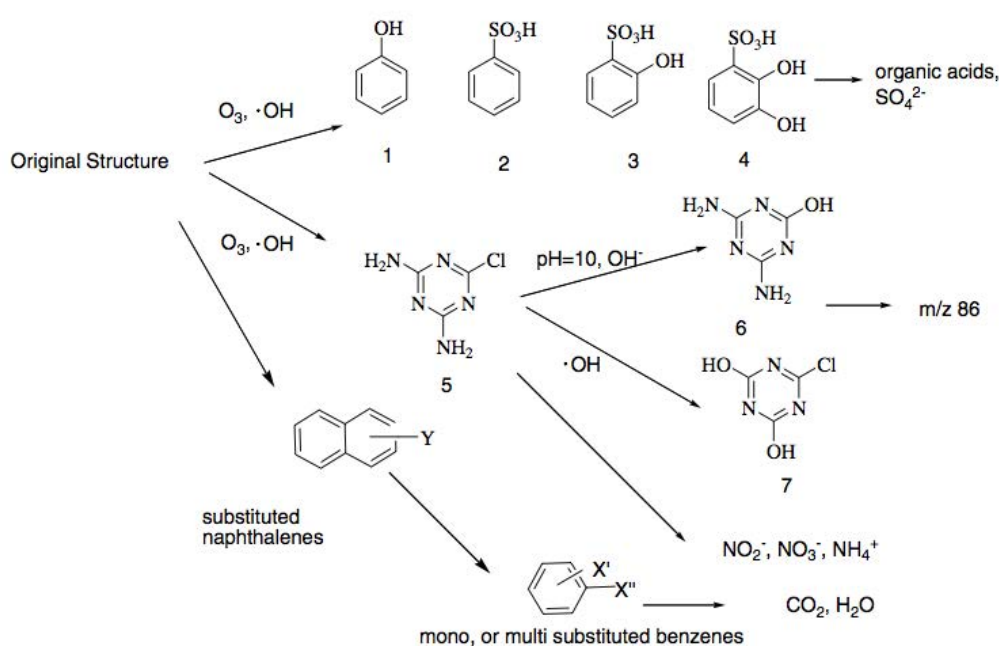


**Figure 2.9** The products of ozonation of purified, hydrolyzed RR 120 and its simplified reaction pathway

## 2.6 Durability and stability of membranes when exposed to oxidizing conditions

The application of membrane process is impeded by membrane fouling that leads to deterioration of permeate water quality, flux reduction and shortening of membrane life. Among the various probabilities that could lead to membrane degradation, the use of chemicals for membrane cleaning is the main cause for membrane damage. The cleaning or oxidizing agents (i.e. NaOCl solution, ozone and chlorine gases) can be used to remove inorganic fouling because they were powerful oxidant. Nevertheless, the oxidizing agents can affect the membrane structure, resulting in changes in the permeation properties. If the backbone of polymer chains is broken, the membranes are degraded. The change of membranes can be detected by exposing the membranes to the relevant agents, i.e. chlorine, ozone gas or acidic condition, over the time and concentration, and then measure the changes including flux, sorption and by analyzing membrane structures, leading to providing the information of membrane stability.

Sodium hypochlorite solution (NaOCl) is widely used as cleaning solution for membranes. Arkhangelsky *et al.* [35] found that The ultimate tensile strength, ultimate elongation and elasticity modulus of UF membranes were decreased after exposed to NaOCl, additionally, the degree of degradation being directly related to the dosage of oxidant and being more intense for cellulose acetate than for polyethersulfone membranes. Wang *et al.* [36] also reported that the tensile strength and the elongation of PVDF membranes became more weaker and flexible, additionally, the contact angles of membrane decreased after NaOCl cleaning. The results of ATR-FTIR indicated that the NaOCl cleaning did not damage to the chemical structure of PVDF membrane, but affected the surface properties. The study of Puspitasari *et al.* [37] also showed that NaOCl could cause ageing on membrane after prolonged exposure and changes in membrane chemical groups, hydraulic performances, mechanical properties and physical structures. The water flux increased, whereas, the salt rejection decreased due to the chlorination, resulting in the increased fragility and resultant defects of the oxidized fully-aromatic polyamide network [38].

It has been reported that the flux of membrane declined after exposed to chlorine, resulting in membrane degradation and decrease of membrane lifetime [104, 105]. Glater *et al.*[106] studied the sensitivity of reverse osmosis membranes to ozone and halogen disinfectants. The results showed that cellulose acetate membranes were resistant to halogens but polyamide membranes were sensitive to chlorine and bromide. The polyamide membranes were very sensitive to ozone in which the salt rejection declined within the first few hours of exposure and membrane failure completely occurred after 15 hours [106]. Bamperng *et al.* [34] reported that the ozone flux of PVDF membranes decreased, as a result of the membrane wetting and possibly due to the change of membrane morphology because of the ozone oxidation.

## **2.7 Membrane Characterization**

Membranes need to be characterized to determine the suitability for the applications. Membrane characterization methods allow determining of the physical and chemical properties of the membranes. In this section, the most familiar methods used for characterization of membranes are described.

### **2.7.1 Contact angle**

Contact angle measurement, which is the quantitative analysis, is the most commonly used method of solid surface tension measurement. The contact angle value is an angle between liquid and solid, which describes the edge of the two-phase boundary, where it ends at a third phase. The wettability of a solid surface by a liquid surface decreases as the contact angle increases. For the hollow fiber membrane, the contact angles can be measured in form of the dynamic contact angle based on the Wilhelmy method by tensiometer as presented in Figure 2.10. Dynamic contact angle is the contact angle when the three phase line is in controlled motion. It can be divided into the advancing and receding contact angles. The advancing contact angle is the contact angle when three phase line is moving over and wetting the surface or pushing away the gas phase, while the receding contact angle is the contact angle when the three phase line is withdraw over a pre-wetted surface or pushing a way the liquid phase. A contact angle of less than  $90^\circ$  means that the liquid tends to wet the substrate (hydrophilic), whereas with a contact angle of greater than  $90^\circ$  the liquid tends to wet

the surface (hydrophobic). If a dry microporous hydrophobic hollow fiber membrane with air-filled pores is surrounded by water, the water cannot penetrate into the pores until the water pressure exceeds a certain critical breakthrough pressure as expressed by equation 2.4.

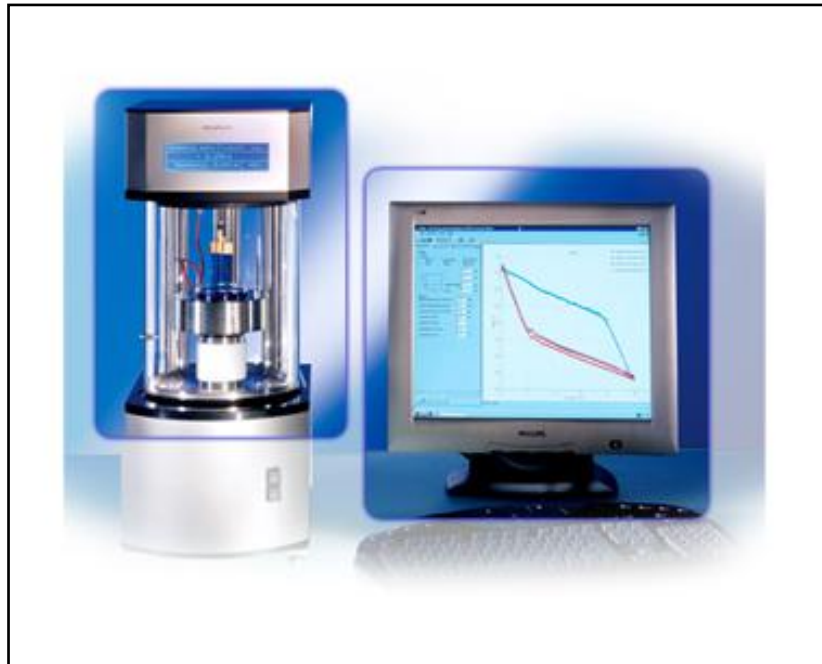


**Figure 2.10** Tensiometer for the contact angle measurement



### **2.7.2 X-ray Photoelectron Spectroscopy (XPS)**

X-ray photoelectron spectroscopy is a quantitative spectroscopic technique that measures the elemental composition, empirical formula, chemical state and electronic state of the elements that exist within a material. XPS is a highly surface-specific analytical technique (3-10 nm) used to obtain the chemical structure and atomic composition of a material. XPS utilizes photo-ionization and energy-dispersive analysis of the emitted photoelectrons to study the composition and electronic state of the surface region of a sample. The atomic sensitivity of XPS is  $10^{-3}$ - $10^{-2}$ , therefore, 0.1-1.0% can be detected (except H and He). The photon is absorbed by an atom on the surface, leading to ionization and the emission of a core (inner shell) electron. The kinetic energy distribution of the emitted photoelectrons can be measured using any appropriate electron energy analyzer and a photoelectron spectrum can thus be recorded. For each element, there is a characteristic binding energy associated with each core atomic orbital. The presence of peaks at particular energies therefore indicates the presence of a specific element in the sample under study. XPS has been commonly used to confirm the chemical reaction of the membrane after surface modification [19, 23, 24, 87].

### **2.7.3 Fourier Transform-Infrared Spectroscopy (FT-IR)**

Fourier Transform Infrared Spectroscopy (FTIR) technique provides excellent quality data in conjunction with the best possible reproducibility of any IR sampling technique. FT-IR is a single beam instrument which is based on the absorption or reflection of electromagnetic radiation with the wavelength in the range of 1 to 1000  $\mu\text{m}$ . In this frequency domain, the absorption bands present from a molecular fingerprint, thus allowing the detection of compounds and the deduction of the structural details. The spectral composition of the reflected beam depends on the variation of the reflection index of the compound with the wavelength. This can lead to attenuated total reflection (ATR). By the angle of incidence and difference in the refractive indices of the media, the sample is penetrated only half a wavelength at each reflection of the radiation. The accumulation of absorption comes from the succession of many total reflections attenuated. Then, the final spectrum is identical to

the spectrum obtained by transmission. FT-IR has been commonly used to confirm the chemical reaction of the membrane after surface modification [107-109].

#### **2.7.4 Scanning Electron Microscopy (SEM) or FE-SEM**

SEM provides a very convenient and simple method for characterizing and investigating the structure of microporous membranes. In a scanning electron microscope (SEM), a fine beam of electrons scans the membrane surface. This causes several kinds of interactions generating different signals, of which secondary electrons (SE) and back scattered electrons (BSE) are used in the image forming. Secondary electron images can be used in membrane characterization in imaging of membrane morphology, for example, pore geometry, pore size, pore size distribution, and surface porosity. Due to the large depth of field, the SE images visualize the membrane surface morphology three-dimensionally. The lateral resolution of a conventional SEM is 10–50 nm. However, with Field Emission Scanning Electron Microscopy (FE-SEM), which has a resolution of 1–5 nm, also visualization of the fine morphology of ultrafiltration membranes is possible. The depth resolution in SE imaging is 1–10 nm and in BSE imaging 10–1000 nm. To observe cross sections of flat-sheet membranes or the inner surfaces of hollow-fiber membranes, the samples are usually briefly frozen in liquid nitrogen and then broken manually. In addition to the visualization of the sample surface, SE and BSE images provide information on sample topography and chemical composition of the sample (BSE images).

Polymers are generally insulators, therefore, polymeric membrane samples (and other non-conducting samples) have to be coated with a conductive coating (carbon, gold, platinum, or palladium) to eliminate surface charging and to minimize sample damage caused by the electron beam. However, the electron beam might still damage the polymeric membrane sample, and the coating process might cause artificial changes to the membrane surface. Furthermore, the coating layer can lead to an underestimation of the pore size [110].

#### **2.7.5 Pore size and pore size distribution**

The main methods used to determine pore size and pore size distribution are gas-liquid displacement. This method is based on the fact that a pressure is needed to

force a non-wetting liquid to flow through the pore of a membrane. The gas pressure differential across the membrane should be able to overcome the capillary force caused by the surface tension of the liquid. This force can be calculated by Laplace-Yong equation, as indicated by equation 2.4. Pure nitrogen is allowed to flow into the chamber gradually. When the increased nitrogen pressure reaches a point that overcomes the capillary flow of the fluid within the largest pore, the bubble point is found. After determining the bubble point, the pressure is increased continuously and the nitrogen permeation rate is measured until all pores are empty of solution, and the sample is considered dry. Nitrogen pressure and permeation flow rates through the dry sample are also recorded. Based on the nitrogen flow rates through the wet and dry membranes, the pore size distribution is calculated.

### **2.7.6 Surface roughness (Atomic Force Microscopy)**

AFM has been widely used to study the morphology of membrane surface. This method is operated by measuring attractive and repulsive forces between a sharp tip and the sample. The advantage of this technique is that the membranes can be scanned without the pretreatment. AFM has a resolution of 1 nm and provide information about the mean surface roughness. In general, roughness of the surfaces is related with the membrane hydrophobicity in term of contact angle. The roughness of the membrane surfaces increases with contact angles leading to high membrane hydrophobicity [111]. Zhang *et al.* [93] studied the outer surfaces of modified PAI hollow fiber membranes by AFM. The results showed that the surface roughness and contact angle of modified PAI membrane surface were increased with the modification time.

### **2.7.7 Mechanical strength**

The mechanical strength is the test in material properties that determines the tensile strength and elongation at fracture as a toughness measurement of the material. The tensile strength is the maximum test force applying to the sample until its fails, while the elongation at fracture is the change in length of the sample compared with its original length which is the degree of deformation. It is necessary to observe the change in tensile properties of the membrane after modification.

# **CHAPTER III**

## **HYDROPHOBIC SURFACE MODIFICATION OF PVDF HOLLOW FIBER MEMBRANE**

### **3.1 Introduction**

The membranes applied in membrane contactors are typically fabricated from hydrophobic polymers to reduce the membrane wetting. Even though the membranes are highly hydrophobic, the membrane wetting can occur leading to the reduction in the performance. Membrane wetting depends on the structural characteristics of the porous material and hydrophobicity. The common hydrophobic membrane materials are polyethylene (PE), polypropylene (PP), polyvinylidene fluoride (PVDF), and polytetrafluoroethylene (PTFE). Based on the contact angle data, the hydrophobicity of the membranes is in the order of PTFE > PE > PP > PVDF [112, 113]. However, PTFE is much more expensive than PVDF due to the use of thermal method for fabrication. On the contrary, PVDF has received much attention as a membrane material due to its high mechanical strength, thermal stability and chemical resistance [77]. Fabrication of PVDF membrane by phase inversion method is also much more simpler.

Recently, several studies have shown success in ceramic membrane modification to improve hydrophobicity since ceramic membranes are hydrophilic. The ceramic membranes had been successfully grafted by fluoroalkylsilanes (FAS) [114-121]. FAS are the group of compounds, which can be efficiently used to create the hydrophobicity. Grafting process, leading to the increase of the hydrophobic properties, can be performed by the reaction between OH groups of the ceramic membrane and ethoxy groups (O-Et) presented in organosilane compounds.

The methods used for modification of ceramic membranes can be applied to modify PVDF membranes. However, PVDF membranes have no hydroxyl groups. Therefore, hydroxyl groups must be introduced on the membrane surface. There are several

methods to produce OH groups on the PVDF membrane surface. Examples are the chemical method (alkaline treatment), plasma treatment, and radiation. Basically, the alkaline treatment is a simple method that has been investigated to introduce OH groups on the membranes. However, it was reported in the literature that the properties of PVDF membrane were destroyed by NaOH solution because NaOH had chemically attacked PVDF membrane and caused the dehydrofluorination in the polymer chain [25, 26]. For example, the mechanical strength and crystallinity of PVDF membranes were decreased even at 4wt% NaOH solution at 70°C within 24h or in 10wt% NaOH solution within 8h [25]. The reduction in mechanical strength of membrane treated by NaOH was due to the degradation of membrane as a result of the chemical reaction between PVDF membrane and NaOH. Liu *et al.* [26] also reported the hydrophilic PVDF membrane modification by alkaline treatment. The results showed that the alkaline treatment changed the membrane surface structure based on the results of pore size distribution.

Plasma treatments can alter the surface energy of membranes and change the surface polarity which is the less damaging method of membrane modification. Plasma treatment of membranes was used in order to increase hydrophilicity by the reaction between hydrophilic monomers and membrane [28, 33, 90]. During the plasma treatment, the membranes were exposed to a reactive environment of excited atomic, ionic, and free radical species by hydrogen abstraction and radical formation, which resulted in modification of only the top-most nanometers of the membrane structure being altered [27, 28]. Therefore, the surface can be selectively modified for a specific application while the bulk properties of membrane are unaffected [27, 29].

As mentioned above, plasma treatment can be used to activate the PVDF membrane surface in order to have the reaction with modifying agent which can replace the alkaline treatment. There is no work reported on the surface modification of PVDF membrane using plasma activation, followed by grafting with organosilane. This work aimed to modify PVDF hollow fiber membranes to increase hydrophobicity using two different activation methods, alkaline treatment and plasma activation, followed by grafting with organosilanes. Three organosilanes, i.e., hexadecyltrimethoxysilane, 1H,

1H, 2H, 2H-perfluorooctyltriethoxysilane and 1H, 1H, 2H, 2H-perfluorodecyltriethoxysilane, were selected for the study. To the best of our knowledge, these organosilanes have not been used to modify PVDF membranes. Effects of NaOH concentration and grafting time were investigated. The chemical and physical changes of original and modified membranes were investigated. The stability of the modified membranes was examined by testing the CO<sub>2</sub> absorption flux by 2M Taurine sodium for 15 days. The modified membranes were expected to be the potential membranes for membrane contactor applications.

## 3.2 Methodology

### 3.2.1 Materials and chemicals

PVDF hollow fiber membrane was supplied by Altrateck (China). The specifications of the membrane were reported by the manufacturer as listed in Table 3.1. The PVDF hollow fiber membranes are shown in Figure 3.1. Aqueous sodium hydroxide (NaOH) solutions were prepared from NaOH pellets (Carlo Erba, 97%). The different organosilanes used in this study are listed in Table 3.2. Hexane (AR<sup>®</sup> (ACS), 98.5%) was used as a solvent and deionized water was used in aqueous solution.

**Table 3.1** Specifications of the PVDF hollow fiber membrane

Fiber o.d. (mm)	1.16
Fiber i.d. (mm)	0.8
Membrane pore size (μm)	0.16
Membrane porosity	70%



**Figure 3.1** PVDF hollow fiber membranes

**Table 3.2** Description of organosilanes used

Name	Formula	Code	Supplier
Hexadecyltrimethoxysilane	$C_{16}H_{33}Si(OCH_3)_3$	AS-C16	(Sigma-Aldrich, 85%)
1H, 1H, 2H, 2H-perfluorooctyltriethoxysilane	$C_6F_{13}C_2H_4Si(OCH_2CH_3)_3$	FAS-C6	(Sigma-Aldrich, 98%)
1H, 1H, 2H, 2H-perfluorodecyltriethoxysilane	$C_8F_{17}C_2H_4Si(OCH_2CH_3)_3$	FAS-C8	(Sigma-Aldrich, 97%)

### 3.2.2 Methods

In order to increase hydrophobicity of PVDF hollow fiber membranes, two surface modification methods were applied to modify the original PVDF hollow fiber membrane as follows.

#### – Chemical modification (CM)

The chemical modification involves the hydroxylation of the PVDF membrane, namely alkaline treatment, by an aqueous NaOH solution followed by immersing in organosilane solution. Firstly, the PVDF hollow fiber membranes (30 cm in length) were immersed in NaOH aqueous solution (2–7.5M) under magnetic stirring for 3-

12h in the plastic container by putting in the water bath for controlling the temperature, then the membranes were rinsed with deionized (DI) water for five times in order to stop reaction. After rinsing, the membranes were immersed in an organosilane solution at fixed concentration using hexane as solvent for 6-24h in the plastic container. Then, the grafted membranes were rinsed with pure hexane for 5 times to remove any unreacted chemicals from the membranes and were hung in an oven at 100°C for 2h in order to dry the membranes. Finally, the membranes were kept at room temperature (25°C) before characterization.

– **Plasma-activated modification (PAM)**

Plasma activation of the original PVDF hollow fiber membranes was conducted using a Plasma Enhancement machine (Model HD-1B) from Chang Zhou Zhongke Changtai Plasma Technology Ltd. Power was inductively supplied at a power of 80W and the sample chamber (30cm×30cm×30cm) was kept under vacuum. Plasma was sustained by a radio frequency (13.56 MHz) generator and was induced to the sample chamber. The plasma modification involved two steps: (1) the 30 hollow fiber membranes were exposed for surface activation by plasma wave with helium gas for 180 seconds and working pressure at 10Pa by hanging in the chamber and (2) the membranes were immersed in organosilane solution with the same method as chemical modification.

### **3.2.3 Membrane characterizations**

Dynamic contact angle was measured using a tensiometer (DCAT11 Dataphysics, Germany) as illustrated in Figure 2.10. The sample fibers were cut into the small pieces with 1-2 cm in length and a lumen of fiber was glued by epoxy to measure only the outer surface contact angle. A piece of hollow fiber membrane was hung to the sample holder on the arm of the electro-balance. Then, the sample was immersed into Milli-Q water with 5 cycles of immersion and the contact angle was calculated from the wetting force based on the Wilhelmy method. The membrane morphology was observed by scanning electron microscopy (SEM) (ZEISS EVO 50), dried membrane samples were fractured in liquid nitrogen and sputtered with a thin layer of gold. The surface infrared spectra were recorded between 650  $\text{cm}^{-1}$  and 4000  $\text{cm}^{-1}$  on an IR



Prestige-21 Fourier transform infrared (FTIR) spectrophotometer (SHIMADZU). All spectra were required by signal averaging 50 scans at a resolution of  $4\text{ cm}^{-1}$  in attenuated total reflection (ATR) mode.

The chemical composition of sample surface was investigated by X-ray photoelectron spectrometer (XPS; AXIS ULTRA<sup>DLD</sup>, Kratos analytical, Manchester UK.). The base pressure in the XPS analysis chamber was about  $5 \times 10^{-9}$  torr. The samples were excited with X-ray hybrid mode  $700 \times 300\ \mu\text{m}$  spot area with a monochromatic Al  $K_{\alpha}$  radiation at 1.4 keV. X-ray anode was run at 15 kV 10 mA 150 W. The photoelectrons were detected with a hemispherical analyzer positioned at an angle of  $45^{\circ}$  with respect to the normal to the sample surface. The mean pore size and pore size distribution of the fibers were measured using a capillary flow porometer (Porous Materials Inc., model CFP-1500A), of which working principle is based on gas permeation and bubble point tests. The samples were potted into the sample holder and soaked in the Galwick<sup>®</sup> solution as the wetting liquid till completely wet. The surface tension of Galwick<sup>®</sup> solution is  $16\text{ mJ/m}^2$ . During the test, the gas flow rate was increased stepwise and passed through the saturated sample until the applied pressure exceeded the capillary attraction of the fluid in the pores. By comparing the gas flow rates of a wet and dry sample at the same pressures, the percentage of flow passing through the pores larger than or equal to the specified size can be calculated from the pressure-size relationship.

The mechanical strength of the fibers was measured using a Zwick/Roell BT1-FR0.5TN.D14 testing machine under room temperature. The tensile strength and tensile modulus were measured in order to examine the mechanical strength and deformation of membranes. The sample fiber was clamped at both ends and pulled under tension at a constant elongation. The surface roughness of the membrane was recorded by atomic force microscopy (AFM, SPA 400, SEIKO instrument) operated in tapping mode. Silicon nitride tips coated with Al on the reflective side, resonance frequency of 200-400 kHz and a spring constant of 25-75N/m were used. The rate of  $2\ \mu\text{m} \times 2\ \mu\text{m}$  images was 1Hz.

### 3.2.4 Long-term stability study of modified PVDF membranes for CO<sub>2</sub> absorption

In order to examine the stability of the modified membranes, long term performance test for 15 days of operation was conducted. The membrane modules were made to test the CO<sub>2</sub> flux. The module consisted of four fibers with an effective length of 20 cm and inner diameter of 7.4 mm as presented in the Figure 3.2. The liquid absorbent, 2M Taurine sodium, flowed on the shell side and CO<sub>2</sub> in the lumen side of the hollow fiber membrane under counter current mode at room temperature. The feed gas flow rate was adjusted by mass flow controllers (Cole-Parmer) and measured by digital bubble meters (Bios Dender 510L). A digital peristaltic pump (MasterFlex) was used to control the liquid flow and pumped the liquid into the shell side of the hollow fibers from a 10 L container. The CO<sub>2</sub> flux was calculated by the difference of CO<sub>2</sub> flow rate before and after the membrane module. Experimental data were recorded after the contactor system was stabilized. The experimental setup of CO<sub>2</sub> absorption in the membrane contactor over 15 days is presented in Figure 3.3.



**Figure 3.2** Hollow fiber membrane modules

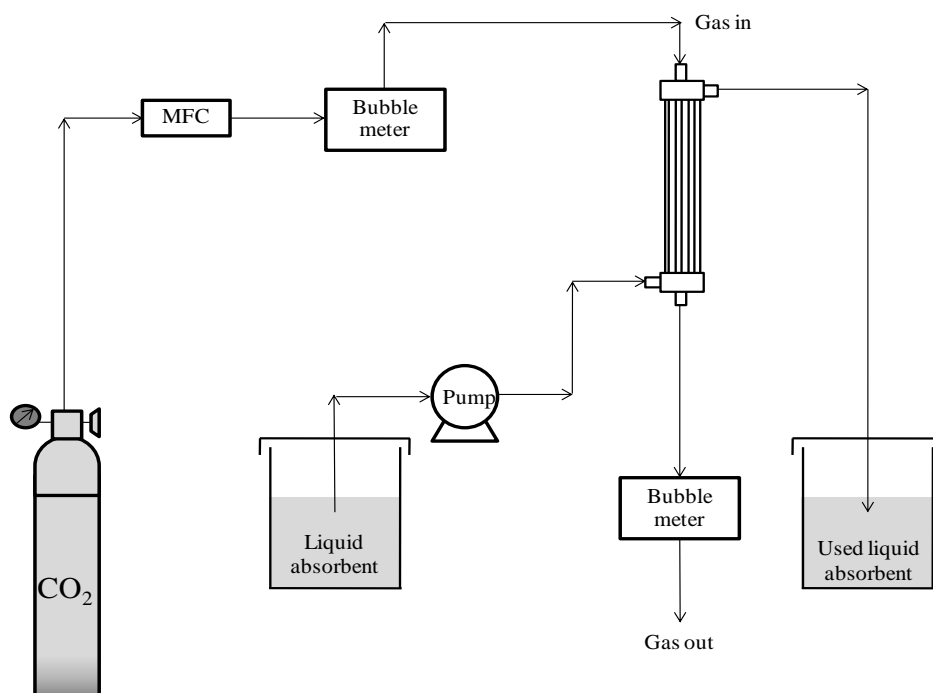


**Figure 3.3** Experimental setup of CO<sub>2</sub> absorption in a membrane contactor

### 3.3 Results and discussion

#### 3.3.1 Effect of NaOH Concentrations and Organosilanes

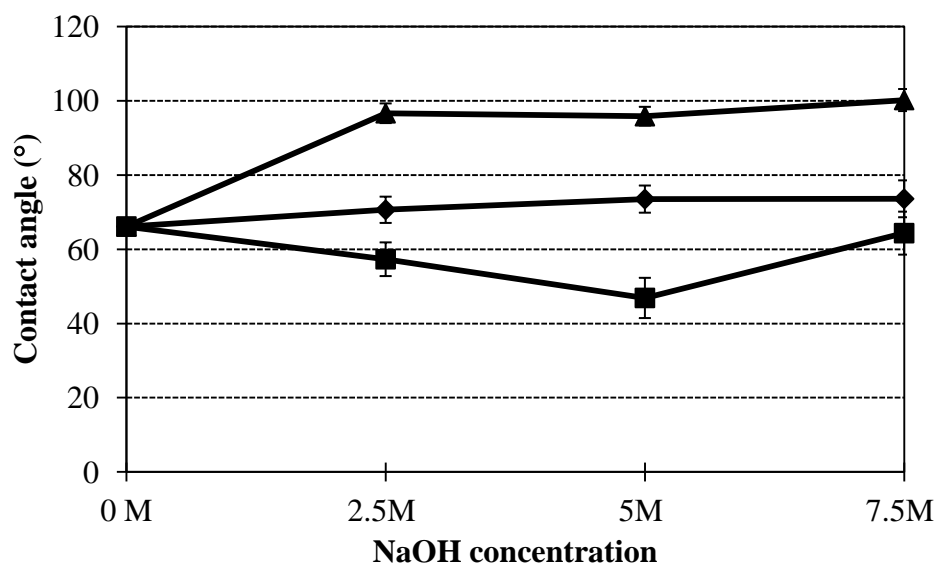
##### – Contact Angle

The contact angle of the original membrane was 68.91°. By increasing the concentration of NaOH from 2.5M to 7.5M, the contact angle of membranes was decreased from 44.23° to 31.27°, respectively as shown in Figure 3.4. Zheng *et al.*[122] reported that with the concentration of 7.5M NaOH and treatment time for 3h, the contact angle gradually decreased with more hydroxide and carbonyl groups found on the membrane. Dehydrofluorination mechanisms of PVDF occur by the reactions of defluorination and oxygenation, formation of hydroxide and carbonyl groups as shown in Figure 3.5 [123, 124].

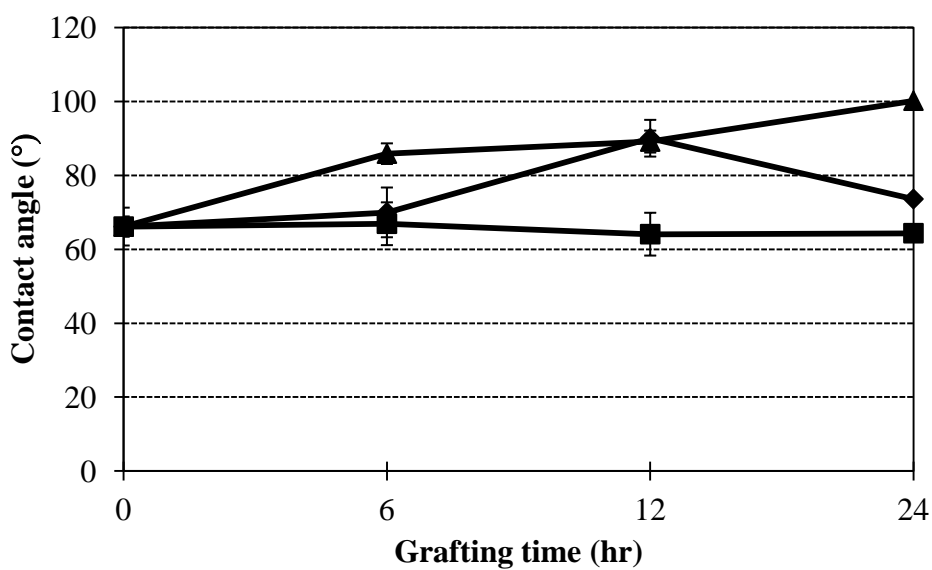


After membrane modification by organosilanes, the results showed that the modified membranes had higher contact angles than original membrane because organosilane with three inorganic reactive groups on silicon (ethoxy) reacted with OH groups on the membrane surface. Increasing the concentration of NaOH, the contact angles of membranes were increased as shown in Figure 3.6a. This was because more OH groups were generated on PVDF membrane surface. Therefore, more organosilane molecules reacted with OH groups. As the results, the modified membranes showed higher hydrophobicity. The contact angles of the modified membrane by FAS-C8 were higher than 90 (increasing hydrophobicity) compared to AS-C16 and FAS-C6 because the FAS-C8 has higher molecular weight, carbon and fluorine atoms than AS-C16 and FAS-C6.

The C-F bonds of FAS-C8 act as the hydrophobic part of the molecule and the Si-(OR)<sub>3</sub> act as anchor at the membrane. In contrast, the element compositions of AS-C16 have no F atoms. Picard *et al.*[114] found that the contact angle should increase with increasing length of fluorinated chains. However, the contact angles of FAS-C6 modified membranes were decreased. This is likely due to the unsuccessful FAS-C6 grafting by a self assembly of FAS-C6 molecules. Therefore, FAS-C6 molecules were not grafted with the OH groups on the treated membrane, resulting in the reduction of contact angles.



a)



b)

◆ AS-C16    ■ FAS-C6    ▲ FAS-C8

**Figure 3.6** a) Influence of NaOH concentration (60°C for 3h) in 0.01M of organosilane modification for 24 h; b) Influence of grafting time and organosilane under 7.5M NaOH (60°C for 3h)

In addition, it was observed that increasing the grafting time of organosilane, the contact angles were increased as shown in Figure 3.6b. Lu *et al.* [117] reported that after increasing multiplicity of grafting time, the contact angles were also increased. Zhang *et al.* [125] reported that the contact angles of the modified PAI membrane by 3-aminopropyltrimethoxysilane (APTMS) were increased from 108° to 118° with the increase in grafting time from 30 to 120 min. The highest contact angle of modified membrane in this study was 100.2° under the condition of 7.5M NaOH at 60°C for 3h, followed by grafting 0.01M FAS-C8 for 24h. The contact angles from this study were lower than those of Zheng *et al.* [122], Yang *et al.*[126] and Wongchitpimon *et al.* [127], which were in range of 110°-135°. Zheng *et al.* [122] used mixed organosilanes (DDS and MTS) which were more hydrophobic. Yang *et al.*[126] performed the alkaline treatment at lower NaOH concentration (2M). Wongchitpimon *et al.* [127] used mixed solution of cross-linking agent and organosilane which was also more hydrophobic.

#### – SEM Images

The SEM images of the cross section and outer surface of the original and modified membranes are as shown in Figures 3.7 and 3.8. The needle-like structures were formed on the modified membrane surface by 7.5M NaOH treatment, followed by grafting with 0.01M FAS-C8 for 24h, which are randomly arranged and intertwined together as shown in Figures 3.7 and 3.8. It is known that a needle-like structure is one of the ideal surfaces for hydrophobicity [117]. Additionally, the surface of AS-C16 modified membrane was the same as original membrane. In contrast, there were some needle-like structure on AS-C16 but they were very small compared to FAS-C8 because AS-C16 molecules have no F atoms, leading to a lower hydrophobicity. FAS molecules were hydrolyzed to a silanol, which can react with OH groups on the PVDF membrane, resulting in the formation of a self-assembled needle like structures on the membrane. It was reported in the literature that FAS molecules are covalently attached and the nanometer-scale aggregates are generated through the further polymerization and the FAS-C8 molecular axis is predominantly oriented perpendicular to the membrane surface (needle like structure) and partly oriented parallel on the surface. Zheng *et al.* [89] also reported that the frosts or needle like

structure were also found on the modified membrane by DDS/MTS. Meanwhile the vertical polymerization to form grafted polysiloxane could be induced on the surface. Lu *et al.* [117] reported that for the membrane surface modified with FAS many needle-like structures were formed that is responsible of the superhydrophobicity of the surface.

#### – Pore Size and Pore Size Distribution

The membrane pore size and pore size distributions of modified membrane were analyzed. Compared to the original membrane which had a maximum pore size of 0.282  $\mu\text{m}$  and mean pore size of 0.1305  $\mu\text{m}$ , the mean pore size and maximum pore size of modified membranes were in the range of 0.136-0.147  $\mu\text{m}$  and 0.283-0.3  $\mu\text{m}$ , respectively. In other words, no significant change was observed.

#### – FT-IR

The FT-IR spectra of the modified PVDF membrane with organosilanes compared to the spectrum of the original membrane were given in Figure 3.9 and Figure 3.10. There were three new peaks detected in the spectra of Figure 3.9. The 1634  $\text{cm}^{-1}$  was assigned to the Si-O-Si bending. This was due to the difunctional or trifunctional silanes forming a polymerized chain on the OH groups of membrane surface [115, 128]. The 2890-2970  $\text{cm}^{-1}$  broad band of medium intensity was  $\text{CH}_2$  asymmetric stretching. The 3480  $\text{cm}^{-1}$  was OH group. However, there were OH groups on the modified membrane surface indicating that all OH may not react with the silanols in the FAS molecules. The OH peak was smaller under the higher FAS concentration because the more FAS-C8 molecules were able to react and graft with OH groups more completely. The presence of Si and  $\text{CH}_2$  implied that there were FAS molecules and the grafting was successful. From Figure 3.10, the peak of Si-O-Si and  $\text{CH}_2$  were found on the modified membranes by three organosilanes modification. The  $\text{CH}_2$  peaks of AS-C16 modification were stronger than FAS-C6 and FAS-C8 modifications due to the composition of AS-C16 which is consisted of  $\text{CH}_2$  groups on its structure. Organosilanes with three reactive groups on silicon (usually methoxy, ethoxy or acetoxy) bond well to the hydroxyl groups on the treated membrane. The alkoxy groups on silicon were hydrolyzed to silanols, either through the addition of water or



from residual water. Then, the silanols coordinate with hydroxyl groups on the membrane surface to form an oxane bond and eliminate water as shown in Figure 3.11.

– **XPS**

The presence of FAS on the membrane was confirmed by XPS analysis as shown in Table 3.3. The fluorine (F) content on the surface of modified PVDF membranes decreased compared to the original membranes, except for 0.02M of FAS-C8. This is caused by the elimination of H-F during the alkaline treatment. In case of AS-C16 modification, F content was lowest because it has no F atom on its structure. In addition, oxygen (O) content of modified membranes was found because of the silanols formed. On the other hand, the amount of silicon (Si) was also found on the modified membranes. The XPS results implied that there were organosilane molecules and the grafting was successful even after rinsing with hexane for five times.

– **Mechanical strength**

The mechanical properties of the original and modified PVDF hollow fiber membranes are summarized in Table 3.4. The results showed that the tensile modulus and tensile stress of modified membranes were increased by 11-18% and 0.4-7%, respectively, in contrast, the strain at break of modified membranes was decreased by 4-17%. This implied that the rigidity of modified membranes was increased, whereas, the elasticity of modified membranes was decreased. In addition, the tensile modulus and tensile stress of modified membranes were higher than those reported by Yang *et al.* [126] and Wongchitphimol *et al.* [97].

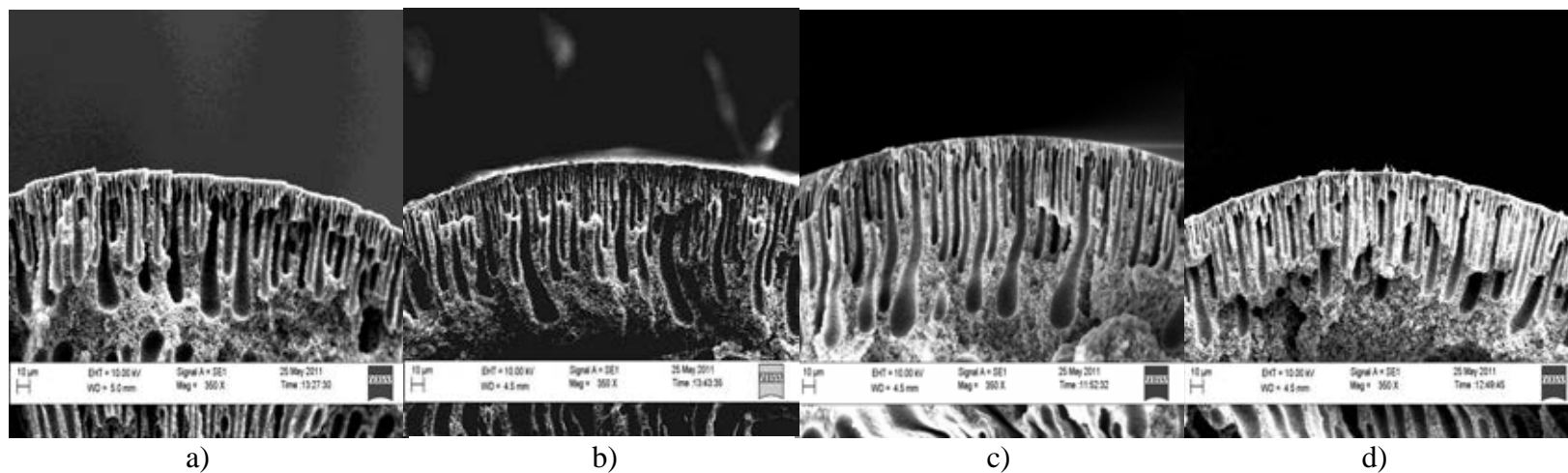


**Figure 3.7** Cross section morphology of PVDF membrane: a) original membrane; b) AS-C16 modified membrane; c) FAS-C6 modified membrane; d) FAS-C8 modified membrane

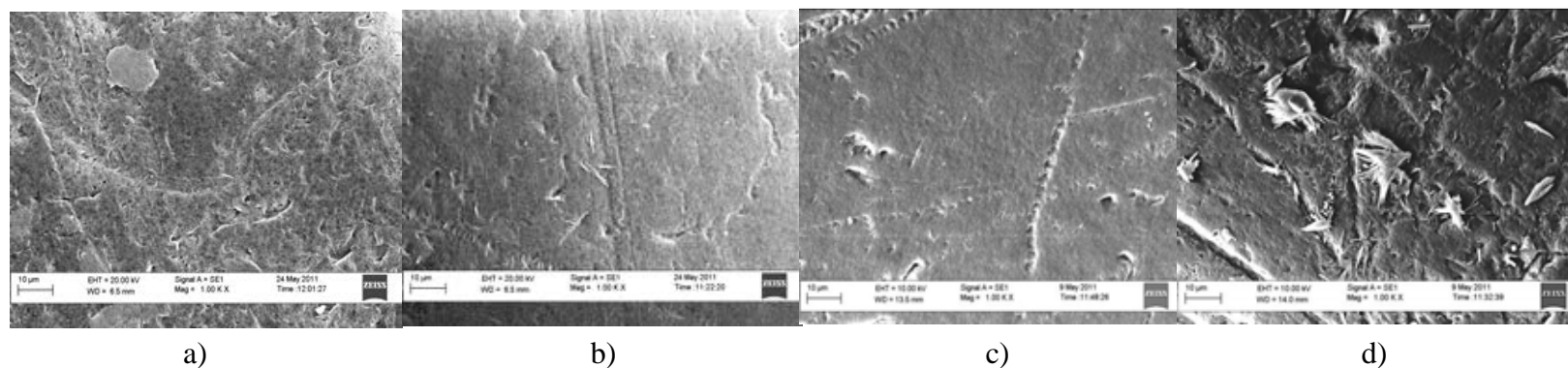


**Figure 3.8** Outer surface morphology of PVDF membrane: a) original membrane; b) AS-C16 modified membrane; c) FAS-C6 modified membrane; d) FAS-C8 modified membrane

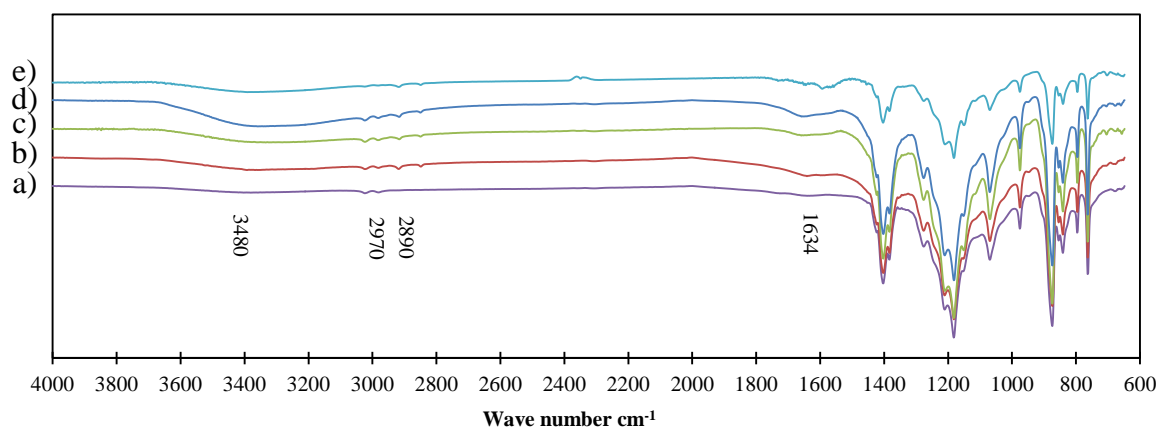


**Figure 3.9** FT-IR spectra of PVDF membrane: a) original membrane; b) 2.5M NaOH, 0.01M FAS-C8 for 24h; c) 5M NaOH, 0.01M FAS-C8 for 24h; d) 7.5M NaOH, 0.01M FAS-C8 for 24h; e) 7.5M NaOH, 0.02M FAS-C8 for 24h

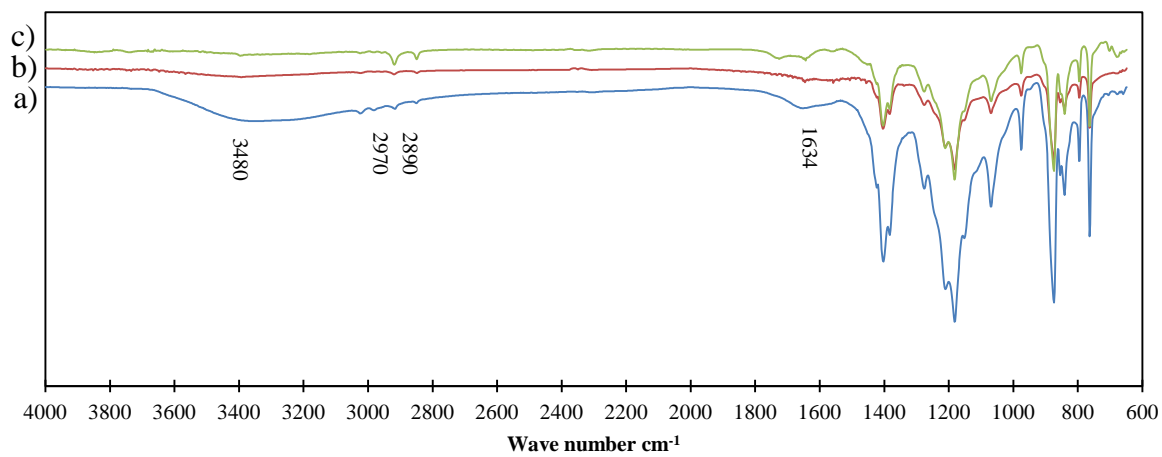


**Figure 3.10** FT-IR spectra of modified PVDF membrane by 7.5M NaOH: a) 0.01M FAS-C8 for 24h; b) 0.01M FAS-C6 for 24h; c) 0.01M AS-C16 for 24h

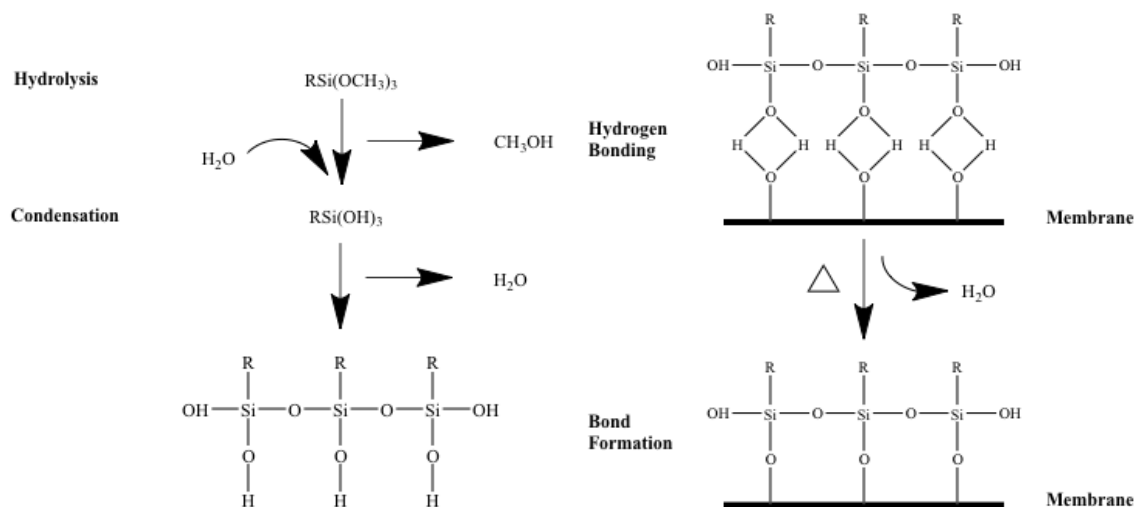


**Figure 3.11** The hydrolysis reaction of the organosilane and the addition of the silanol groups onto the PVDF membrane surface

**Table 3.3** Changes of the chemical structure of membrane surface

Surface	Atomic concentration (%)			
	C	F	O	Si
Original	52.5	38.9	7.1	-
Alkaline treatment: 7.5M NaOH at 60°C for 3h				
0.01M AS-C16 for 24h	58	7.3	27.6	1.3
0.01M FAS-C6 for 24h	48.1	29.9	14.6	2.0
0.01M FAS-C8 for 24h	48.7	32.9	14.6	1.9
0.02M FAS-C8 for 24h	36.4	49.8	8.5	3.8

**Table 3.4** Mechanical properties of original and modified PVDF membranes

Membrane	Tensile Modulus (MPa)	Tensile stress (MPa)	Strain at break (%)
Original PVDF	50.5±2.1	2.81±0.05	219.4±10.2
Alkaline treatment: 7.5M NaOH at 60°C for 3h			
0.01M AS-C16 for 24h	56.5±3.2	2.84±0.05	188.6±9.8
0.01M FAS-C6 for 24h	59.6±0.9	2.89±0.06	191.9±10.1
0.01M FAS-C8 for 24h	58.8±5.8	3.01±0.07	180.6±8.5
0.02M FAS-C8 for 24h	56.3±2.3	2.82±0.06	208±11.2

### 3.3.2 Comparison of chemical modification (CM) and plasma-activation modification (PAM)

The grafting conditions, 0.01M FAS-C8 for 24h, were selected to modify PVDF hollow fiber membrane in order to increase hydrophobicity. The two chemical modifications, which were 2M NaOH under room temperature for 12h and 7.5M NaOH at 60°C for 3h, namely PVDF-CM2 and PVDF-CM7.5, respectively, were selected to compare with original membrane and plasma-activation modification (PAM).

#### – Contact Angle

The contact angles of modified membrane treated by CM and PAM are summarized in Table 3.5. Overall, the contact angles of the modified membranes were increased. Both conditions of chemical modification (PVDF-CM2 and PVDF-CM7.5) resulted increased the contact angle but the PVDF-CM2 showed higher contact angle than PVDF-CM7.5. The contact angles of the modified by PVDF-CM2 and PVDF-PAM were 119.46° and 145.61°, respectively. Wongchitphimon *et al.* [127] found that the contact angle of modified membranes at 2.5M NaOH concentration was higher than 7.5M NaOH.

Additionally, Yang *et al.*[126] reported that the contact angles of the modified membrane using chemical and plasma modifications, compared to the original membranes were increased by 20% and 30%, respectively. The contact angles of

modified membrane by PVDF-CM2 and PVDF-PAM in this study were higher than the study of Yang *et al.* [126], which were 105° and 115° by plasma modification and chemical modification, respectively. The membranes of Yang *et al.* [126] were modified by plasma polymerization that the monomers were added in the plasma enhancement machine for 21ms; while the membranes in this study were immersed in FAS-C8 for 24h.

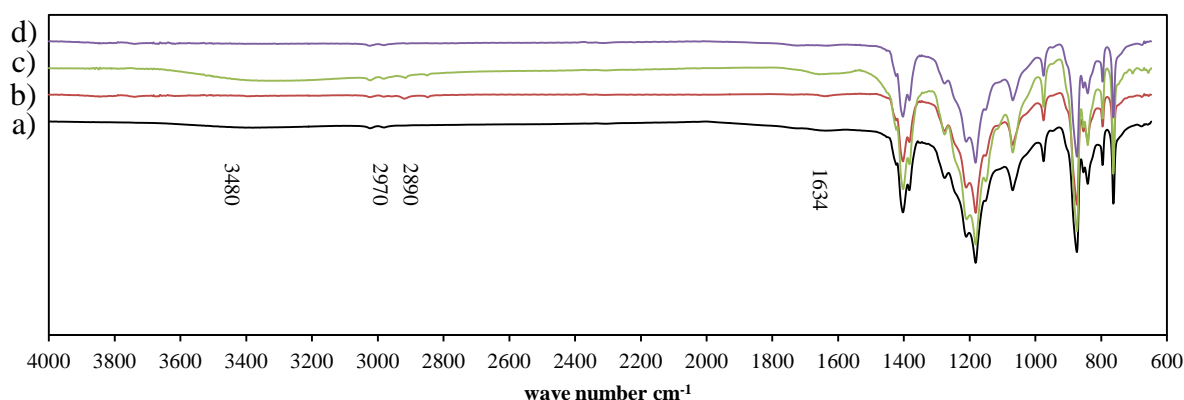
Hashim *et al.* [25] reported that the PVDF membrane was attacked by NaOH solution which led to the decrease in the melting temperature, melting enthalpy and crystallinity. Additionally, the decrease was accelerated by either a high temperature, or a concentrated NaOH solution. The degree of crystallinity of PVDF membranes was reduced after the NaOH treatment. In contrast, plasma activated modification showed the highest contact angle. PAM is the less damaging method of membrane modification compared to the alkaline treatment. Plasma only activates the surface of membrane to generate oxide or hydroxide groups without membrane destruction.

**Table 3.5** Contact angle and surface roughness of the original and the modified membranes by 0.01M FAS-C8 (24h) after chemical and plasma activations

<b>Membrane modification</b>	<b>Contact angle (°)</b>	<b>R<sub>rms</sub> (nm)</b>
Original membrane	68.91±0.89	31.13
2M NaOH at room temperature for 12h (PVDF-CM2)	119.46±1.64	49.67
7.5M NaOH at 60°C for 3h (PVDF-CM7.5)	100.20±2.97	48.77
Plasma-activated modification (PVDF-PAM)	145.61±3.11	53.65

### – FT-IR

In Figure 3.12, the FT-IR spectra of the original membrane and the modified membrane with organosilanes by PVDF-CM and PVDF-PAM are compared. There were three new peaks detected in the spectrum of Figure 3.12. The  $1634\text{ cm}^{-1}$  was assigned to the Si-O-Si bending. The  $2890\text{-}2970\text{ cm}^{-1}$  broad band of medium intensity was  $\text{CH}_2$  asymmetric stretching. The  $3480\text{ cm}^{-1}$  was OH group. For the PVDF-CM7.5, there were OH groups on the membrane surface since all OH groups may not react with silanol of the FAS molecules. Under the PVDF-PAM, membrane surfaces were activated by helium plasma activation, which followed by grafting with FAS-C8. Polar functional groups can be introduced on membrane surface after breaking C-C and C-H bonds [30]. The OH peak was undetected due to the complete chemical reaction between OH and silanol forms. As a result, the contact angles of membrane modified by PVDF-PAM were higher than by PVDF-CM.



\*The membranes were modified in 0.01M FAS-C8 for 24h

**Figure 3.12** FT-IR spectra of the PVDF membrane: a) original membrane; b) PVDF-CM2; c) PVDF-CM7.5; d) PVDF-PAM

### – XPS

The XPS analytical results were shown in Table 3.6. The fluorine (F) content on the surface of modified PVDF membranes increased compared with that of the original membranes, except the PVDF-CM7.5. This is caused by the elimination of H-F during the alkaline treatment due to high NaOH concentration in which F atoms were released from the PVDF membrane.

In case of PVDF-PAM, Si content was higher and the XPS results implied that there were organosilane molecules and the grafting was successful. The exposure of the He plasma treated membrane to atmosphere caused the attachment of oxygen molecules on the PVDF membranes resulting in the OH groups on the membrane surface. Wavhal and Fisher [90] and Liu *et al.* [77] reported that when the membrane was exposed to argon plasma, and then to air, there were the formations of oxide and peroxide. Figure 3.13 shows XPS spectra obtained from the PVDF membrane surface grafted with FAS-C8 solution. Three elemental compositions (Si 2s at 153 eV, Si 2p at 102.4–102.7 eV, C 1s at 284.8 eV and O 1s at 531.71-533.12eV) were clearly observed. The Si 2p, Si 2s, C 1s and O 1s components originated from the Si-CH<sub>3</sub>, Si-O, CH<sub>3</sub>-Si and O-Si groups, respectively. The Si 2p and Si 2s were from FAS-C8. Zheng *et al.* [122] reported that the Si-CH<sub>3</sub>, Si-O, CH<sub>3</sub>-Si and O-Si groups were found on the membrane surface modified by polydimethylsiloxane and polymethylsiloxane solution. Additionally, Na was found on the membrane surface as shown in Figure 3.13d due to the residue of NaOH in the cleaning step which due to high concentration of NaOH. The O 1s spectra in Figure 3.13b showed that the membranes were activated by helium plasma, and then were attacked by the oxygen in the atmosphere followed by the reaction with the silanol of FAS-C8, which is indicated by a stronger increase of the corresponding peak at 531.71 eV than the original membrane. In contrast, there was a significant increase in the intensity of O 1s in 7.5M NaOH treated membrane as shown in Figure 3.13d. This may be the results of oxygen in the ether group at 533.12 eV [90].



**Table 3.6** Changes of the chemical structure of membrane surface

Membrane modification	Atomic concentration (%)			
	C	F	O	Si
Original membrane	52.5	38.9	7.1	-
PVDF-CM2	43.99	48.98	4.85	1.07
PVDF-CM7.5	48.7	32.9	14.6	1.9
PVDF-PAM	39.44	46.96	10.21	2.7

\*The membranes were modified in 0.01M FAS-C8 for 24h

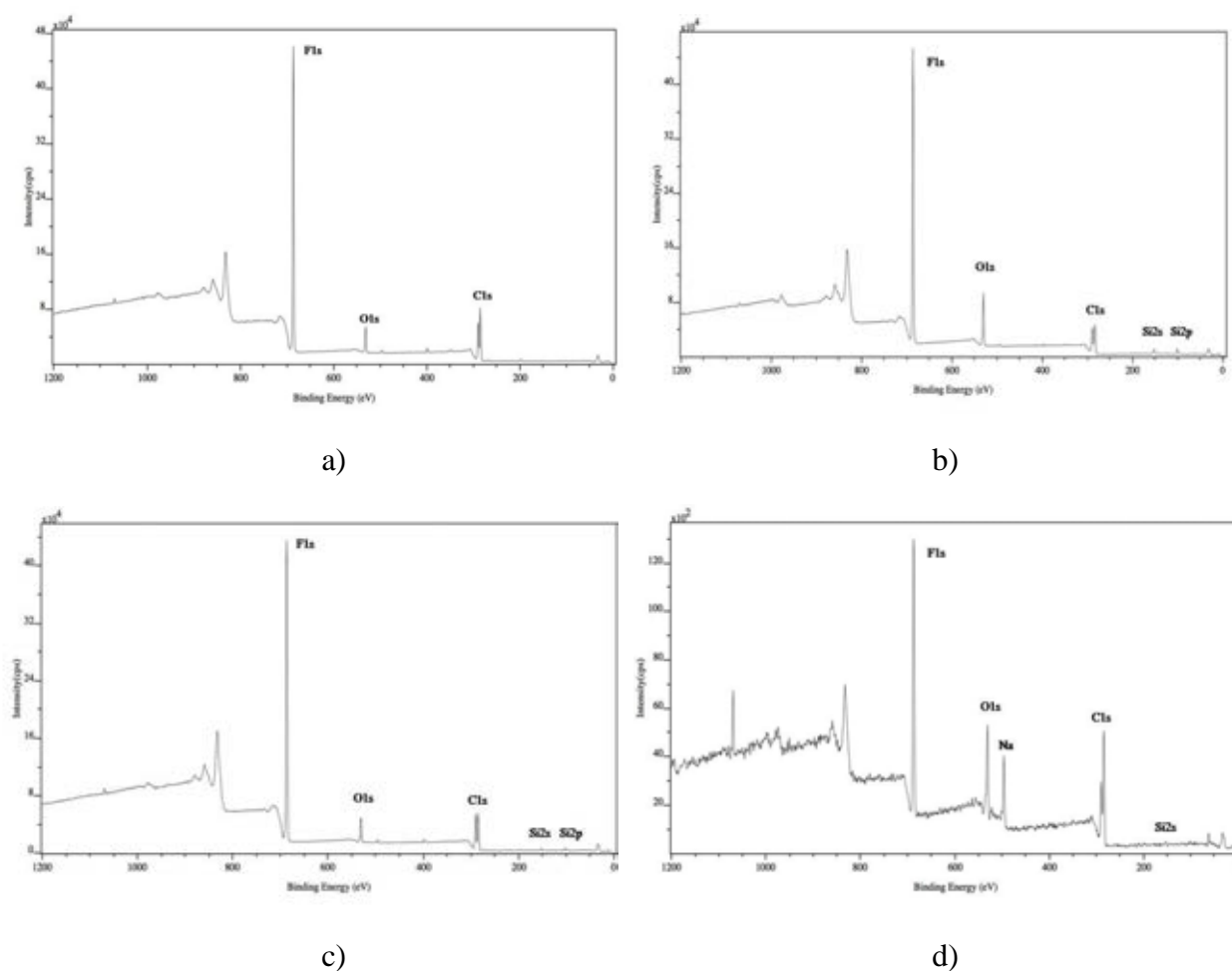


**Figure 3.13** XPS spectra: a) original membrane; b) PVDF-PAM; c) PVDF-CM2; d) PVDF-CM7.5

#### – Pore Size and Pore Size Distribution

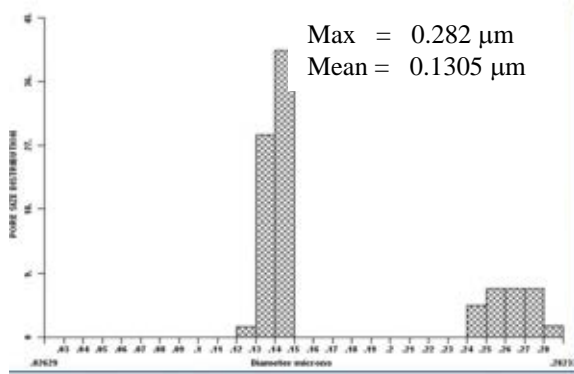
The membrane pore size and pore size distributions were illustrated in Figure 3.14. Compared to the original membrane which had a maximum pore size of 0.282  $\mu\text{m}$  and mean pore size of 0.1305  $\mu\text{m}$ , the pore size and pore size distribution after modification were in the range of 0.136-0.1396  $\mu\text{m}$  and 0.2361-0.3  $\mu\text{m}$ , respectively.

#### – SEM Images

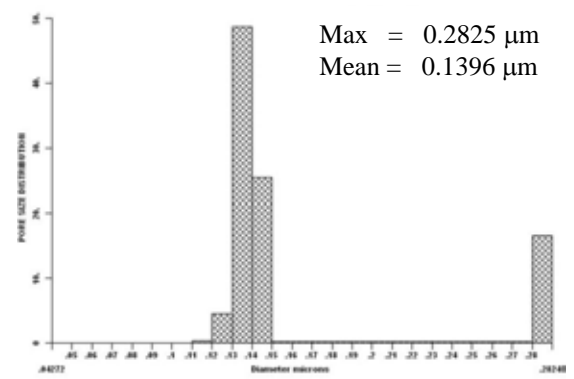
Figure 3.15 displays the morphology observations of the outer surface of the original and modified membranes. The outer surfaces of the modified membrane from both PVDF-CM2 and PVDF-PAM were not significantly different.

#### – AFM Images

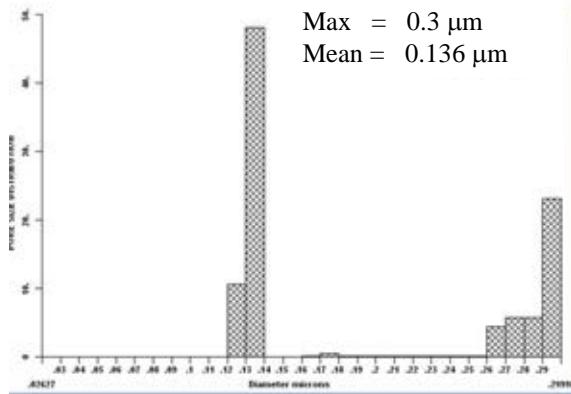
The effect of modification on surface roughness was shown in Figure 3.16 at a scan size 2  $\mu\text{m} \times 2 \mu\text{m}$ . The root-mean-squared roughness ( $R_{\text{rms}}$ ) was used to report the data in Table 3.5. The 3D images indicated that the surface modifications increased the surface roughness of membrane. The  $R_{\text{rms}}$  of membrane was increased from 31.13 nm for original membrane to 53.65 nm for modified membranes. The modified membrane surfaces were covered by many small peaks. The modified surfaces became rougher and revealed numerous bumps. The increase of surface roughness after modification can confirm the grafting of organosilane on the surface that also led to the increase in the contact angles. The roughness of the membrane surfaces increases with contact angles leading to high membrane hydrophobicity [111].



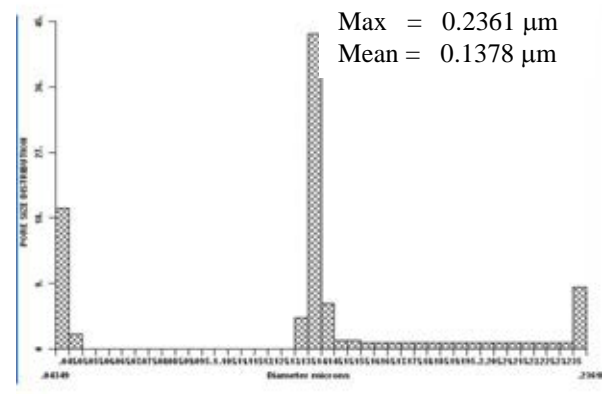
a)



b)

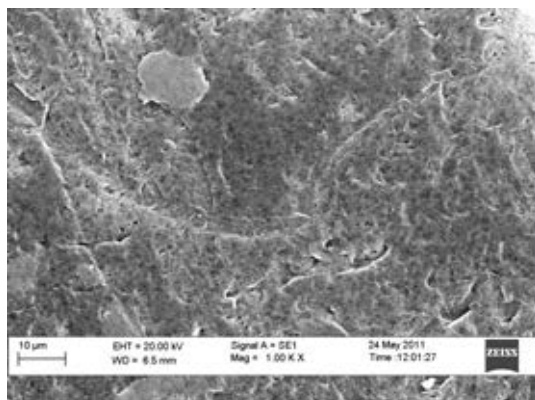


c)

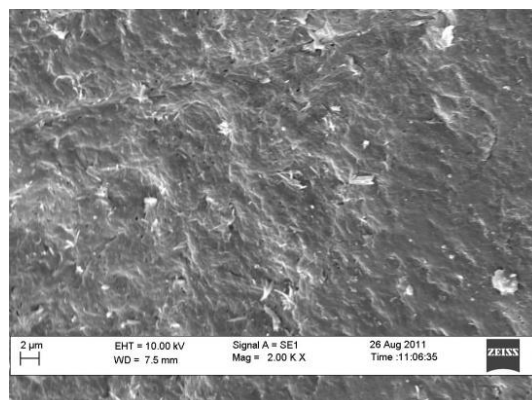


d)

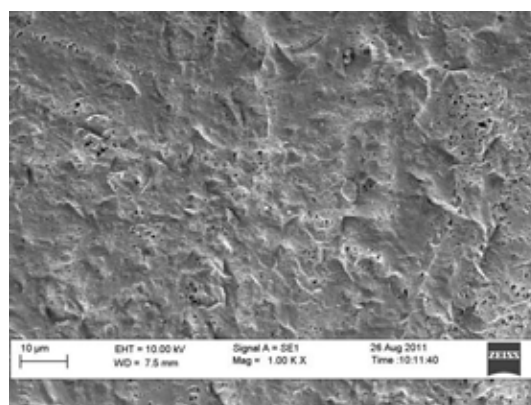
**Figure 3.14** Pore size and pore size distribution of the original and modified membranes: a) original membrane; b), PVDF-PAM; c) PVDF-CM2; d) PVDF-CM7.5



a)



b)



c)

**Figure 3.15** SEM images of the original membrane and modified membrane: a) original membrane; b) PVDF-CM2; d) PVDF-PAM

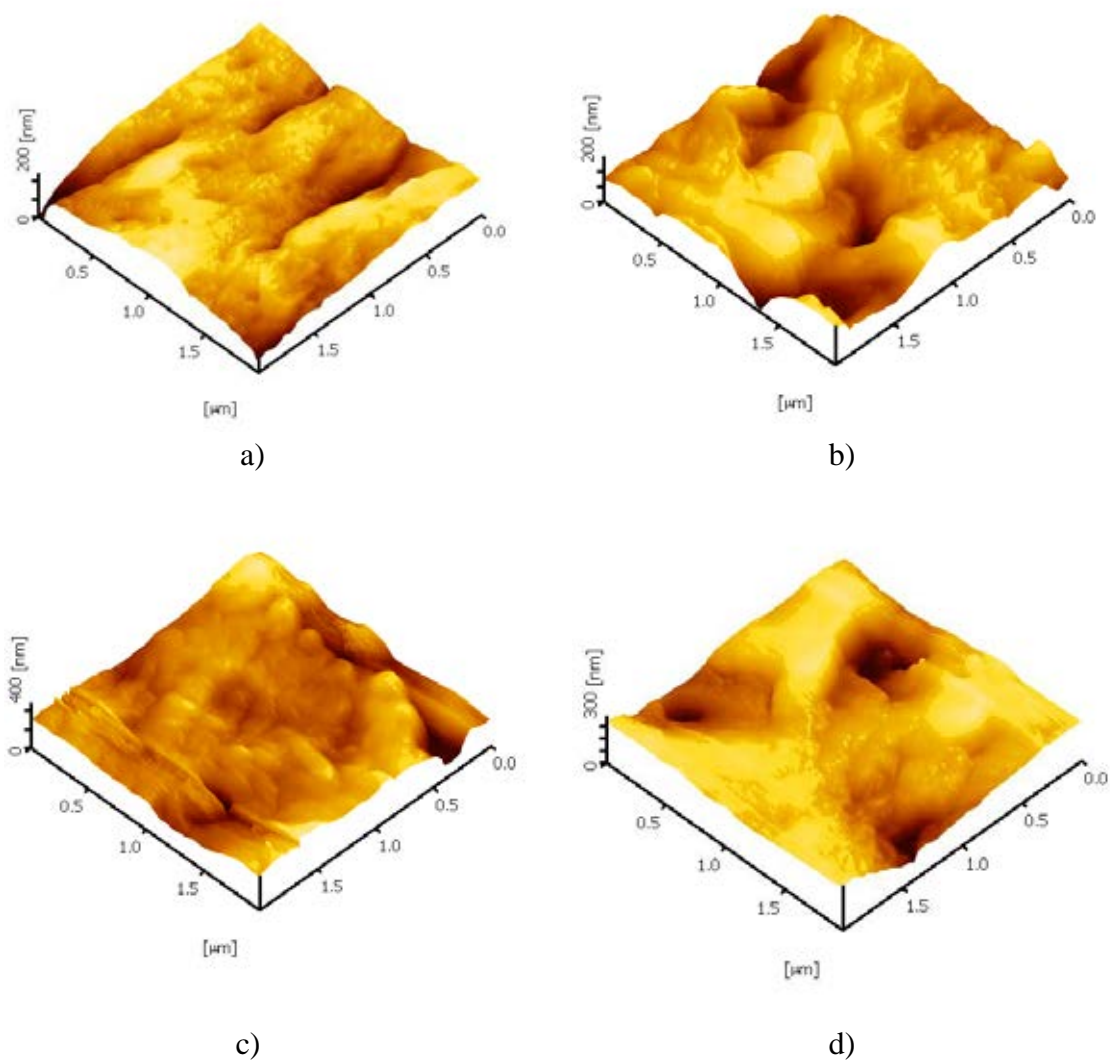


**Figure 3.16** AFM 3D images of membranes: a) original membrane; b) PVDF-CM2; c) PVDF-CM7.5; d) PVDF-PAM (all modified by 0.01M FAS-C8 (24h))

Table 3.7 shows the comparison of modified membrane's properties with reported ones by different groups in the literature. The contact angle of modified membrane by the condition of PVDF-CM7.5 was  $100.2^\circ$ , which was lower than those of Zheng *et al.* [89] and Yang *et al.* [126], which were in range of  $105^\circ$ - $135^\circ$ . Zheng *et al.* [89] used mixed organosilanes (DDS and MTS) which were more hydrophobic. Yang *et al.* [126] performed the alkaline treatment at lower NaOH concentration (2M), while

Rahbari-Sisakht *et al.* [94] used surface modifying macromolecule which was also more hydrophobic.

However, both conditions of PVDF-CM2 and PVDF-PAM in the current work resulted in an increased contact angle higher than PVDF-CM7.5. The contact angles of the modified by PVDF-CM2 and PVDF-PAM were 119.46° and 145.61°, respectively which were higher than those of Zheng *et al.* [89] and Yang *et al.* [126].

Moreover, the modified membranes in this study presented good performance of mechanical strength in term of tensile modulus and tensile strength which are similar to the study of Zheng *et al.* [89]. However, the strain at break of membrane in this study was decreased while the modified membranes of Yang *et al.* [126] were increased. It is worthy to mention that the mean pore sizes of modified membranes in this study show an insignificant change, whereas the modified membrane of Yang *et al.* [126] and Rahbari-Sisakht *et al.* [94] became bigger, which may play an adverse impact on the membrane performance.

### **3.3.3 Stability test of modified PVDF membranes for CO<sub>2</sub> absorption**

The modified membranes were applied to study that used as membrane contactor for CO<sub>2</sub> absorption. The CO<sub>2</sub> absorption flux of original and modified membranes is shown in Figure 3.17. The CO<sub>2</sub> flux of the original membranes decreased from  $7.7 \times 10^{-3}$  to  $3.1 \times 10^{-3}$  mol/m<sup>2</sup>.s, which is 40.3% of the initial value during the 15 days operation. In the case of modified membrane by PVDF-PAM and PVDF-CM2, the CO<sub>2</sub> fluxes were stable during 15 days operation. The CO<sub>2</sub> flux of PVDF-PAM was higher than PVDF-CM2. This is because the modified membranes were more hydrophobic than the original membranes in term of contact angle; the modified membranes can reduce the membrane wetting. Therefore, the grafted hydrophobic layer (the chain side of organosilane) can resist the water penetration to the membrane. According to the results, the membrane showed a stable performance for 15 days, suggesting that the reactions between membrane and organosilane were relatively stable within this period of time.

**Table 3.7** Comparison of various PVDF hydrophobic membrane modifications

Reference	Membrane	Treatment condition	Contact angle (°)	Mechanical properties			Mean pore size
				Tensile Modulus	Tensile stress	Strain at break	
[89]	PVDF film	7.5M NaOH at 60°C for 3h, 20%DDS/MTS for 30 min	157	-	-	-	-
[94]	PVDF hollow fiber	Surface modifying macromolecule	92±1.25	-	-	-	Bigger
[126]	PVDF hollow fiber	(1) 1-2M NaOH for 12h, grafting with perfluoropolyether with ethoxysilane	115	Increase	-	Increase	Bigger
		(2) polymerization with 1H, 1H, 2H, 2H-perfluorodecyl acrylate	105	Decrease	-	Increase	Bigger
<b>Current work</b>	PVDF hollow fiber	(1) 7.5M NaOH for 3h at 60°C, 0.01M FAS-C8 for 24h (CM7.5)	100.2 ±2.97	Increase	Increase	Decrease	No significant change

---

(2) 2M NaOH for 12h, 0.01M FAS-C8 for 24h (CM2)	119.46± 1.64	Increase	Increase	Decrease	No significant change
(3) Helium plasma activation, 0.01M FAS-C8 for 24h (PAM)	145.61± 3.11	Increase	Increase	Decrease	No significant change

---

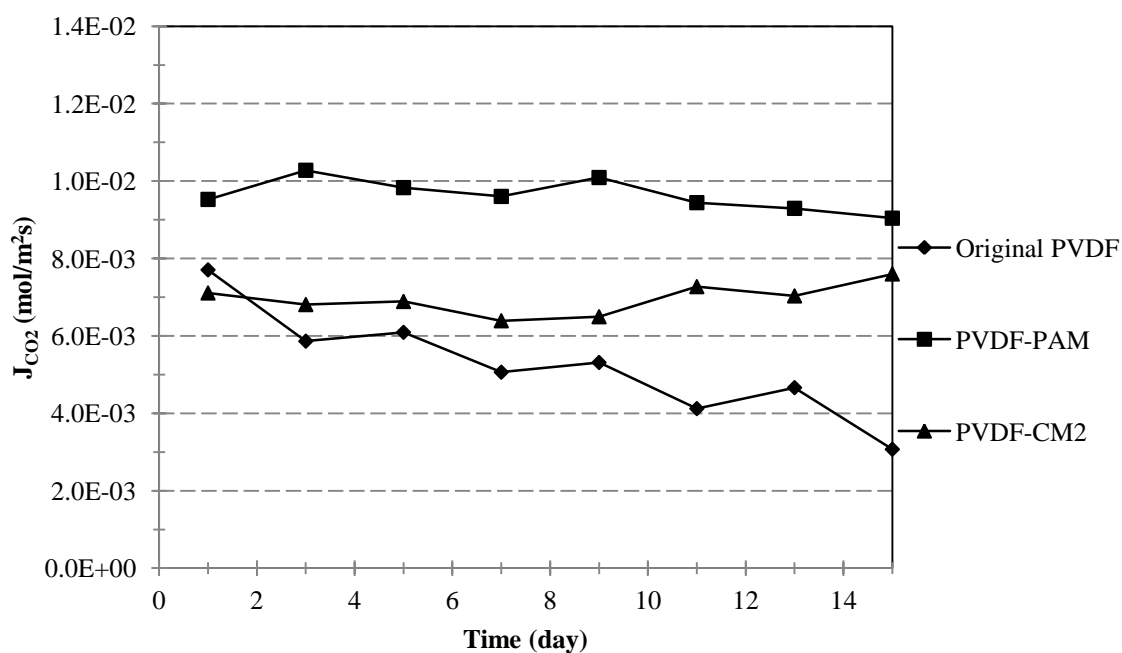


**Figure 3.17** Membrane performances for CO<sub>2</sub> absorption over 15 days of operation



### 3.4 Conclusions

The modification conditions of this study by chemical and plasma-activated modifications were investigated by varying the modification parameters including NaOH and organosilane concentrations, types of organosilanes and grafting time. The original and modified membranes were characterized for FT-IR, XPS, contact angle, SEM and AFM images, pore size and pore size distribution, and mechanical strength. The results showed that the contact angle of original membrane ( $68.91^\circ$ ) were decreased after alkaline treatment from  $44^\circ$  to  $31^\circ$  with increasing NaOH concentration from 2.5M to 7.5M at  $60^\circ\text{C}$  for 3h. For the chemical modification, the contact angle of NaOH treated membranes was increased to  $100.2^\circ$  after modification with 0.01M FAS-C8 for 24h. Additionally, the contact angles increased with grafting time and number of functional groups of organosilanes. A need-like structure was observed on membrane surface after modification while there was no significant change in pore size and pore size distribution. Moreover, FT-IR and XPS data showed the peak and chemical composition of Si. The mechanical strength of membranes was also improved after modification. In contrast, the contact angle of the modified membrane was increased to  $119.46^\circ$  after decreasing NaOH concentration from 7.5M to 2M and immersing the membrane for 12h under room condition, followed by grafting of 0.01M of FAS-C8 for 24h.

The comparison between chemical modification and helium plasma activation followed by grafting 0.01M FAS-C8 for 24h showed that the contact angle of modified membrane under helium plasma activation followed by grafting 0.01M FAS-C8 for 24h ( $145.61^\circ$ ) was higher than the 2M NaOH followed by grafting 0.01M FAS-C8 for 24h ( $119.46$ ). The mechanical strength and surface roughness of modified membranes were also enhanced while other physical properties did not change.

In the long-term performance, the modified PVDF membranes were more stable and durable than the original PVDF membranes. This result clearly indicated the feasibility of improving the membrane performance in membrane contactor by surface modification.

## CHAPTER IV

### THE STABILITY OF MODIFIED MEMBRANES EXPOSED TO OZONE

#### 4.1 Introduction

The membrane is a major component in the membrane contactor. Under the extreme oxidizing agent as ozonation oxidation in membrane contactor for wastewater treatment, the formation of hydroxyl radicals and reactive ozone which aim to degrade the pollutants may change the properties of membranes. PTFE and PVDF membranes are widely used for membrane contacting process, which are hydrophobic membranes, because the main chains consist the chemically strong bonding between carbon and fluorine. Mori *et al.* [11] reported that the O<sub>3</sub> resistance of PTFE membranes was higher than that of PVDF and PE membranes. Bamperng *et al.* [34] presented the changes in SEM image of PVDF membrane after long-term testing by ozonation with membrane contactor. Glater *et al.* [106] found that the membranes were damaged during ozone exposure by decrease of salt rejection in reverse osmosis. Recently, the degradation of polymeric membranes by sodium hypochlorite solution (NaOCl) as the cleaning solution and oxidizing agent have been widely studied in the literature [35-39], little is known on the changes on chemical and physical properties of membranes by ozone.

The results in CHAPTER 3 showed that the hollow fiber PVDF membranes activated by 2M NaOH, at 60°C for 12h and by helium plasma, followed by grafting with 0.01M FAS-C8 for 24h (referred to as PVDF-CM2, and PVDF-PAM, respectively) exhibited increased hydrophobicity. The CO<sub>2</sub> absorption fluxes were also more stable than original membranes. Kukuzaki *et al.* [40] reported that the modified Shirasu porous glass (SPG) membranes by an organosilane compound not only increased the hydrophobicity but also resisted the ozone oxidation. Therefore, examination of changes of membrane of membrane hydrophobicity and ozone resistance after ozone

exposure would give useful results for the application of membrane contactor for ozonation process.

In this chapter, we performed a systematic experiment to investigate the effect of ozone concentration and time on the membrane structure and properties using the modified membranes (PVDF-CM2 and PVDF-PAM), in comparison with the original PVDF and commercial PTFE hollow fiber membranes. Detailed characterizations were performed for all membranes before and after ozone contact.

## **4.2 Methodology**

### **4.2.1 Materials and chemicals**

The PVDF membranes selected for in this study were PVDF-CM2 and PVDF-PAM which was obtained from the CHAPTER 3. The PTFE hollow fiber membrane was supplied by Markel Corporation (U.S.A). The specifications of the membranes are listed in Table 4.1.

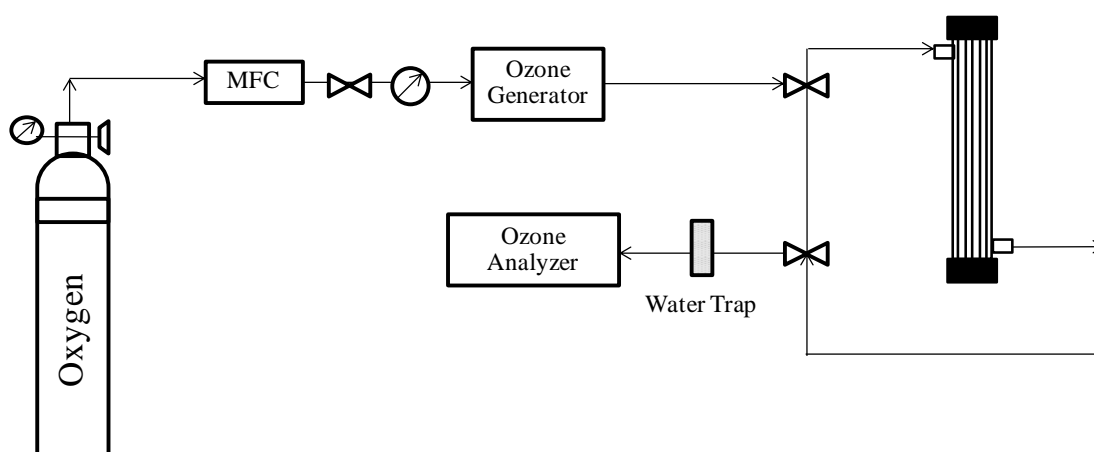
### **4.2.2 Methods**

#### **– The stability test of membranes exposed to ozone**

The experimental setup is illustrated in Figure 4.1. The ozone was produced with ozone generator (Model: VGsa 010, Siamese twins Ltd., Thailand) using pure oxygen. The ozone concentration in the gas phase was measured by the ozone analyzer (OLD/DL-5, Canada). The membrane module was prepared using 5 hollow fibers assembled in a glass tube with an inner diameter of 10 mm and an effective length of 25 cm. The fiber ends were completely sealed with the epoxy. The ozone gas at a fixed concentration (0-60 ppm) was continuously fed in the shell side or on the outer surface of the fibers for a fixed period of time (0-36h).

**Table 4.1** Specifications of the hollow fiber membranes

Membranes	Original PVDF	PVDF- CM2	PVDF- PAM	PTFE
Fiber o.d. (mm)	1.16	1.16	1.16	2
Fiber i.d. (mm)	0.8	0.8	0.8	1.6
Membrane pore size ( $\mu\text{m}$ )	0.13	0.14	0.14	0.089
Membrane porosity (%)	85	83	80	50
Contact angle ( $^{\circ}$ )	68	119	145	105

**Figure 4.1** Schematic diagram of the stability test of membranes exposed to ozone

After testing, the membranes were taken out of the modules and then were characterized for the contact angles using a tensiometer (DCAT11 Dataphysics, Germany). A lumen of fiber was glued by epoxy to measure only the outer surface contact angle. The sample was immersed into Milli-Q water and the contact angle was calculated from the wetting force based on the Wilhelmy method. The membrane morphology was observed by Field Emission Scanning Electron Microscopy (FE-SEM) (JSM-7001F). The surface infrared spectra were recorded using an IR Prestige-21 Fourier transform infrared (FTIR) spectrophotometer (SHIMADZU) at a resolution of  $4\text{ cm}^{-1}$  in attenuated total reflection (ATR) mode.

The pore sizes of the fibers were measured using a capillary flow porometer (Porous Materials Inc., model CFP-1500A). The pores of the samples were filled with the Galwick<sup>®</sup> solution as the wetting liquid. The mechanical strength of the fibers was measured using a Zwick/Roell BT1-FR0.5TN.D14 testing machine at a constant elongation under room temperature.

### **4.3 Results and discussion**

#### **4.3.1 Change of membrane properties and structures**

The contact angles of PVDF membranes exposed to ozone from 0 to 36h for 0-60 ppm are as shown in Figure 4.2. The contact angle of original PVDF membranes increased approximately 26% after 2h of ozone treatment and remained relatively constant afterwards, as illustrated in Figure 2a. It is possible that some additive groups on the membrane surface used by the manufacturer to make the membranes were removed, resulting in the observed increase of contact angle [37]. The result of FT-IR spectra to be discussed. In contrast, Figure 2b and c present the contact angles of the PVDF-CM2 and PVDF-PAM membranes which decreased approximately 10% and 20%, respectively, after 2h of ozone treatment, followed by insignificant change with time and ozone concentrations. Based on this result, the contact angles of all ozone treated membranes did not change significantly after 20 ppm ozone concentration and 2h ozonation time. Levitsky *et al.* [129] and Wang *et al.* [36] reported that the contact angles of PVDF membranes decreased with time after cleaning by NaOCl solution (hypochlorite), even though the oxidation potential of hypochlorite ( $E^0=1.48\text{V}$ ) is

lower than that of ozone ( $E^0=2.08V$ ) [70, 130, 131]. On the contrary, the contact angles of original and PTFE membranes, for 60 ppm ozone, 36h, were  $108^\circ\pm 0.86$  and  $108^\circ\pm 1.8$ , respectively, or were rather constant. This is because the PTFE membrane consists of the strong carbon-fluorine (C-F) bonds which contribute to excellent chemical resistance including ozone oxidation. Basically, the role of fluorine and C-F bond in achieving a high degree of solvent resistance and stability is well known in organic polymers. Although the contact angles of PVDF-PAM membrane decreased, the PVDF-PAM membrane still showed the higher hydrophobicity than the original PVDF and PTFE membranes in term of contact angle due to surface modification using FAS-C8, resulting in the changes of intramolecular bonding with C-F and layer during grafting.

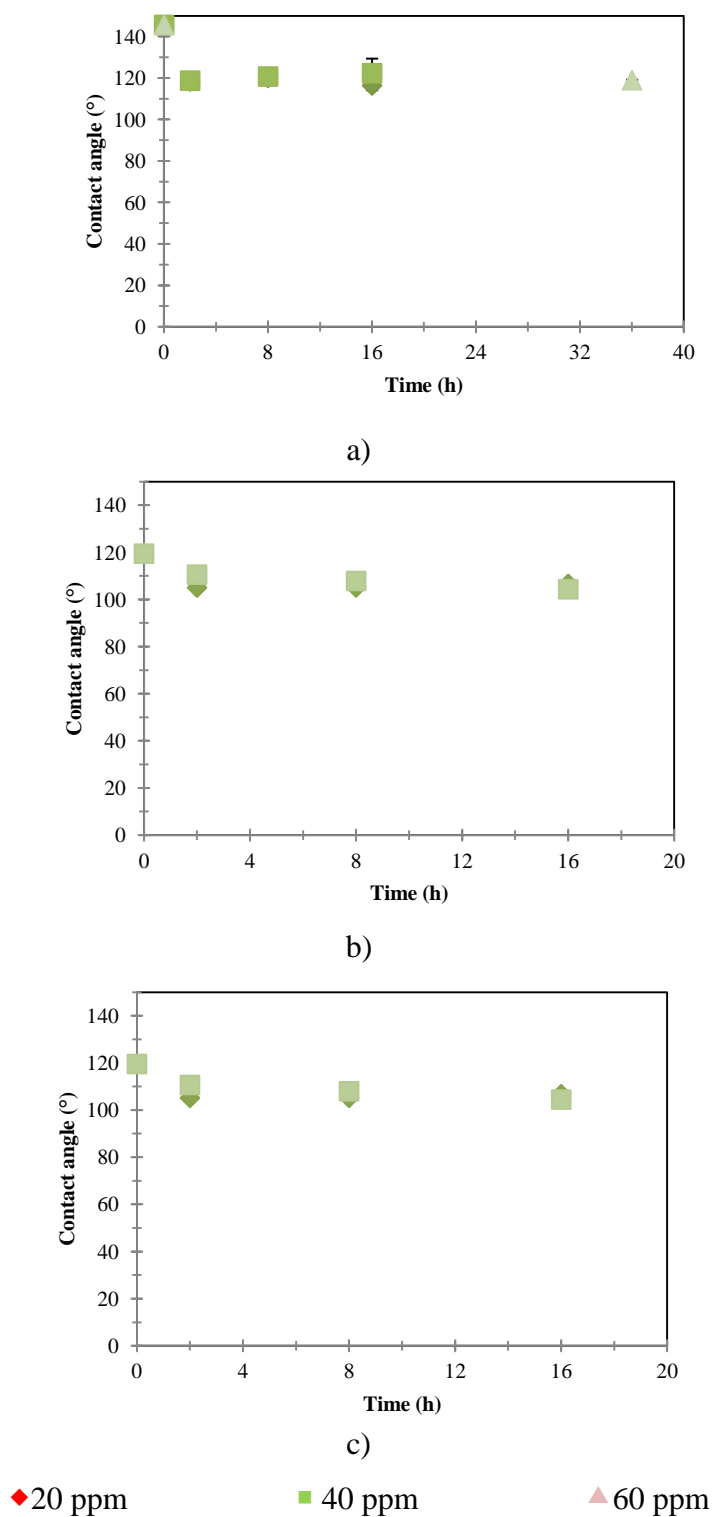


**Figure 4.2** Contact angles of PVDF membranes after exposing to ozone: a) original; b) PVDF-PAM; c) PVDF-CM2

The changes in the chemical functionality of membrane surface after exposing to ozone were confirmed by observing the changes in the position of hydroxyl and carbonyl bands. Figure 4.3 shows the FT-IR spectra of PVDF and PTFE membranes exposed to ozone under ozone concentration of 60 ppm for 36h. In the commercial PVDF membrane manufacturing process, the solvent for the post-treatment (e.g. water, isopropanol), is used to wash membranes to remove the impurity from the membranes that may contain the OH group on the membrane surface. As shown in Figure 4.3, the functional groups of original PVDF membrane presented a very strong band at  $3313\text{ cm}^{-1}$ . Original PVDF membranes exposed to ozone did not exhibit a broad band from  $3300\text{ cm}^{-1}$  to  $3400\text{ cm}^{-1}$  which may be attributed to the stretching hydroxyl group (-OH), but presented a broad band from  $2850\text{ cm}^{-1}$  to  $3000\text{ cm}^{-1}$  which may be attributed to the stretching alkyl groups (C-H) after ozone oxidation of hydroxyl groups. As -OH groups were destroyed, the membranes became more hydrophobic, as seen by the increase in the contact angle in Figure 4.2a. This is similar to the study of Puspitasari *et al.* [37] that the -OH groups were destroyed after cleaning membrane with NaOCl solution. Comparing the spectra of unexposed and ozone exposed PVDF-PAM at 60 ppm for 36h, the main difference was the strong broad band at  $1644\text{ cm}^{-1}$  and  $1740\text{ cm}^{-1}$  during the ozone exposure. These two bands are characteristics for the stretching carbonyl groups (C=O). The C=O groups most likely impart the hydrophilic character to the PVDF membranes. As C=O groups were found, the membrane became more hydrophilic, as seen by the decrease in contact angle in Figure 4.2b. These observations suggested that the modified PVDF membrane using FAS-C8 as a modifying agent may be degraded by ozone oxidation. In addition, the unsaturated bond after modification may be effectively degraded on the membrane surface by ozone oxidation because ozone is highly powerful to modify the hydrophilicity and can form free oxygen groups on the membrane surface. Figure 4.4 illustrates the bond energy of modified PVDF membranes. The bond energies of C-F, C-H and Si-O are higher than that of Si-C and C-C [132, 133]. As the result, part of Si-C bond may be oxidized and C-C bond may be changed to C=O or C-O bond by ozone oxidation. In contrast, the FT-IR spectra of PTFE membranes exposed to ozone showed no significant change. This result indicated that the PTFE membranes were



not oxidized by ozone due to the high bond energy of C-F which is resistant to ozone oxidation.

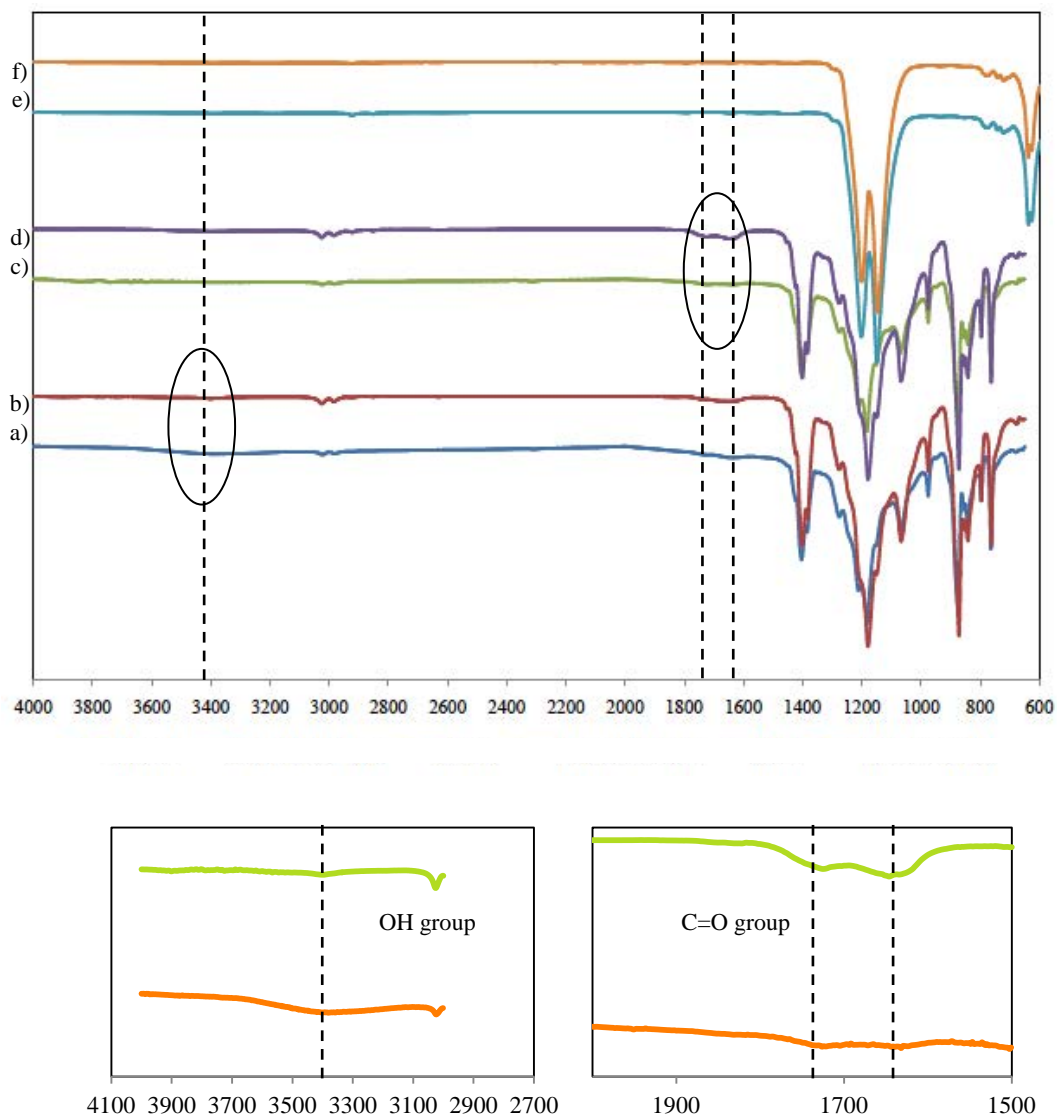


**Figure 4.3** FT-IR spectra of membranes before and after exposing to ozone, 60 ppm for 60h: a) original PVDF; b) O<sub>3</sub>-original PVDF; c) PVDF-PAM; d) O<sub>3</sub>-PVDF-PAM membranes; e) PTFE; f) O<sub>3</sub>-PTFE membrane





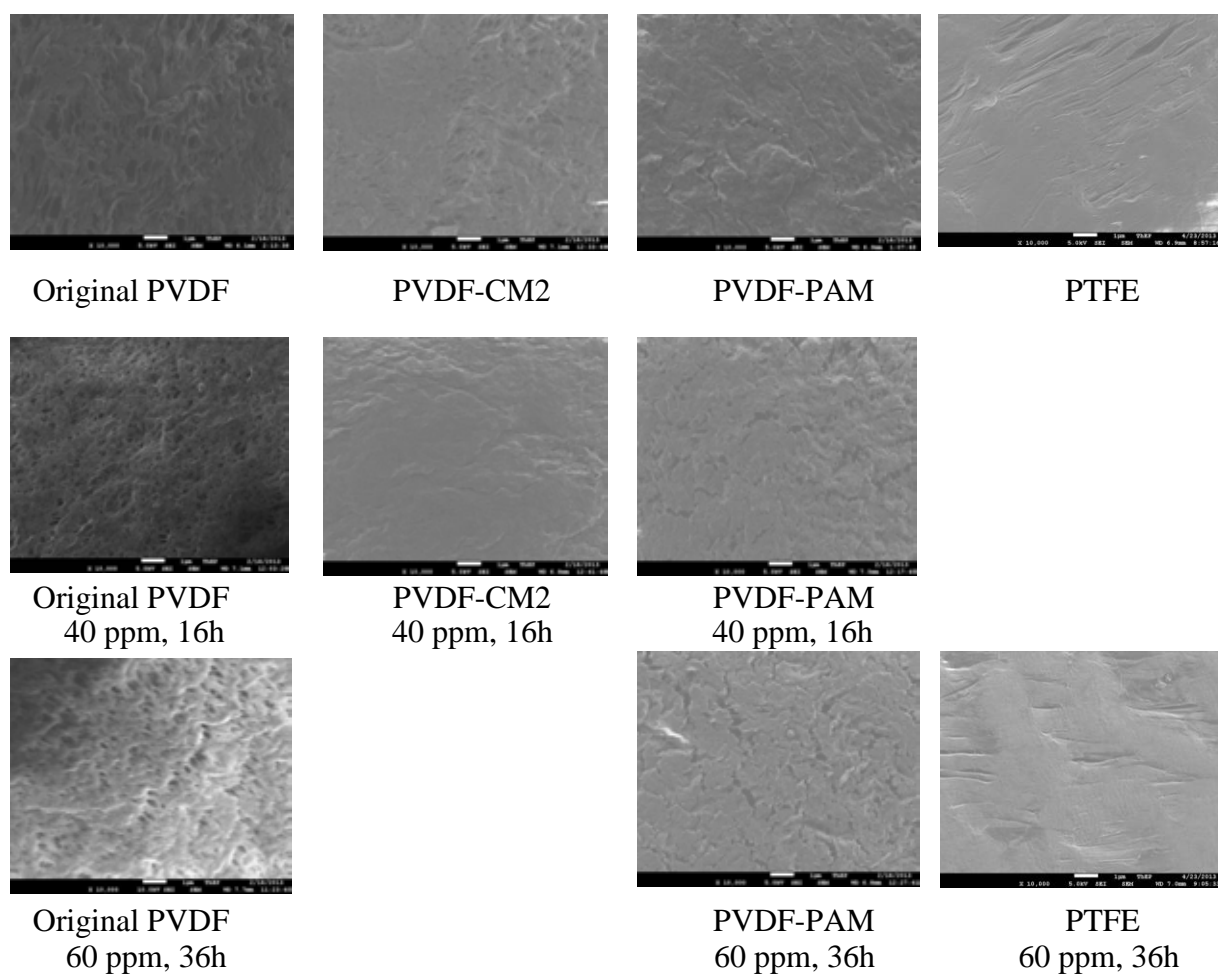


**Figure 4.6** FE-SEM images of membranes before and after exposing to ozone

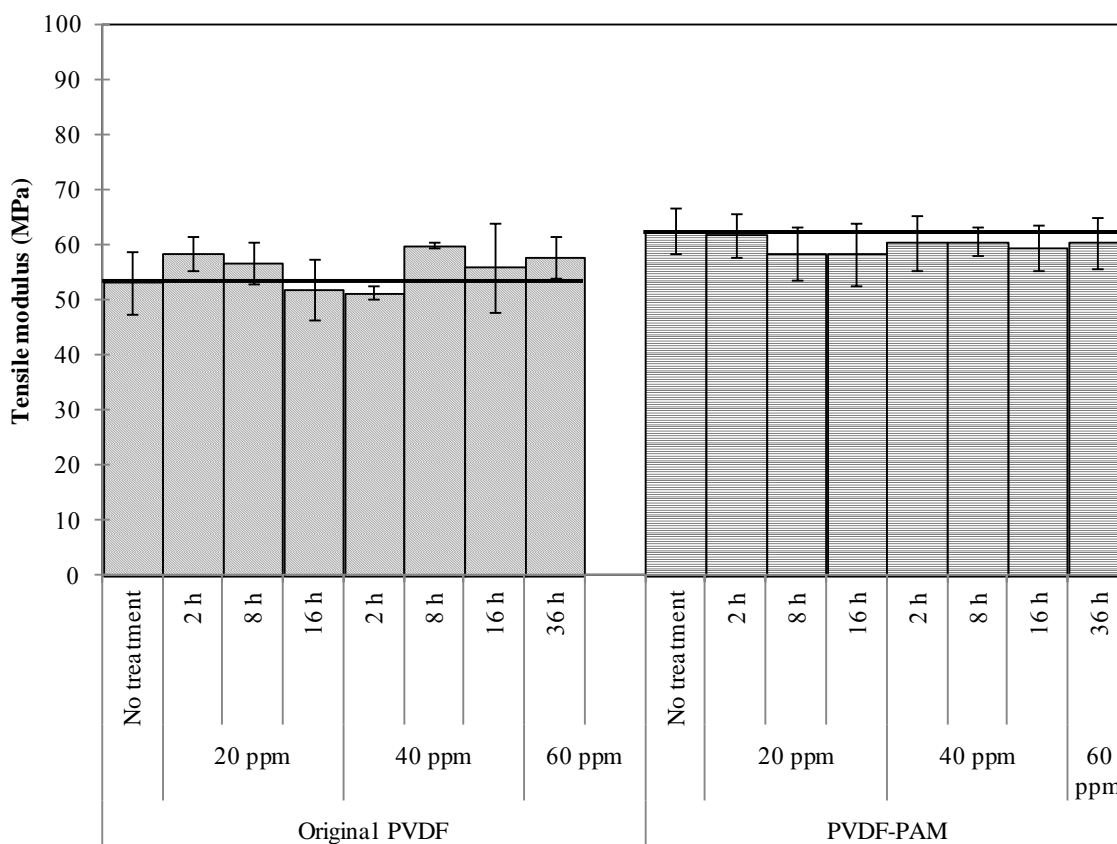


**Figure 4.7** Tensile modulus of PVDF membranes after exposing to ozone

#### 4.4 Conclusions

An investigation of the stability and durability of PVDF hollow fiber membranes exposed to ozone has been presented. The original PVDF membrane, the modified PVDF-CM2 and PVDF-PAM membranes, and PTFE membrane were selected to study. According to the stability test of membranes exposed to ozone at different ozone concentrations and durations, the results showed that the contact angles of the PVDF-PAM and PVDF-CM2 membranes decreased at the initial period of ozone exposure (2h, 20 ppm) and remained constant afterwards. In contrast, the contact angles of original membranes increased. The reduction of hydroxyl peak and presence of carbonyl peak were confirmed by FT-IR. The mean pore size and outer surface of membranes exposed to ozone showed insignificant change but the tensile modulus of PVDF-PAM membranes exhibited more stability than that of original PVDF and PVDF-CM2 membranes. The properties of PTFE membranes showed insignificant

change after ozone exposure. The modified PVDF membrane showed the increase in hydrophobicity, the membrane stability, and durability towards ozone. The stability of modified PVDF membranes was due to the enhancement of C-F bonding of FAS-C8, which resisted the ozone oxidation.

## **CHAPTER V**

### **APPLICATION OF MODIFIED MEMBRANE IN MEMBRANE CONTACTOR FOR DYE SOLUTION TREATMENT**

#### **5.1 Introduction**

Wastewater from the textile industries is the significant source of environmental pollution. Color is usually the first contaminant to be recognized in textile wastewaters. The high strength colored effluents are visual eyesore, cause aesthetic pollution, eutrophication and perturbations in aquatic life which have been found to be toxic and carcinogenic to aquatic environments [2, 45, 134-136]. The ozonation process has been recommended in recent years as a potential alternative method for decolorization. Ozone specifically attacks the conjugated chains that show color to the dye molecule. During the ozonation process, ozone molecule is selective and attacks preferentially the unsaturated bonds of the chromophores, as a result, the color is removed [41, 70, 99, 136, 137]. The process of ozonation can take place in two ways which are directly by ozone molecule itself or indirectly by changing to hydroxyl radicals [41, 70, 99, 136, 137]. The conventional methods of gas-liquid contact for the ozonation of wastewater, such as bubble columns and packed beds, are limited by low mass transfer of ozone into the aqueous phase [9]. In addition, the efficiency of ozone mass transfer depends on the hydrodynamic behavior of the fluid, solubility ratio, and mass transfer coefficient [71]. The effectiveness of ozonation can be increased by increasing surface area of ozone through the generation of smaller bubbles [5, 6]. However, the drawbacks of the bubble column are flooding, uploading, emulsion, and foaming [7, 8]. These problems can be solved by using a gas-liquid membrane contactor [8, 13], a method employing a combination of membrane with ozonation which has been developed for the effective absorption of CO<sub>2</sub> by liquid absorbents [8].

Membrane contactors are systems in which hydrophobic porous membranes are used to promote gas-liquid or liquid-liquid mass transfer without dispersion of one phase

into the other [9]. The advantages of the membrane contactors over conventional contactors are given by the fact that contacting membrane provides much higher interfacial area [13, 138], the hydrodynamic decoupling of the phases [10], and requires small areas [11, 13]. Also, increasing mass transfer coefficients results in higher gas transfer rate and a smaller process volume for installation [12]. Several studies have been conducted on use of ozonation by membrane contactor for oxidation of organic compounds such as humic substance, phenol, acrylonitrile, nitrobenzene, dyes [7, 10, 12, 13]. However, there has been a limited study on the application of the membrane contactor for treatment of dye wastewater.

Recently, several studies have shown success of using modified hydrophobic membranes in membrane contactor applications. Wongchitphimon *et al.* [97] reported that the modified PVDF-HFP had a higher CO<sub>2</sub> absorption flux than the original membranes due to higher hydrophobicity. Sisakht *et al.* [95] found that the CO<sub>2</sub> fluxes of modified polysulfone membranes by surface modifying macromolecule were higher than those of unmodified membranes. Razmjou *et al.* [139] modified PVDF membranes via coating TiO<sub>2</sub> on the membrane surface followed by perflorododecyltrichorosilane for membrane distillation. The results showed that the permeate conductivity, using the modified membranes, was stable whereas, it was sharply increased for the original membrane. It can be concluded that the improvement of membrane hydrophobicity is effective for the application of membrane contactor for CO<sub>2</sub> absorption and membrane distillation process.

The results in CHAPTERS 3 and 4 showed that the contact angle, CO<sub>2</sub> absorption flux and membrane stability after ozone contact of modified PVDF-PAM membrane was higher than that of original PVDF and PVDF-CM2 membranes. Therefore, in this chapter, the PVDF-PAM membranes fabricated as hollow fiber modules were applied for treatment of dye solutions by ozonation to compare ozone flux, COD and TOC removals, including BOD<sub>5</sub>/COD, by-products and pH changes during ozonation, in comparison with original PVDF and PTFE membranes.



## 5.2 METHODOLOGY

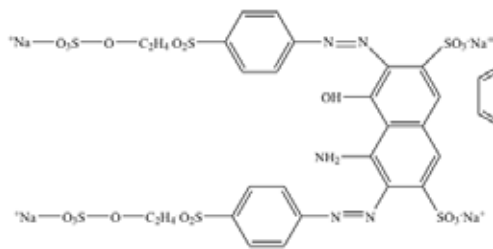
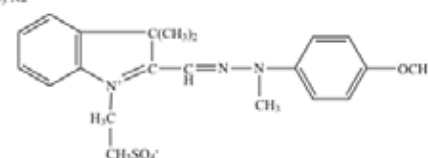
### 5.2.1 Materials and chemicals

The membranes selected for in this study were original PVDF, PVDF-PAM and PTFE membranes as reported in Table 4.1, in the CHAPTER 4. Dyes, Reactive Black 5 (RB5) and Basic Yellow 28 (BY28), were kindly provided by DyStar Thai Ltd. The properties of RB5 and BY28 are shown in Table 5.2.

**Table 5.1 Specifications of hollow fiber membranes and modules**

Properties	Original PVDF	PVDF- CM2	PVDF- PAM	PTFE
<b>Membrane</b>				
Fiber o.d. (mm)	1.16	1.16	1.16	2.0
Fiber i.d. (mm)	0.8	0.8	0.8	1.6
Membrane pore size ( $\mu\text{m}$ )	0.13	0.14	0.14	0.089
Membrane porosity (%)	85	83	80	50
Number of fibers	30	30	30	24
Effective contact area ( $\text{m}^2$ )	0.01885	0.01885	0.01885	0.03137
Contact angle ( $^\circ$ )	68	119	145	105
<b>Module</b>				
Module o.d. (mm)	12	12	12	26
Module i.d. (mm)	10	10	10	38
Effective module length (mm)	250	250	250	260

**Table 5.2** Dyes properties used in this study

Dye	Reactive Black 5	Basic Yellow 28
Code	RB5	BY28
Chemical structure		
Molecular weight (g/mol)	991	433
$\lambda_{\max}$ (nm)	600	450

### 5.2.2 Methods

#### – The long-term ozone fluxes of PVDF and PTFE membranes

In order to study the deterioration of ozone flux; possibly due to membrane wetting and ozone oxidation, the long-term experiments were conducted. The experimental setup is schematically shown in Figure 5.1. The 30 hollow fibers of original PVDF and PVDF-PAM, and 24 hollow fibers of PTFE membranes were potted in the glass modules as presented in Figure 5.2. The ozone gas at fixed concentration (40 mg/L) was continuously fed in the shell side with the velocity of 0.12 m/s, while 100 mg/L of RB5 dye feed solution was pumped through the lumen side of the fibers using peristaltic pump (L/S<sup>®</sup> Easyload<sup>®</sup> II, Masterflex) in a counter current mode. The RB5 dye solution was fed as a single pass, shown by the solid line (Mode I) in Figure 5.1, with the velocity of 0.46 m/s. The outlet ozone concentrations in the gas phase were measured every 1h (after a steady state was reached) for 20h using the ozone analyzer. The ozone flux ( $J_{O_3}$ ) can be determined by the following equation:

$$J_{O_3} = \frac{Q_{O_3}(C_{O_3,in} - C_{O_3,out})}{A} \quad 5.1$$

Where  $Q_{O_3}$  is the ozone flow rate.  $C_{O_3,in}$  and  $C_{O_3,out}$  are the ozone concentrations in the gas phase at inlet and outlet, respectively.  $A$  is an effective area of the membrane.

– **Decolorization performance of dye solution by ozonation using membrane contactor**

This part is the study of continuous ozonation to determine the decolorization performance. The experimental setup was similar to the previous section, except the outlet dye solution was recycled back to the feed tank as illustrated by the dashed line (Mode II) in Figure 5.1. The conditions of the experiments were also the same as the previous section with fixed ozone concentration 40 mg/L and dye solution 300 mg/L, gas velocity 0.12 m/s, and liquid velocity 0.46 m/s. The liquid samples were collected from the feed tank at 5, 10, 20, 40 and 60 min and were analyzed for the dye concentration using U3000 spectrophotometer (Hitachi) at specific wavelength of each dye solution. The COD and BOD of treated dye solutions were determined by the Standard Methods [140] as described in Appendix A. Analysis of total organic carbon (TOC) was performed by an elemental liquid TOC analyzer with high temperature catalytic oxidation mode coupled with non-dispersive infrared (NDIR) detector. The carrier gas was air zero with a flow rate of 200 ml/min. Calibration of the analyzer was achieved with potassium hydrogen phthalate (99.5%, Merck) and sodium carbonate (secondary reference material, Merck) as the standards for total carbon (TOC) and inorganic carbon (IC), respectively. The difference between total carbon and IC gives TOC data of the sample. The removal efficiency, including color, COD and TOC, is defined by the following expression:

$$\text{Removal efficiency (\%)} = \left(1 - \frac{C}{C_0}\right) \times 100 \quad 5.2$$

Where  $C_0$  and  $C$  are the concentrations at time 0 and  $t$ , respectively.

The volatile organic acids (VOCs) in the liquid phase were analyzed by a Shimadzu GC-14B gas chromatography equipped with a flame ionization detector and a packed column unisole 30T 3 mm in diameter and 3 m in length. 1  $\mu$ L of each sample was

injected into the injection port. The temperature of the column was initially set at 180°C. The injector and detector temperatures were set at 130°C and 200°C, respectively.

The oxalic and acetic acids after the degradation of RB5 and BY28 were determined by high-performance liquid chromatography (HPLC). Analysis was done using a Agilent 1260Infinity equipped Inertsil ODS-3 with guard (column with 4.6 mm × 250 mm inside diameter, 5 μm) with a mobile phase of KH<sub>2</sub>PO<sub>4</sub> and acetonitrile. The sample was fed into the HPLC at a flow rate of 20 μL/min. The determination of ammonium ion has been performed by ion chromatography (IC) adopting a Shodex IC YS-50 with guard (4.6 mm × 125 mm) column and 4mM methanesulfonic acid as eluent with flow rate of 1 ml/min and temperature at 40°C. The anions, including sulphate and nitrate, have been analyzed by using a Shodex IC NI-424 with guard (4.6 mm × 100 mm) column and a mixture of 6mM 4-hydroxybenzoic, 2.8mM Bis-Tris, 2mM phenylboronic acid and 0.005mM CyDTA at a flow rate 1 mL/min and temperature at 50°C.

GC/MS analysis was employed to identify the presence of by-products in the dye solution. Prior to GC/MS analysis, the samples were pre-concentrated using solid phase microextraction (SPME). Extraction was performed at room temperature and under intensive magnetic stirring using a glasscoated flea micro spin-bar. The 100 μm polydimethylsiloxane SPME fiber type and a SPME fiber holder assembly purchased from Supelco were used for extraction. For extraction, the fiber holder assembly was clamped at a fixed location above glass vial containing the sample. The fiber was immersed to the aqueous phase and after sampling for 30 min at room temperature it was retracted and transferred to the heated injection port (250 °C) of the GC/MS for desorption, where it remained for 5 min. A fiber clean-up procedure was followed between runs to eliminate the possibility of analyte carry over between runs. A Shimadzu GC-17A (Version 3) QP-5050A GC/MS system equipped with a 30m×0.25mm×0.25 mm HP-5MS capillary column (Agilent Technologies) was used. The injector was operating at 250°C in the splitless mode with the split closed for 5

min. Helium (99.999% purity) was used as the carrier gas at a flow-rate of 1.2 mL/min. The column oven was initially set at 50°C for 5 min, then programmed to 160°C at a 3°C/min rate where it was held for 2 min, then to 310°C at a 5°C/min rate. The interface temperature was set at 320°C and the detector voltage at 1.50kV. The ionization mode was electron impact (70 eV) and data was collected in the full scan mode ( $m/z$  50–450). For a compound to be considered as a likely reaction intermediate with a certain degree of confidence, its mass spectrum should match that of the GC/MS mass spectrum library by at least 75%.

The pH of treated dye solution was measured by a Suntext Digital pH/mV meter (TS-1). The conductivity was measured by a WTW InoLab Cond 720.

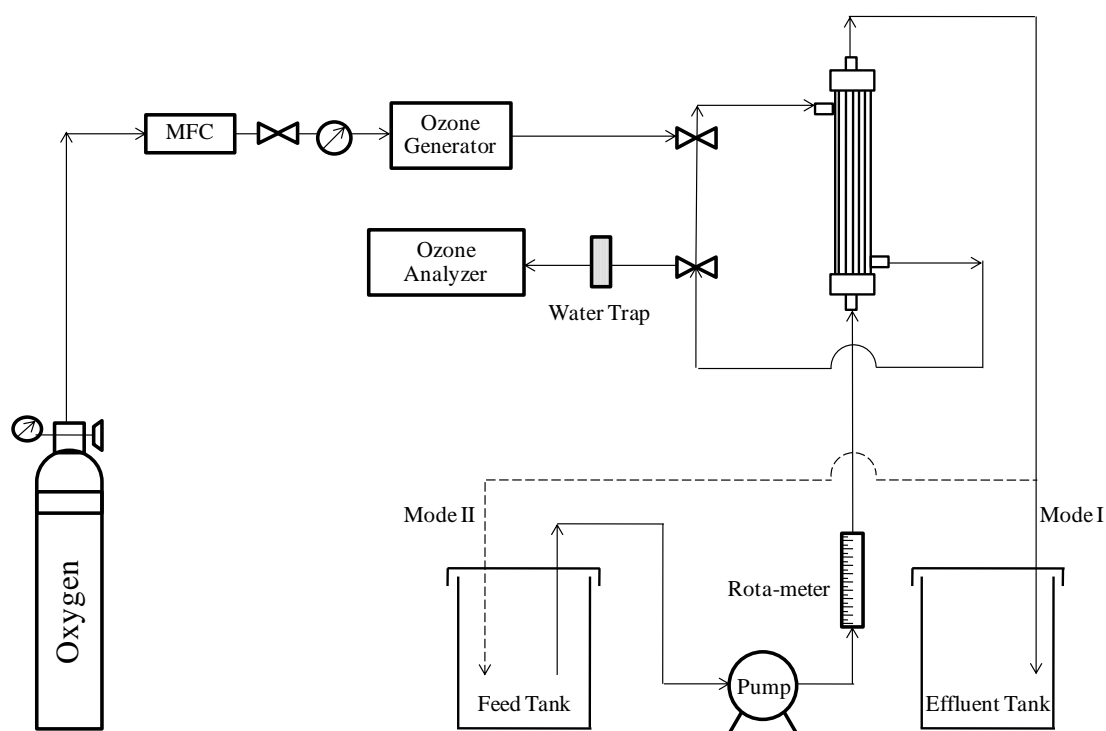


**Figure 5.1** Schematic diagram of the membrane contactor for ozonation of dye solution

### 5.3 Results and discussion

#### 5.3.1 Long-term ozone flux of PVDF and PTFE membranes

The comparison of ozone mass fluxes in the long term test of the original and modified PVDF membranes for Reactive Black 5 solution feed was investigated. PVDF-PAM was selected due to the good properties after exposing to ozone. The experimental results are shown in Figure 5.2. It is very clear that the ozone fluxes of original PVDF and PVDF-PAM membranes decreased with the operation time. The ozone flux of original PVDF membrane decreased from  $1.23 \times 10^{-3}$  to  $7.53 \times 10^{-4}$   $\text{g/m}^2 \cdot \text{s}$ , or the decrease was 39% after 5h of the operation, and then remained quite constant. On the contrary, the ozone flux of PVDF-PAM membrane showed a slight decrease (16%) from  $1.08 \times 10^{-3}$  to  $9.04 \times 10^{-4}$   $\text{g/m}^2 \cdot \text{s}$  in 6h. The CHAPTER 3 reported that the pore size and pore size distribution of the original and PVDF-PAM membranes were in the range of 0.10-0.30  $\mu\text{m}$ . According to the Laplace equation, the penetration of water takes place more easily for the bigger pores [98], therefore, the big pores of PVDF-PAM membrane may be filled by water, resulting in the initial reduction of ozone flux. Similar performance decline by wetting was reported by Bamperng *et al.* [34] for PVDF membranes in ozonation of dye wastewater. The reason for the slight decrease of ozone flux for PVDF-PAM membrane during long term operation was the increase in contact angle after membrane modification, from  $68^\circ$  to  $145^\circ$ . Also, the ozone flux stability of PVDF-PAM membrane could be explained by the enhancing of intermolecular hydrogen bonding of FAS-C8, leading to reduced membrane wetting and ozone oxidation on the membrane surface as discussed in the previous section. It should be noted that the ozone flux of the modified membrane was a little lower than that of original membrane in the first 2h. It was due to the decrease of porosity and an increase the thickness after membrane modification [98].

In the case of PTFE membrane, ozone flux decreased slightly from  $8.67 \times 10^{-4}$  to  $8.19 \times 10^{-4}$   $\text{g/m}^2 \cdot \text{s}$  and was constant during 20h. It was noted that the PVDF-PAM membrane exhibited the higher ozone flux than PTFE membrane since the contact angle of the modified PVDF-PAM membrane ( $145^\circ$ ) was higher than PTFE membrane ( $105^\circ$ ). Moreover, PTFE membrane had the lower porosity than original PVDF and PVDF-PAM membranes. The high porosity membranes have the higher

gas-liquid interfacial area, leading to higher ozone mass transfer [40]. The pore size of membrane had also influence on the ozone flux. Since the pore size of PVDF-PAM membrane ( $0.14\ \mu\text{m}$ ) was larger than PTFE membrane ( $0.089\ \mu\text{m}$ ) as reported in Table 5.1, partial wetting of PVDF-PAM membrane could be the reason for the decrease of ozone flux [95, 98]. In conclusion, in the long-term operation, the modified membrane exhibited more stable and better performance. This result clearly indicated the feasibility of improving flux stability of long-term performance by modifying the PVDF hollow fiber membranes with FAS-C8.

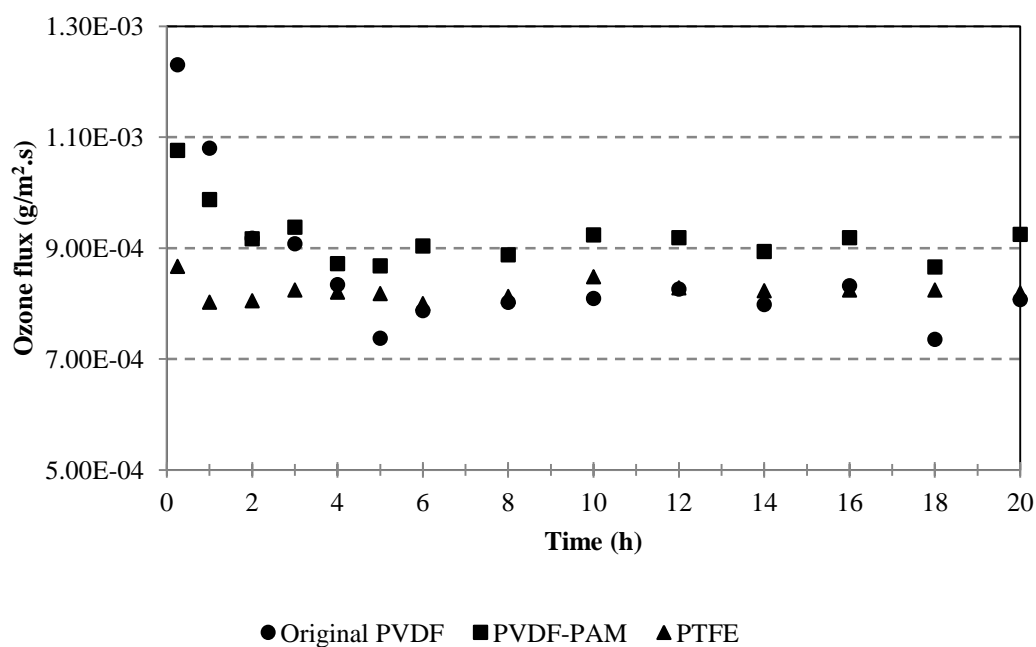


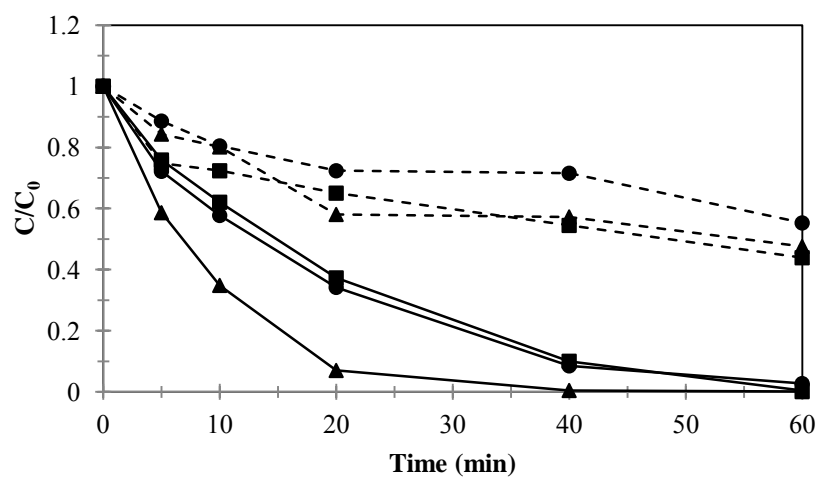
**Figure 5.2** Long term performance of PVDF and PTFE membranes

### 5.3.2 Decolorization performance of dye solution using modified PVDF and PTFE membranes

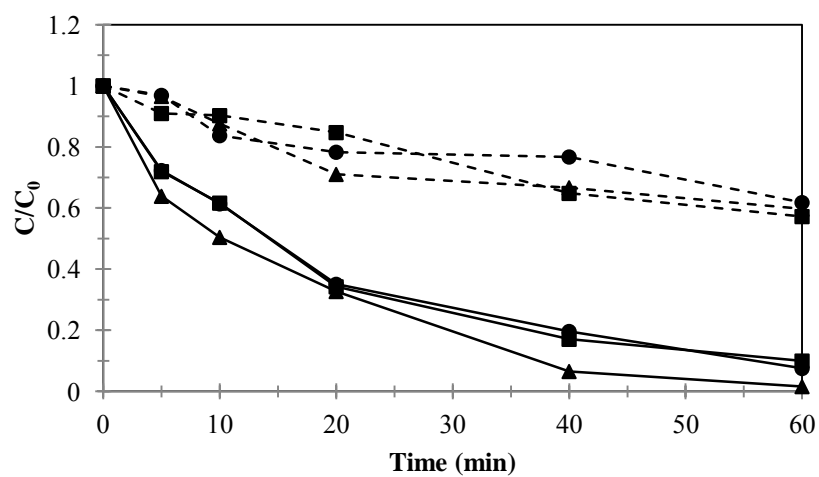
In Figure 5.3, for both RB5 and BY28, the decolorization performance using the PVDF-PAM membrane was higher than that of original PVDF membranes. After 60 min of ozonation time, the decolorization by original PVDF and PVDF-PAM membranes was almost completed. Moreover, after 60 min, the decolorization performance of PVDF-PAM was as high as PTFE membrane. This phenomenon was due to the cleavage of the chromophore structures in the dye molecules, resulting in the rapid decolorization [141]. It is worth mentioning that the ozone flux of PTFE was lower than that of the original PVDF and PTFE membranes, as presented in previous section (5.3.1) but the decolorization of PTFE membrane, which had lower contact angle, was faster than that of original PVDF and PVDF-PAM membranes. This was possibly due to the effect of pore size. The pore sizes of original PVDF and PVDF-PAM membranes were bigger than that of PTFE membranes which were partially wetted, therefore, the decolorization performance of PTFE membrane was better. It is noted that the complete decolorization did not mean that the degradation of dyes was completed, as indicated by the COD removal in Figure 5.3.

COD removals of RB5 and BY28 by PVDF-PAM membrane were 56% and 42%, respectively. On the contrary, COD removals of RB5 and BY28 by PTFE membrane were 52% and 42%, respectively. The COD removal of RB5 for PVDF-PAM membrane was slightly higher than that of original and PTFE membranes. This is because the PVDF-PAM membrane was more hydrophobic than the original PVDF and PTFE membranes in term of contact angle, resulting in reduced the membrane wetting. It is possible that the pores of original PVDF and PTFE membrane were filled by the liquid, hence, the diffusivity of gas in the liquid-filled membrane pores is much lower than that of in the gas-filled pores [142, 143]. Therefore, ozone molecules could continually react with by-products, which were produced after dye degradation, using PVDF-PAM membrane, resulting in high reduction of COD.





a)



b)

● Original PVDF    ■ PVDF-PAM    ▲ PTFE  
 — Decolorization    - - - COD removal

**Figure 5.3** Comparison of decolorization performance using different membranes:

a) Reactive black 5; b) Basic yellow 28

### 5.3.3 Effect of dye solution types

The decolorization performance of RB5 and BY28 using original PVDF, PVDF-PAM and PTFE membranes showed the similar results. Therefore, the results of PVDF-PAM were selected to present as illustrated in Figure 5.4. The decolorization of RB5 was higher than BY28. After 60 min of ozonation time, the concentrations of RB5 and BY28 decreased approximately 100% and 92%. The colors of RB5 and BY28 after 60 min of ozonation time are presented in Figure 5.5. The reason is that the initial pH of RB5 (5.8) was lower than that of BY28 (6.55), therefore, most ozone was presented as molecules. Generally, ozone reacts with organic compounds via two mechanisms either direct ozone attack or indirect free radical attack [99, 136]. Ozone molecule dominates oxidation process under low pH, whereas, the hydroxyl radical dominates under high pH [41, 136]. Ozone molecule is selective and attack preferentially the unsaturated bonds of azo-chromophores [136, 144]. Hydroxyl radicals have a greater oxidative power and are less selective than molecular ozone, leading to a decrease in decolorization at higher pH [69, 70, 99]. For this reason, color removal by action of ozone molecule is better. Hence, this implied that the predominant reaction in this study was the direct oxidation of dye molecules by ozone molecule at acidic pH. Therefore, the decrease in the pH from the 5.8 to 3.2 of RB5, and 6.55 to 3.2 of BY28 was found during the ozonation as shown in Figure 5.6, due to the formation of by-products and ions in the solution. In addition, the result showed that the color of RB5 solution was clear after 60 min which implied that the wastewater containing RB5 solution with ozonation by membrane contacting process can be discharged. In contrast, the color of BY28 after 60 min was still yellowish which could not be discharged into the environment. However, the COD and TOC removals of RB5 and BY28 were not high as presented in Figure 5.6 which implied that both RB5 and BY28 could not be discharged.

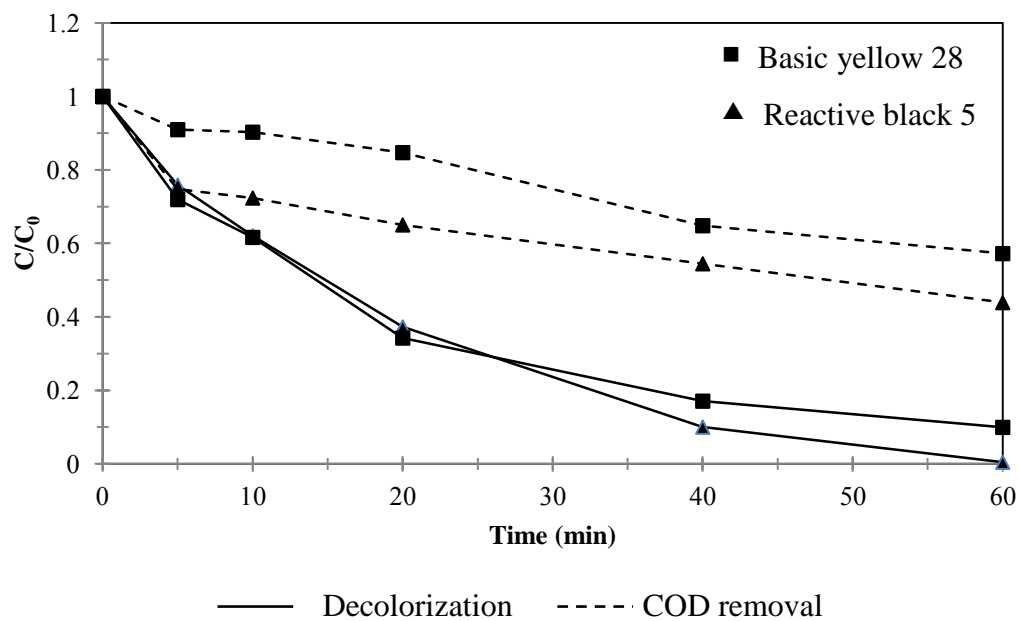


**Figure 5.4** Comparison of Reactive black 5 and Basic yellow 28 removal using PVDF-PAM membrane

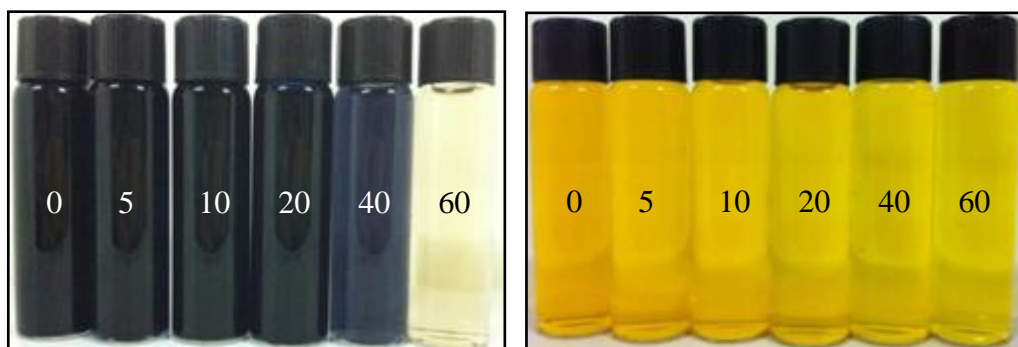


**Figure 5.5** Illustration of Reactive Black 5 and Basic Yellow 28 with different ozonation time by PVDF-PAM membrane

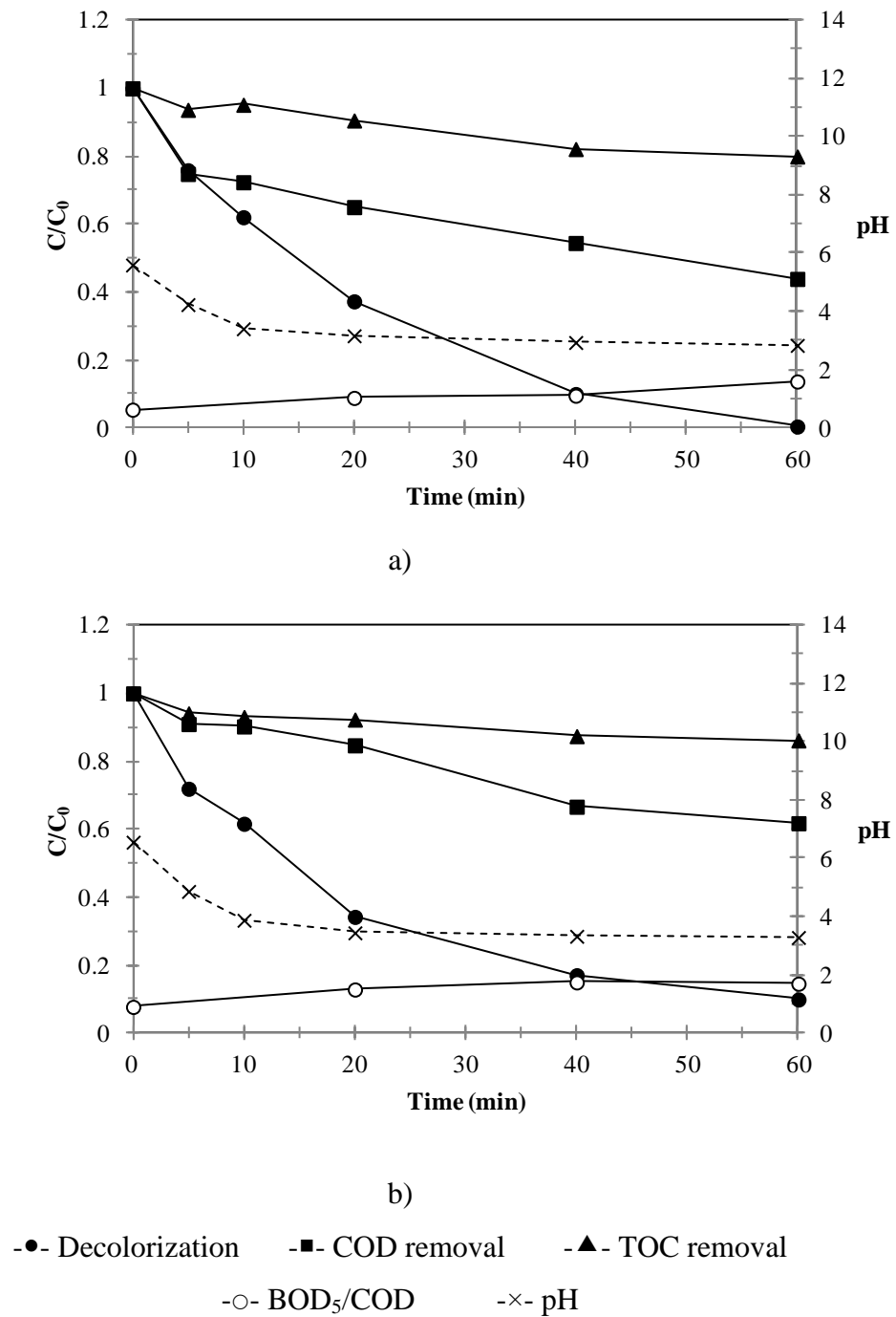


**Figure 5.6** The performance of PVDF-PAM in membrane contactor for dye wastewater containing: a) Reactive black 5; b) Basic Yellow 28

Figure 5.7 depicts decolorization and ozone consumption of RB5 and BY28. The decolorization of RB5 and BY28 was approximately 100% and 92% after 60 min of ozonation time, but about 65% of the colors were removed in the first 20 min. Initially, the ozone used and the RB5 removal were rapid, as the treatment progressed, both the ozone consumption and decolorization decreased. In contrast, the ozone consumption of BY28 was lower than that of RB5. Therefore, the reaction between the BY28 molecule and ozone proceeded slowly and required a significant time for complete degradation.

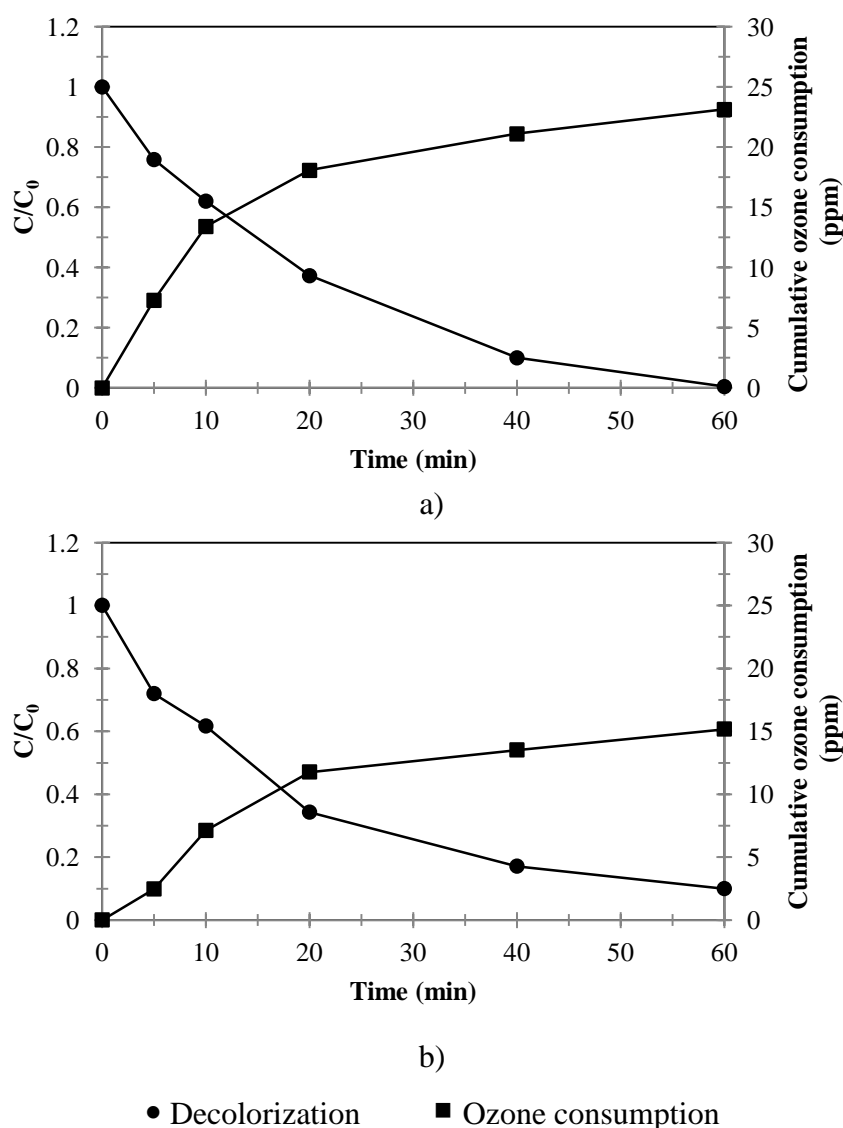


**Figure 5.7** Color removal and ozone consumption: a) Reactive Black 5; b) Basic Yellow 28

### 5.3.4 Determination of by-products from ozonation of dye solutions

Since the chemical reduction of azo linkage (N=N) by ozonation commonly results in the formation of lower molecular weight by-products and eliminates the color RB5. From the results of color and COD reductions by ozonation membrane contacting process, it was observed that the COD removal efficiency was always lower than decolorization. Comparing the three membranes in Figure 5.3, the COD removal by PVDF-PAM membranes was highest. Therefore, the PVDF-PAM membranes were selected to study in this part.

After 60 min, the COD removals of RB5 and BY28 were 56% and 42%, respectively. In addition, a slight removal of TOC was noted, as shown in Figure 5.6, indicating that RB5 and BY28 were converted mainly to the intermediate products and complete mineralization did not occur. The low TOC removal under ozonation can be explained by the resistance of aromatic structures to cleavage and the productions of small organic molecule fragments not being completely mineralized under oxidation. TOC values may not be the total TOC concentrations due to the removal of volatile organic compounds (VOCs) formed during ozonation, i.e., formaldehyde and acetaldehyde [69]. In this study, isovaleric acid, butyric acid, propionic acid and acetic acid were found as VOCs by gas chromatograph. The 4-(2-Methylamino-ethyl)-phenol was also found after dye degradation by ozonation process. The results confirmed that RB5 and BY28 could not be completely oxidized to carbon dioxide and water during the ozonation but rather transformed to some intermediates.

Figure 5.8 (a-b) illustrates representative time profile of RB5 and BY28 solution subjected to ozonation at 40 ppm. RB5 at  $t=0$  is represented mainly by three peaks: (1) 595 nm, (2) 310 nm, (3) 255 nm, as shown in Figure 5.8a. It may be noted that each molecule of RB5 consists of two molecule of benzene rings and one molecule of naphthalene ring connected by  $-N=N-$  bonds. The peak at 595 nm corresponds to chromophore group ( $-N=N-$ ), and the peaks at 255 nm and 310 nm corresponds to benzene and naphthalene rings, respectively [69, 145, 146]. The peak located at 230 nm correspond to the benzoic ring [131]. It may be observed that as the ozonation proceeded, peak at 255 nm and 310 nm decreased as well as decreased the peak at 595

nm, indicating that the benzene and naphthalene rings were decreased by the reduction of RB5. Finally, it can be concluded that the intensity of visible band disappeared after 60 min of ozonation time and remained to zero, leading to the cleavage of azo group from aromatic rings.

BY28 at  $t=0$  is represented mainly by two peaks: (1) 440 nm, (2) 255 nm, as shown in Figure 5.8b. The decrease peak at 440 nm was also meaningful with respect to the carbon-nitrogen double bond of BY28, as the active site for oxidative attack [147]. The peak at 255 nm corresponds to benzene ring. It may be observed that as the ozonation proceeded, peak at 255 nm decreased as well as decreased the peak at 440 nm, indicating that the benzene ring was decreased by the reduction of a BY28.

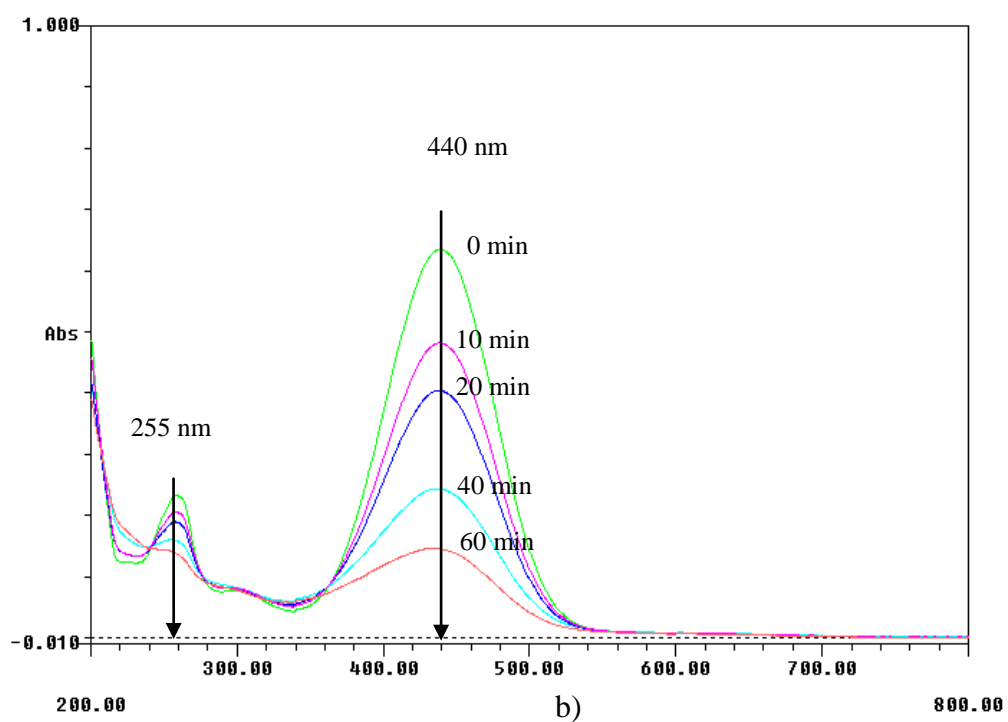
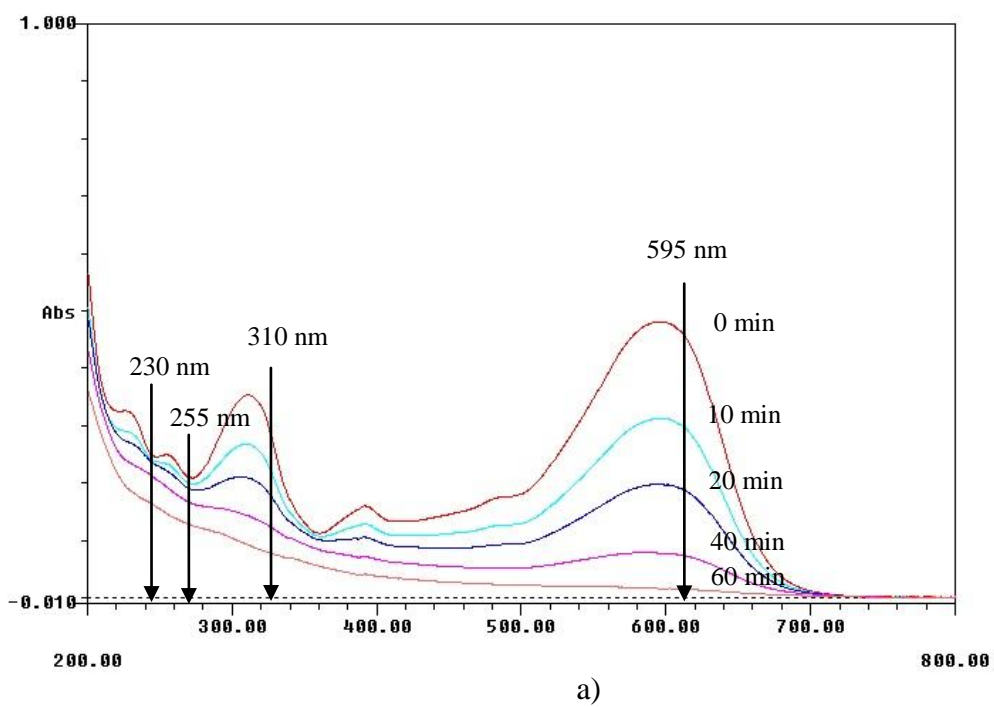
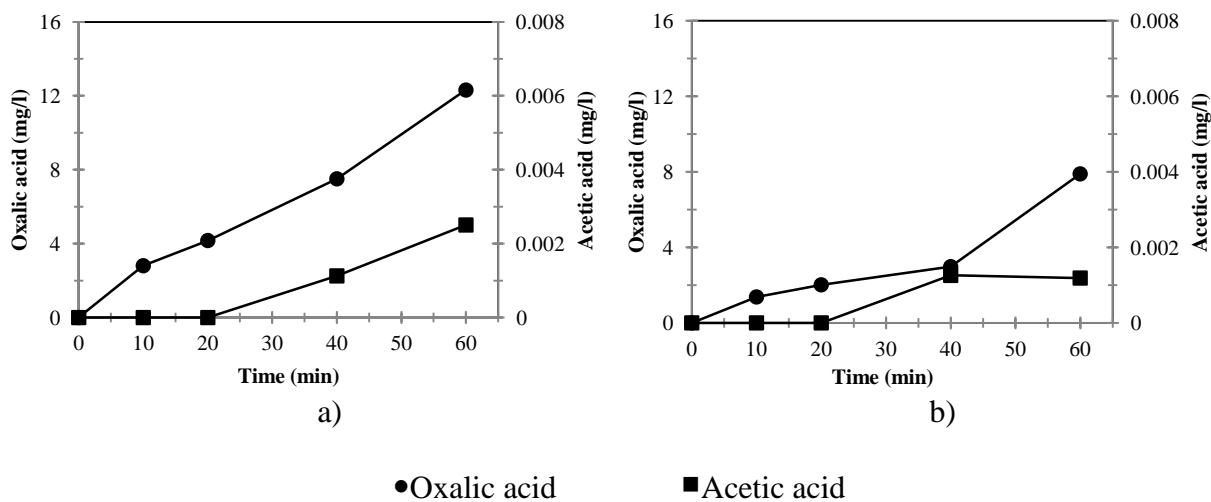


**Figure 5.8** UV-Vis spectra of RB5 solution at different ozonation time: a) Reactive Black 5; b) Basic Yellow 28



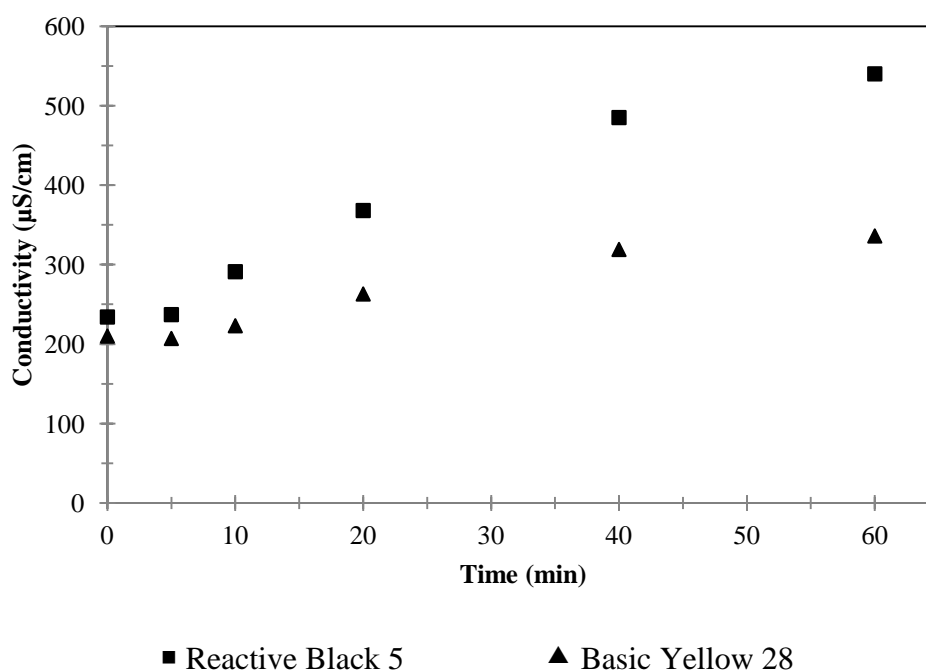
In addition, it is worth mentioning that the reduction of aromatic structures (i.e. 255 and 310 nm) can be observed, indicating that the membrane contactor with ozonation process has a powerful oxidative ability for not only a complete decolorization but also a continuous destruction of aromatic intermediates.

In addition to the aromatic intermediates, the carboxylic acids were also detected, including oxalic and acetic acids, which are the most successive organic products prior to conversion to CO<sub>2</sub>. Concentration of acetic acid increased on ozonation time, whereas oxalic acid was detected after 20 min of ozonation time as illustrated in Figure 5.9. This implies that under the studied conditions within 60 min of ozonation time, the dye solutions could not be completely mineralized to CO<sub>2</sub>. This is in agreement with the total organic carbon profile as shown in Figure 5.6(a-b) in which only 20% of dye solutions could be converted to CO<sub>2</sub>. It was observed that acetic acid and oxalic acid concentrations of RB5 were higher than that of BY28, leading to rapid removals of COD and TOC.



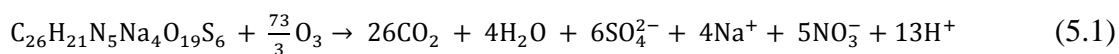
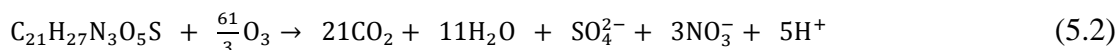
**Figure 5.9** Oxalic and acetic acids produced at different ozonation time: a) Reactive Black 5; b) Basic Yellow 28

Figure 5.10 illustrates the conductivity of RB5 and BY28 solutions with ozonation time. It can be seen that the conductivity of RB5 and BY28 increased with increasing ozonation time, and the change was consistent with the decolorization efficiency and pH. This means that ionic solution increased with increasing ozonation time and the dyes were transformed to ions and other products. From the result of the pH decrease during the ozonation time, it also can be presented that the treated dye solution contained the anions in the formation of corresponding acids.



**Figure 5.10** The conductivity of dye solution during the ozonation

It has been reported that ozonation induces denitration and desulfuration of phenols at the initial reaction step [72, 148, 149]. The concentration profiles for ions, including nitrate, ammonium and sulfate ions, are also illustrated in Figure 5.11. According to the molecular formulas of RB5 and BY28 in Table 5.1, the following theoretical mineralization equation could be considered for the ozone reaction:

**RB5:****BY28:**

Stoichiometrically, reactions (5.1) and (5.2) indicate that each 300 mg/l of RB5 and BY28 will produce 174.37 and 93.84 mg/l, and 66.51 and 128.86 mg/l of sulfate and nitrate, respectively. It was assumed that excess ozone was added and the RB5 was completely mineralized. However, the results in Figure 5.11 showed that the sulfate concentration gradually increased from 39.4 to 56.6 mg/l with in 60 min of ozonation time. Therefore, the increase of sulfate concentration was approximately 32% of the theoretical release value, implying that the vinyl sulfonyl group (-SO<sub>2</sub>CH<sub>2</sub>CH<sub>2</sub>OSO<sub>3</sub>Na) on the mono benzene ring, or sulfonic group (-SO<sub>2</sub>Na) on the anthraquinone rings of RB5 were partially oxidized. Oxidation and cleavage of sulfonic acid group from the naphthalene ring leads to the accumulation of sulphate during ozonation [150]. Similar results for the partial release of sulfate have also been found in the ozonation of other dyes containing sulfonate groups [69, 72, 150, 151]. In contrast, an increase of sulfate concentration of BY28 was not observed during the 60 min of ozonation time in this study, implying that the sulfonyl group (-CH<sub>3</sub>SO<sub>4</sub>) was not oxidized by ozone [68].

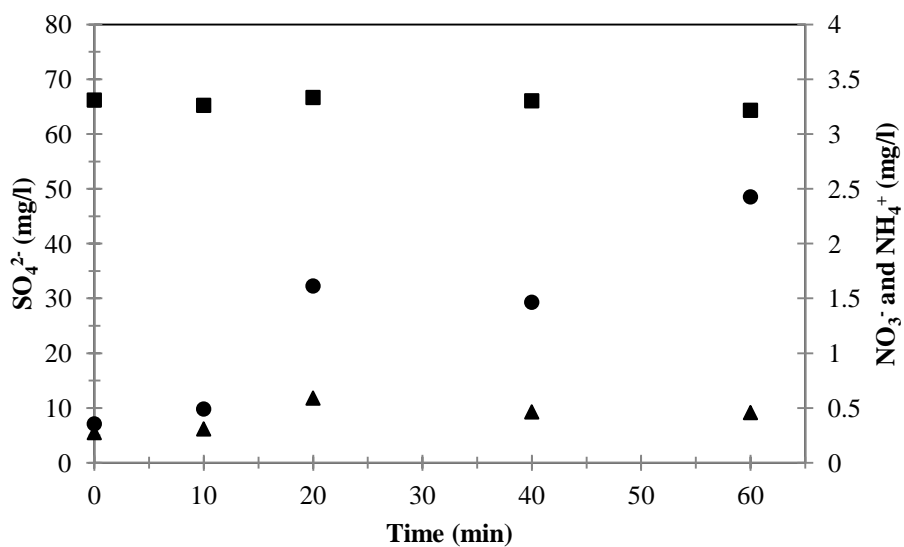
The increase in nitrate of RB5 and BY28 were not observed during 10 min of ozonation time. The results of releasing nitrate are also consistent with ozonation of RY84 [50], RB19 [69], Procion red (MX-5B) [150], and RR120 [151] which contain nitrogen atoms in the dye structures. Therefore, the increase of nitrate concentration of RB5 and BY28 were approximately 2% of the theoretical release value, implying that the nitrogen was not completely oxidized to nitrate.

It was because the nitrogen would be transformed to NH<sub>4</sub><sup>+</sup> as presented in the Figure 5.11. Nevertheless, the total nitrogen contents of NH<sub>4</sub><sup>+</sup> and NO<sub>3</sub><sup>-</sup> were less than the initial dye solution.

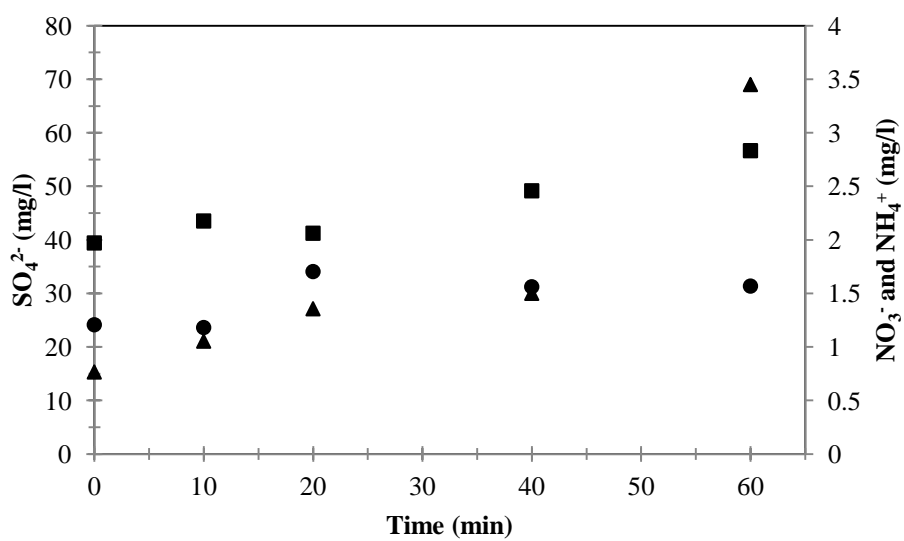
In contrast, azo dye ( $-N=N-$ ) are easily attacked by ozone. As a consequence, a remarkable release of nitrate was found during the ozonation of azo dyes. Konstantinou *et al.* [152, 153] reported that the total amount of nitrogen-containing ions present in the solution at the end of the experiments is usually lower than that expected from stoichiometry indicating that N-containing species have been produced and transferred to the gas phase such as  $N_2$  and  $NH_3$ . Therefore, in this study the increase of conductivity in dye solutions was interpreted as indirect evidence of sulfate and nitrate ions accumulation related to the dyes denitration and desulfuration [149].

### **5.3.5 Investigation on biodegradability**

The extremely low  $BOD_5/COD$  ratio (0.05 and 0.08 as RB5 and BY28, respectively) indicated that both dyes are resistant to biodegradation.  $BOD_5/COD$  ratio for RB5 and BY28 increased to 0.12 after 60 min of ozonation due to the presence of more easily degradable compounds [41, 49, 72, 151]. Wang *et al.* [148] also showed that first by-product after partial ozonation (10-150 min) of Reactive Black 5 was more biodegradable than the parent compound and ozonation can enhance the biodegradability of the azo dyes.



a)



b)

-●- Nitrate    -■- Sulfate    -▲- Ammonium

**Figure 5.11** Concentration profiles of ions during the ozonation

#### 5.4 Conclusions

The long-term ozone flux by PVDF-PAM membrane was higher and more stable than original PVDF membrane, while PTFE membrane was more stable and gave lower flux than the PVDF-PAM membrane. The decolorization performance of PVDF-PAM membrane was more effective than the original PVDF membrane and was as high as PTFE membrane. The decolorization performance of Reactive Black 5 was higher than that of Basic Yellow 28. The COD reductions of RB5 and BY28 using PVDF-PAM membranes were higher than the original PVDF and PTFE membranes. The results confirmed that RB5 and BY28 could not be completely oxidized to carbon dioxide and water during the ozonation but rather transformed to some intermediates. The experimental results showed that the use of the PVDF-PAM membrane as the membrane for contactor with ozonation is very beneficial to not only the complete decolorization but also to the degradation efficiency of its derivative aromatic fragments. The reduction of RB5 disappeared the benzene and naphthalene rings, leading to the cleavage of azo group from aromatic rings. Additionally, reduction of a BY28 which disappeared the benzene ring leading to cleavage of the C=N bonding. The sulfate, nitrate, acetic and oxalic acids were identified as the products during 60 min ozonation of RB5 and BY28, implying that the vinyl sulfonyl group and azo group were partial oxidized by ozone.

## **CHAPTER VI**

### **CONCLUSIONS AND RECOMMENDATIONS**

The thesis aimed to study the surface modification of hollow fiber PVDF membranes by organosilanes, test membrane stability after ozone contact, then apply the modified membrane for decolorization of dye solution by ozonation using membrane contacting process. The main conclusions and recommendations obtained are discussed as the followings:

#### **6.1 Conclusions**

##### **6.1.1 Hydrophobic membrane modification of PVDF hollow fiber membranes**

1. The contact angle of original membranes ( $68^\circ$ ) was decreased from  $44^\circ$  to  $31^\circ$  with increasing NaOH concentration from 2.5M to 7.5M at  $60^\circ\text{C}$  for 3h and the contact angle of NaOH treated membranes was increased to  $100^\circ$  after modification with 0.01M FAS-C8 for 24h.
2. A needle-like structure was observed on the membrane surface while there was no significant change in pore size and pore size distribution.
3. The Si peak and compositions were found on the membrane surface and the mechanical strength was improved.
4. A comparison of chemical modification (CM) and plasma-activation modification (PAM) indicated that the surface modified membranes under helium plasma activation (PVDF-PAM) followed by grafting with 0.01M FAS-C8 for 24h showed higher contact angle, mechanical strength and surface roughness than that obtained by NaOH activation (PVDF-CM2) method while other physical properties did not change.
5. The  $\text{CO}_2$  absorption flux by PVDF-PAM membrane was reasonably higher and more stable than original PVDF and PVDF-CM2 membranes.

### **6.1.2 The stability of modified membranes exposed to ozone**

1. The contact angle of original PVDF membranes exposed to ozone were increased, while the contact angles of PVDF-CM2 and PVDF-PAM were decreased at low concentration and time, and remained constant.
2. The structural changes in the original and modified PVDF membranes after ozone contact were observed by FT-IR with the peak corresponding to the decrease of OH and increase of C=O peaks with exposure time and concentration, respectively.
3. The membrane morphologies after ozone contact were insignificantly changed and the tensile modulus of PVDF-PAM membranes did not change. Nevertheless, the ozone oxidation had no impact on the properties of PTFE membrane.

### **6.1.3 Application of modified membrane in membrane contactor for dye solution treatment**

1. PVDF-PAM membrane provided higher and more stable ozone flux than original PVDF membrane, but PTFE membrane flux was lower than PVDF-PAM membrane for a long operation period.
2. The decolorization performance of PVDF-PAM membrane was more effective than the original PVDF membrane and was as high as PTFE membrane.
3. The decolorization performance of Reactive Black 5 was higher than that of Basic Yellow 28.
4. The COD reductions of RB5 and BY28 using PVDF-PAM membranes were higher than the original PVDF and PTFE membranes.
5. The results confirmed that RB5 and BY28 could not be completely oxidized to carbon dioxide and water during the ozonation but rather transformed to some intermediates.
6. The PVDF-PAM membranes showed a potential use as the membrane for contactor with the improved stability and decolorization performance.
7. The modified PVDF membranes were feasible for improving the membrane performance in other membrane contactor applications.



## 6.2 Recommendations

In the case of surface modification, the results of plasma activation/modification was better than the chemical activation/modification since plasma treatment is justified to be one of the less damaging membrane modification method. The condition for the plasma activation of PVDF membrane in this study was kept constant by helium gas for 180 seconds and working pressure at 10Pa with a power of 80W. In order to optimize the plasma activation of the membranes, the number of reactive species produced in the plasma and lifetime has to be regarded. Hence, the gas mixture and the pressure are important parameters beside power input and treatment time. Therefore, the conditions of plasma activation can also be varied to find the optimum required for the desirable properties of PVDF membranes. Recently, PVDF membranes have been already successfully modified to increase hydrophobicity. There are new membrane materials that present high performance in terms of flux with high resistance to aggressive chemicals. For example, poly(ethylene chlorotrifluoroethylene) (ECTFE) is a promising material due to its excellent chemical and thermal stability compared with PVDF and better processability compared with PTFE, giving the potential for MD, pervaporation, and gas separation [154].

In the study of membrane stability toward ozone, a systematic experiment was conducted to investigate the effect of ozone concentration and time on the membrane structure and properties using the modified membranes (PVDF-CM2 and PVDF-PAM), compared to the original PVDF and commercial PTFE hollow fiber membranes. Furthermore, the experiment on physical absorption (using pure water and ozone) could be useful to determine the membrane degradation by measuring the TOC or organic compounds in the effluent water after ozone contact. If the membranes are destroyed by ozone oxidation, the elemental composition of membrane in the effluent water will be detected or the TOC will be increased.

In the study of long-term ozone flux of PVDF and PTFE membranes, the ozone flux was measured every 1h for 20h in order to study the deterioration of ozone flux,

possibly due to membrane wetting and ozone oxidation. However, the observation of ozone flux is recommended to study longer time than 20h.

In the case of decolorization by membrane contactor with ozonation process, the experiment in this study was carried on the decolorization of individual dye solution, whereas the industrial effluents contain mixture of dyes. Therefore, an experiment using the mixture of dye solution or the industrial effluent should be conducted by measuring the reduction of BOD, COD and TOC values. Moreover, our findings found that the decolorization by membrane contacting process was almost completed, however, the COD and TOC removals and biodegradability were not high. Therefore, the enhancing efficiency of those values is recommended for the future work by combination with other processes. Additionally, the ozone flux of PTFE membrane was lower than that of PVDF-PAM membrane, but the decolorization performance of dye solution was better than that of PVDF-PAM membrane. Therefore, it was possible that the ozone concentration in this study was excessive which can destroy the membrane surface. The investigation of ozonation kinetic for dye solution should be taken in to the consideration due to presenting an important role in evaluating the efficiency and feasibility of decolorization process by varying the parameters including ozone and dye concentrations.

Finally, the long-term stability and performance of decolorization are important from an economic point of view for the future application. Therefore, the cost analysis of the process will be very beneficial. The cost analysis should include the cost of raw material, cost of membrane modification and operating cost. Therefore, the cost analysis of both modified and unmodified used as the membrane for the contactor with ozonation process should be carried out, and then compared with PTFE membrane.

## REFERENCES

- [1] Sirianuntapiboon, S., and Srisornsak, P. 2007. Removal of disperse dyes from textile wastewater using bio-sludge. Bioresource Technology 98 (5):1057-1066.
- [2] Gad-Allah, T. A., Kato, S., Satokawa, S., and Kojima, T. 2009. Treatment of synthetic dyes wastewater utilizing a magnetically separable photocatalyst ( $\text{TiO}_2/\text{SiO}_2/\text{Fe}_3\text{O}_4$ ): Parametric and kinetic studies. Desalination 244 (1-3):1-11.
- [3] Zhang, H., Zhang, J. H., Liu, F., and Zhang, D. B. 2009. Decolorization of Ci Acid Orange 52 by Ozonation in a Hollow Fiber Membrane Reactor. Fresenius Environmental Bulletin 18 (3):275-279.
- [4] Zhang, H., Jiang, M., Xia, Q., and Zhang, D. B. 2010. Decomposition of 4-Nitrophenol by Ozonation in a Hollow Fiber Membrane Reactor. Chemical Engineering Communications 197 (3):377-386.
- [5] Chu, L. B., Xing, X. H., Yu, A. F., Sun, X. L., and Jurcik, B. 2008. Enhanced treatment of practical textile wastewater by microbubble ozonation. Process Safety and Environmental Protection 86 (B5):389-393.
- [6] Chu, L. B., Xing, X. H., Yu, A. F., Zhou, Y. N., Sun, X. L., and Jurcik, B. 2007. Enhanced ozonation of simulated dyestuff wastewater by microbubbles. Chemosphere 68 (10):1854-1860.
- [7] Atchariyawut, S., Phattaranawik, J., Leiknes, T., and Jiratananon, R. 2009. Application of ozonation membrane contacting system for dye wastewater treatment. Separation and Purification Technology 66 (1):153-158.
- [8] Gabelman, A., and Hwang, S. T. 1999. Hollow fiber membrane contactors. Journal of Membrane Science 159 (1-2):61-106.
- [9] Ciardelli, G., Ciabatti, I., Ranieri, L., Capannelli, G., and Bottino, A. 2003. Membrane contactors for textile wastewater ozonation. Advanced Membrane Technology 984:29-38.

- [10] Jansen, R. H. S., de Rijk, J. W., Zwijnenburg, A., Mulder, M. H. V., and Wessling, M. 2005. Hollow fiber membrane contactors - A means to study the reaction kinetics of humic substance ozonation. Journal of Membrane Science 257 (1-2):48-59.
- [11] Mori, Y., Oota, T., Hashino, M., Takamura, M., and Fujii, Y. 1998. Ozone-microfiltration system. Desalination 117 (1-3):211-218.
- [12] Phattaranawik, J., Leiknes, T., and Pronk, W. 2005. Mass transfer studies in flat-sheet membrane contactor with ozonation. Journal of Membrane Science 247 (1-2):153-167.
- [13] Pines, D. S., Min, K. N., Ergas, S. J., and Reckhow, D. A. 2005. Investigation of an ozone membrane contactor system. Ozone-Science & Engineering 27 (3):209-217.
- [14] Khaisri, S., Demontigny, D., Tontiwachwuthikul, P., and Jiraratananon, R. 2009. Comparing membrane resistance and absorption performance of three different membranes in a gas absorption membrane contactor. Separation and Purification Technology 65 (3):290-297.
- [15] Xi, Z. Y., Xu, Y. Y., Zhu, L. P., Wang, Y., and Zhu, B. K. 2009. A facile method of surface modification for hydrophobic polymer membranes based on the adhesive behavior of poly(DOPA) and poly(dopamine). Journal of Membrane Science 327 (1-2):244-253.
- [16] Bothun, G. D., Peay, K., and Ilias, S. 2007. Role of tail chemistry on liquid and gas transport through organosilane-modified mesoporous ceramic membranes. Journal of Membrane Science 301 (1-2):162-170.
- [17] Castricum, H. L., Sah, A., Mittelmeijer-Hazeleger, M. C., and ten Elshof, J. E. 2005. Hydrophobisation of mesoporous gamma-Al<sub>2</sub>O<sub>3</sub> with organochlorosilanes - efficiency and structure. Microporous and Mesoporous Materials 83 (1-3):1-9.
- [18] Dafinov, A., Garcia-Valls, R., and Font, J. 2002. Modification of ceramic membranes by alcohol adsorption. Journal of Membrane Science 196 (1):69-77.

- [19] Koonaphaptleelert, S., and Li, K. 2007. Preparation and characterization of hydrophobic ceramic hollow fibre membrane. Journal of Membrane Science 291 (1-2):70-76.
- [20] Krajewski, S. R., Kujawski, W., Bukowska, M., Picard, C., and Larbot, A. 2006. Application of fluoroalkylsilanes (FAS) grafted ceramic membranes in membrane distillation process of NaCl solutions. Journal of Membrane Science 281 (1-2):253-259.
- [21] Leger, C., Lira, H. D., and Paterson, R. 1996. Preparation and properties of surface modified ceramic membranes .2. Gas and liquid permeabilities of 5 nm alumina membranes modified by a monolayer of bound polydimethylsiloxane (PDMS) silicone oil. Journal of Membrane Science 120 (1):135-146.
- [22] Picard, C., Larbot, A., Guida-Pietrasanta, F., Boutevin, B., and Ratsimihety, A. 2001. Grafting of ceramic membranes by fluorinated silanes: hydrophobic features. Separation and Purification Technology 25 (1-3):65-69.
- [23] Picard, C., Larbot, A., Tronel-Peyroz, E., and Berjoan, R. 2004. Characterisation of hydrophilic ceramic membranes modified by fluoroalkylsilanes into hydrophobic membranes. Solid State Sciences 6 (6):605-612.
- [24] Sah, A., Castricum, H. L., Blik, A., Blank, D. H. A., and ten Elshof, J. E. 2004. Hydrophobic modification of gamma-alumina membranes with organochlorosilanes. Journal of Membrane Science 243 (1-2):125-132.
- [25] Hashim, N. A., Liu, Y., and Li, K. 2011. Stability of PVDF hollow fibre membranes in sodium hydroxide aqueous solution. Chemical Engineering Science 66:1565-1575.
- [26] Liu, Q. F., Lee, C. H., and Kim, H. 2010. Performance evaluation of alkaline treated poly(vinylidene fluoride) membranes. Separation Science and Technology 45 (9):1209-1215.
- [27] Kull, K. R., Steen, M. L., and Fisher, E. R. 2005. Surface modification with nitrogen-containing plasmas to produce hydrophilic, low-fouling membranes. Journal of Membrane Science 246:203-215.

- [28] Bazaka, K., Jacob, M. V., Crawford, R. J., and Ivanova, E. P. 2011. Plasma-assisted surface modification of organic biopolymers to prevent bacterial attachment. Acta Biomaterialia 7:2015-2028.
- [29] Yan, M. G., Liu, L. Q., Tang, Z. Q., Huang, L., Li, W., Zhou, J., Gu, J. S., Wei, X. W., and Yu, H. Y. 2008. Plasma surface modification of polypropylene microfiltration membranes and fouling by BSA dispersion. Chemical Engineering Science 145:218-224.
- [30] Jaleh, B., Parvin, P., Wanichapichart, P., Saffar, A. P., and Reyhani, A. 2010. Induced super hydrophilicity due to surface modification of polypropylene membrane treated by O<sub>2</sub> plasma. Applied Surface Science 257:1655-1659.
- [31] Kim, E. S., Yu, Q., and Deng, B. 2011. Plasma surface modification of nanofiltration (NF) thin-film composite (TFC) membranes to improve anti organic fouling. Applied Surface Science 257:9863-9871.
- [32] Yu, H. Y., Liu, L. Q., Tang, Z. Q., Yan, M. G., Gu, J. S., and Wei, X. W. 2008. Surface modification of polypropylene microporous membrane to improve its antifouling characteristics in an SBR: Air plasma treatment. Journal of Membrane Science 311:216-224.
- [33] Zou, L., Vidalis, I., Steele, D., Michelmore, A., Low, S. P., and Verberk, J. Q. J. C. 2011. Surface hydrophilic modification of RO membranes by plasma polymerization for low organic fouling. Journal of Membrane Science 369:420-428.
- [34] Bamperng, S., Suwannachart, T., Atchariyawut, S., and Jiratananon, R. 2010. Ozonation of dye wastewater by membrane contactor using PVDF and PTFE membranes. Separation and Purification Technology 72 (2):186-193.
- [35] Arkhangel'sky, E., Kuzmenko, D., Gitis, N. V., Vinogradov, M., Kuiry, S., and Gitis, V. 2007. Hypochlorite cleaning causes degradation of polymer membranes. Tribology Letters 28 (2):109-116.
- [36] Wang, P., Wang, Z. W., Wu, Z. C., Zhou, Q., and Yang, D. H. 2010. Effect of hypochlorite cleaning on the physicochemical characteristics of

- polyvinylidene fluoride membranes. Chemical Engineering Journal 162 (3):1050-1056.
- [37] Puspitasari, V., Granville, A., Le-Clech, P., and Chen, V. 2010. Cleaning and ageing effect of sodium hypochlorite on polyvinylidene fluoride (PVDF) membrane. Separation and Purification Technology 72 (3):301-308.
- [38] Lee, J. H., Chung, J. Y., Chan, E. P., and Stafford, C. M. 2013. Correlating chlorine-induced changes in mechanical properties to performance in polyamide-based thin film composite membranes. Journal of Membrane Science 433:72-79.
- [39] Liu, M. H., Chen, Z. W., Yu, S. C., Wu, D. H., and Gao, C. J. 2011. Thin-film composite polyamide reverse osmosis membranes with improved acid stability and chlorine resistance by coating N-isopropylacrylamide-co-acrylamide copolymers. Desalination 270 (1-3):248-257.
- [40] Kukuzaki, M., Fujimoto, K., Kai, S., Ohe, K., Oshima, T., and Baba, Y. 2010. Ozone mass transfer in an ozone-water contacting process with Shirasu porous glass (SPG) membranes-A comparative study of hydrophilic and hydrophobic membranes. Separation and Purification Technology 72 (3):347-356.
- [41] Sarayu, K., Swaminathan, K., and Sandhya, S. 2007. Assessment of degradation of eight commercial reactive azo dyes individually and in mixture in aqueous solution by ozonation. Dyes and Pigments 75 (2):362-368.
- [42] Kusvuran, E., Gulnaz, O., Samil, A., and Erbil, M. 2010. Detection of double bond-ozone stoichiometry by an iodimetric method during ozonation processes. Journal of Hazardous Materials 175 (1-3):410-416.
- [43] Satapanajaru, T., Chompuchan, C., Suntornchot, P., and Pengthamkeerati, P. 2011. Enhancing decolorization of Reactive Black 5 and Reactive Red 198 during nano zerovalent iron treatment. Desalination 266 (1-3):218-230.
- [44] Kusvuran, E., Gulnaz, O., Samil, A., and Yildirim, O. 2011. Decolorization of malachite green, decolorization kinetics and stoichiometry of ozone-

- malachite green and removal of antibacterial activity with ozonation processes. Journal of Hazardous Materials 186 (1):133-143.
- [45] Kritikos, D. E., Xekoukoulotakis, N. P., Psillakis, E., and Mantzavinos, D. 2007. Photocatalytic degradation of reactive black 5 in aqueous solutions: Effect of operating conditions and coupling with ultrasound irradiation. Water Research 41 (10):2236-2246.
- [46] Iranifam, M., Zarei, M., and Khataee, A. R. 2011. Decolorization of CI Basic Yellow 28 solution using supported ZnO nanoparticles coupled with photoelectro-Fenton process. Journal of Electroanalytical Chemistry 659 (1):107-112.
- [47] Patel, U. D., Ruparelia, J. P., and Patel, M. U. 2011. Electrocoagulation treatment of simulated floor-wash containing Reactive Black 5 using iron sacrificial anode. Journal of Hazardous Materials 197:128-136.
- [48] Damodar, R. A., and You, S.-J. 2010. Performance of an integrated membrane photocatalytic reactor for the removal of Reactive Black 5. Separation and Purification Technology 71 (1):44-49.
- [49] Lackey, L. W., Mines, R. O., and McCreanor, P. T. 2006. Ozonation of acid yellow 17 dye in a semi-batch bubble column. Journal of Hazardous Materials 138 (2):357-362.
- [50] He, Z. Q., Song, S., Xia, M., Qiu, J. P., Ying, H. P., Lu, B. S., Jiang, Y. F., and Chen, J. M. 2007. Mineralization of CI Reactive Yellow 84 in aqueous solution by sonolytic ozonation. Chemosphere 69 (2):191-199.
- [51] Tizaoui, C., and Grima, N. 2011. Kinetics of the ozone oxidation of Reactive Orange 16 azo-dye in aqueous solution. Chemical Engineering Journal 173 (2):463-473.
- [52] Sevimli, M. F., and Sarikaya, H. Z. 2002. Ozone treatment of textile effluents and dyes: effect of applied ozone dose, pH and dye concentration. Journal of Chemical Technology and Biotechnology 77 (7):842-850.
- [53] Aksu, Z., and Donmez, G. 2003. A comparative study on the biosorption characteristics of some yeasts for Remazol Blue reactive dye. Chemosphere 50 (8):1075-1083.



- [54] Chang, J. S., Chou, C., Lin, Y. C., Lin, P. J., Ho, J. Y., and Hu, T. L. 2001. Kinetic characteristics of bacterial azo-dye decolorization by *Pseudomonas luteola*. Water Research 35 (12):2841-2850.
- [55] Walker, G. M., and Weatherley, L. R. 2000. Biodegradation and biosorption of acid anthraquinone dye. Environmental Pollution 108 (2):219-223.
- [56] Papić, S., Koprivanac, N., Božić, A. L., and Metes, A. 2004. Removal of some reactive dyes from synthetic wastewater by combined Al(III) coagulation/carbon adsorption process. Dyes and Pigments 62 (3):291-298.
- [57] Malik, P. K. 2004. Dye removal from wastewater using activated carbon developed from sawdust: adsorption equilibrium and kinetics. Journal of Hazardous Materials 113 (1-3):81-88.
- [58] Can, O. T., Kobya, M., Demirbas, E., and Bayramoglu, M. 2006. Treatment of the textile wastewater by combined electrocoagulation. Chemosphere 62 (2):181-187.
- [59] Hu, H. S., Yang, M. D., and Dang, H. 2005. Treatment of strong acid dye wastewater by solvent extraction. Separation and Purification Technology 42 (2):129-136.
- [60] Capar, G., Yetis, U., and Yilmaz, L. 2006. Membrane based strategies for the pre-treatment of acid dye bath wastewaters. Journal of Hazardous Materials 135 (1-3):423-430.
- [61] Koyuncu, I., Topacik, D., and Yuksel, E. 2004. Reuse of reactive dyehouse wastewater by nanofiltration: process water quality and economical implications. Separation and Purification Technology 36 (1):77-85.
- [62] Nataraj, S. K., Hosamani, K. M., and Aminabhavi, T. M. 2009. Nanofiltration and reverse osmosis thin film composite membrane module for the removal of dye and salts from the simulated mixtures. Desalination 249 (1):12-17.
- [63] Robinson, T., McMullan, G., Marchant, R., and Nigam, P. 2001. Remediation of dyes in textile effluent: a critical review on current treatment technologies with a proposed alternative. Bioresource Technology 77 (3):247-255.

- [64] Rosales, E., Pazos, M., Longo, M. A., and Sanroman, M. A. 2009. Electro-Fenton decoloration of dyes in a continuous reactor: A promising technology in colored wastewater treatment. Chemical Engineering Journal 155 (1-2): 62-67.
- [65] Arslan-Alaton, I., Tureli, G., and Olmez-Hanci, T. 2009. Treatment of azo dye production wastewaters using Photo-Fenton-like advanced oxidation processes: Optimization by response surface methodology. Journal of Photochemistry and Photobiology a-Chemistry 202 (2-3): 142-153.
- [66] Maezawa, A., Nakadoi, H., Suzuki, K., Furusawa, T., Suzuki, Y., and Uchida, S. 2007. Treatment of dye wastewater by using photo-catalytic oxidation with sonication. Ultrasonics Sonochemistry 14 (5): 615-620.
- [67] Tang, W. Z., and An, H. 1995. UV/TiO<sub>2</sub> Photocatalytic Oxidation of Commercial Dyes in Aqueous-Solutions. Chemosphere 31 (9): 4157-4170.
- [68] Fanchiang, J. M., and Tseng, D. H. 2009. Decolorization and transformation of anthraquinone dye Reactive Blue 19 by ozonation. Environmental Technology 30 (2): 161-172.
- [69] Tehrani-Bagha, A. R., Mahmoodi, N. M., and Menger, F. M. 2010. Degradation of a persistent organic dye from colored textile wastewater by ozonation. Desalination 260 (1-3): 34-38.
- [70] Chu, W., and Ma, C.-W. 2000. Quantitative prediction of direct and indirect dye ozonation kinetics. Water Research 34 (12): 3153-3160.
- [71] Lopez-Lopez, A., Pic, J. S., and Debellefontaine, H. 2007. Ozonation of azo dye in a semi-batch reactor: A determination of the molecular and radical contributions. Chemosphere 66 (11): 2120-2126.
- [72] Koch, M., Yediler, A., Lienert, D., Insel, G., and Kettrup, A. 2002. Ozonation of hydrolyzed azo dye reactive yellow 84 (CI). Chemosphere 46 (1): 109-113.
- [73] Konsowa, A. H. 2003. Decolorization of wastewater containing direct dye by ozonation in a batch bubble column reactor. Desalination 158 (1-3): 233-240.

- [74] Oguz, E., Keskinler, B., and Celik, Z. 2005. Ozonation of aqueous Bomaplex Red CR-L dye in a semi-batch reactor. Dyes and Pigments 64 (2): 101-108.
- [75] Pabby, A. K., and Sastre, A. M. 2013. State-of-the-art review on hollow fibre contactor technology and membrane-based extraction processes. Journal of Membrane Science 430: 263-303.
- [76] Mansourizadeh, A., and Ismail, A. F. 2009. Hollow fiber gas-liquid membrane contactors for acid gas capture: A review. Journal of Hazardous Materials 171 (1-3): 38-53.
- [77] Liu, F., Hashim, N. A., Liu, Y., Abed, M. R. M., and Li, K. 2011. Progress in the production and modification of PVDF membranes. Journal of Membrane Science 375: 1-27.
- [78] Bormashenko, E., Bormashenko, Y., Whyman, G., Pogreb, R., Musin, A., Jager, R., and Barkay, Z. 2008. Contact Angle Hysteresis on Polymer Substrates Established with Various Experimental Techniques, Its Interpretation, and Quantitative Characterization. Langmuir 24 (8): 4020-4025.
- [79] Leiknes, T., Phattaranawik, J., Boller, M., Von Gunten, U., and Pronk, W. 2005. Ozone transfer and design concepts for NOM decolourization in tubular membrane contactor. Chemical Engineering Journal 111 (1): 53-61.
- [80] Lv, Y. X., Yu, X. H., Tu, S. T., Yan, J. Y., and Dahlquist, E. 2012. Experimental studies on simultaneous removal of CO<sub>2</sub> and SO<sub>2</sub> in a polypropylene hollow fiber membrane contactor. Applied Energy 97: 283-288.
- [81] Hedayat, M., Soltanieh, M., and Mousavi, S. A. 2011. Simultaneous separation of H<sub>2</sub>S and CO<sub>2</sub> from natural gas by hollow fiber membrane contactor using mixture of alkanolamines. Journal of Membrane Science 377 (1-2): 191-197.
- [82] Mavroudi, M., Kaldis, S. P., and Sakellariopoulos, G. P. 2003. Reduction of CO<sub>2</sub> emissions by a membrane contacting process. Fuel 82 (15-17): 2153-2159.

- [83] Park, H. H., Deshwal, B. R., Kim, I. W., and Lee, H. K. 2008. Absorption of SO<sub>2</sub> from flue gas using PVDF hollow fiber membranes in a gas-liquid contactor. Journal of Membrane Science 319 (1-2): 29-37.
- [84] Brewis, D. M., Mathieson, I., Sutherland, I., Cayless, R. A., and Dahm, R. H. 1996. Pretreatment of poly(vinyl fluoride) and poly(vinylidene fluoride) with potassium hydroxide. International Journal of Adhesion and Adhesives 16 (2): 87-95.
- [85] Crowe, R., and Badyal, J. P. S. 1991. Surface modification of poly(vinylidene difluoride)(PVDF) by LiOH. Journal of the Chemical Society, Chemical Communications (14): 958-959.
- [86] Ross, G. J., Watts, J. F., Hill, M. P., and Morrissey, P. 2000. Surface modification of poly(vinylidene fluoride) by alkaline treatment 1. The degradation mechanism. Polymer 41 (5): 1685-1696.
- [87] Ross, G. J., Watts, J. F., Hill, M. P., and Morrissey, P. 2001. Surface modification of poly(vinylidene fluoride) by alkaline treatment Part 2. Process modification by the use of phase transfer catalysts. Polymer 42 (2): 403-413.
- [88] Zhang, S. C., Shen, J., Qiu, X. P., Weng, D. S., and Zhu, W. T. 2006. ESR and vibrational spectroscopy study on poly(vinylidene fluoride) membranes with alkaline treatment. Journal of Power Sources 153 (2): 234-238.
- [89] Zheng, Z. R., Gu, Z. Y., Huo, R. T., and Luo, Z. S. 2010. Superhydrophobic poly(vinylidene fluoride) film fabricated by alkali treatment enhancing chemical bath deposition. Applied Surface Science 256 (7): 2061-2065.
- [90] Wavhal, D. S., and Fisher, E. R. 2002. Hydrophilic modification of polyethersulfone membranes by low temperature plasma-induced graft polymerization. Journal of Membrane Science 209: 255-269.
- [91] Bazaka, K., Jacob, M. V., Crawford, R. J., and Ivanova, E. P. 2011. Plasma-assisted surface modification of organic biopolymers to prevent bacterial attachment. Acta Biomaterialia 7 (5): 2015-2028.

- [92] Zhang, Y., Wang, R., Yi, S. L., Setiawan, L., Hu, X., and Fane, A. G. 2011. Novel chemical surface modification to enhance hydrophobicity of polyamide-imide (PAI) hollow fiber membranes. Journal of Membrane Science 380 (1-2): 241-250.
- [93] Zhang, Y., Wang, R., Zhang, L. Z., and Fane, A. G. 2012. Novel single-step hydrophobic modification of polymeric hollow fiber membranes containing imide groups: Its potential for membrane contactor application. Separation and Purification Technology 101: 76-84.
- [94] Rahbari-Sisakht, M., Ismail, A. F., Rana, D., and Matsuura, T. 2012. A novel surface modified polyvinylidene fluoride hollow fiber membrane contactor for CO<sub>2</sub> absorption. Journal of Membrane Science 415: 221-228.
- [95] Rahbari-Sisakht, M., Ismail, A. F., Rana, D., and Matsuura, T. 2012. Effect of novel surface modifying macromolecules on morphology and performance of Polysulfone hollow fiber membrane contactor for CO<sub>2</sub> absorption. Separation and Purification Technology 99:61-68.
- [96] Bakeri, G., Ismail, A. F., Rana, D., and Matsuura, T. 2012. Development of high performance surface modified polyetherimide hollow fiber membrane for gas-liquid contacting processes. Chemical Engineering Journal 198: 327-337.
- [97] Wongchitphimon, S., Wang, R., and Jiratananon, R. 2011. Surface modification of polyvinylidene fluoride-co-hexafluoropropylene (PVDF-HFP) hollow fiber membrane for membrane gas absorption. Journal of Membrane Science 381 (1-2): 183-191.
- [98] Lv, Y. X., Yu, X. H., Jia, J. J., Tu, S. T., Yan, J. Y., and Dahlquist, E. 2012. Fabrication and characterization of superhydrophobic polypropylene hollow fiber membranes for carbon dioxide absorption. Applied Energy 90 (1): 167-174.
- [99] Preethi, V., Parama Kalyani, K. S., Iyappan, K., Srinivasakannan, C., Balasubramaniam, N., and Vedaraman, N. 2009. Ozonation of tannery effluent for removal of cod and color. Journal of Hazardous Materials 166 (1): 150-154.

- [100] Wang, J. L., and Xu, L. J. 2012. Advanced Oxidation Processes for Wastewater Treatment: Formation of Hydroxyl Radical and Application. Critical Reviews in Environmental Science and Technology 42 (3): 251-325.
- [101] Hoigne, J., and Bader, H. 1976. The role of hydroxyl radical reactions in ozonation process in aqueous solutions. Water research 10:377-386.
- [102] Gottschalk, C., Libra, J. A., and Saupe, A. 2000. *Ozonation of water and wastewater*. Weinheim: Wiley-VCH.
- [103] Zhang, F. F., Yediler, A., and Liang, X. M. 2007. Decomposition pathways and reaction intermediate formation of the purified, hydrolyzed azo reactive dye C.I. Reactive Red 120 during ozonation. Chemosphere 67 (4): 712-717.
- [104] Cran, M. J., Bigger, S. W., and Gray, S. R. 2011. Degradation of polyamide reverse osmosis membranes in the presence of chloramine. Desalination 283: 58-63.
- [105] Do, V. T., Tang, C. Y. Y., Reinhard, M., and Leckie, J. O. 2012. Effects of Chlorine Exposure Conditions on Physiochemical Properties and Performance of a Polyamide Membrane-Mechanisms and Implications. Environmental Science & Technology 46 (24): 13184-13192.
- [106] Glater, J., Zachariah, M. R., McCray, S. B., and McCutchan, J. W. 1983. Reverse osmosis membrane sensitivity to ozone and halogen disinfectants. Desalination 48 (1): 1-16.
- [107] Sano, T., Hasegawa, M., Ejiri, S., Kawakami, Y., and Yanagishita, H. 1995. Improvement of the Pervaporation Performance of Silicalite Membranes by Modification with a Silane Coupling Reagent. Microporous Materials 5 (3): 179-184.
- [108] Singh, R. P., Way, J. D., and McCarley, K. C. 2004. Development of a model surface flow membrane by modification of porous vycor glass with a fluorosilane. Industrial & Engineering Chemistry Research 43 (12): 3033-3040.
- [109] Oh, S., Kang, T., Kim, H., Moon, J., Hong, S., and Yi, J. 2007. Preparation of novel ceramic membranes modified by mesoporous silica with 3-

- aminopropyltriethoxysilane (APTES) and its application to Cu<sup>2+</sup> separation in the aqueous phase. Journal of Membrane Science 301 (1-2): 118-125.
- [110] Li, N. N., Fane, A. G., Ho, W. S. W., and Matsuura, T. 2008. *Advanced membrane technology and applications*. New Jersey: John Wiley&Sons, Inc.
- [111] Lv, Y., Yu, X., Tu, S. T., Yan, J., and Dahlquist, E. 2010. Wetting of polypropylene hollow fiber membrane contactors. Journal of Membrane Science 362: 444-452.
- [112] Khaisri, S., deMontigny, D., Tontiwachwuthikul, P., and Jiratananon, R. 2009. Comparing membrane resistance and absorption performance of three different membranes in a gas absorption membrane contactor. Separation and Purification Technology 65: 290-297.
- [113] Xi, Z. Y., Xu, Y. Y., Zhu, L. P., Wang, Y., and Zhu, B. K. 2009. A facile method of surface modification for hydrophobic polymer membranes based on the adhesive behavior of poly(DOPA) and poly(dopamine). Journal of Membrane Science 327: 244-253.
- [114] Picard, C., Larbot, A., Tronel-Peyroz, E., and Berjoan, R. 2004. Characterisation of hydrophilic ceramic membranes modified by fluoroalkylsilanes into hydrophobic membranes. Solid State Sciences 6: 605-612.
- [115] Koonaphaddeert, S., and Li, K. 2007. Preparation and characterization of hydrophobic ceramic hollow fibre membrane. Journal of Membrane Science 291: 70-76.
- [116] Krajewski, S. R., Kujawski, W., Bukowska, M., Picard, C., and Larbot, A. 2006. Application of fluoroalkylsilanes (FAS) grafted ceramic membranes in membrane distillation process of NaCl solutions. Journal of Membrane Science 281: 253-259.
- [117] Lu, J., Yu, Y., Zhou, J., Song, L., Hu, X., and Larbot, A. 2009. FAS grafted superhydrophobic ceramic membrane. Applied Surface Science 255: 9092-9099.

- [118] Hendren, Z. D., Brant, J., and Wiesner, M. R. 2009. Surface modification of nanostructured ceramic membranes for direct contact membrane distillation. Journal of Membrane Science 331 (1-2): 1-10.
- [119] Picard, C., Larbot, A., Guida-Pietrasanta, F., Boutevin, B., and Ratsimihety. 2001. Grafting of ceramic membranes by fluorinated silanes: hydrophobic features. Separation and Purification Technology 25: 65-69.
- [120] Krajewski, S. R., Kujawski, W., Dijoux, F., Picard, C., and Larbot, A. 2004. Grafting of ZrO<sub>2</sub> powder and ZrO<sub>2</sub> membrane by fluoroalkylsilanes. Colloids and Surfaces A: Physicochem. Eng. Aspects 243: 43-47.
- [121] Bothun, G. D., Peay, K., and Ilias, S. 2007. Role of tail chemistry on liquid and gas transport through organosilane-modified mesoporous ceramic membranes. Journal of Membrane Science 301: 162-170.
- [122] Zheng, Z., Gu, Z., Huo, R., and Luo, Z. 2010. Superhydrophobic poly(vinylidene fluoride) film fabricated by alkali treatment enhancing chemical bath deposition. Applied Surface Science 256 (7): 2061-2065.
- [123] Ross, G. J., Watts, J. F., Hill, M. P., and Morrissey, P. 2001. Surface modification of poly(vinylidene fluoride) by alkaline treatment Part 2. Process modification by the use of phase transfer catalysts. Polymer 42: 403-413.
- [124] Xu, Z., Li, L., Wu, F., Tan, S., and Zhang, Z. 2005. The application of the modified PVDF ultrafiltration membranes in further purification of Ginkgo biloba extraction. Journal of Membrane Science 255: 125-131.
- [125] Zhang, Y., Wang, R., Yi, S., Setiawan, L., Hu, X., and Fane, A. G. 2011. Novel chemical surface modification to enhance hydrophobicity of polyamide-imide (PAI) hollow fiber membranes. Journal of Membrane Science 380 (1-2): 241-250.
- [126] Yang, X., Wang, R., Shi, L., Fane, A. G., and Debowski, M. 2011. Performance improvement of PVDF hollow fiber-based membrane distillation process. Journal of Membrane Science 369 (1-2): 437-447.



- [127] Wongchitphimon, S., Wang, R., and Jiratananon, R. 2011. Surface modification of polyvinylidene fluoride-co-hexafluoropropylene (PVDF–HFP) hollow fiber membrane for membrane gas absorption. Journal of Membrane Science 381 (1-2): 183-191.
- [128] Sah, A., Castricum, H. L., Bilek, A., Blank, D. H. A., and ten Elshof, J. E. 2004. Hydrophobic modification of  $\gamma$ -alumina membranes with organochlorosilanes. Journal of Membrane Science 243: 125-132.
- [129] Levitsky, I., Duek, A., Arkhangelsky, E., Pinchev, D., Kadoshian, T., Shetrit, H., Naim, R., and Gitis, V. 2011. Understanding the oxidative cleaning of UF membranes. Journal of Membrane Science 377 (1-2): 206-213.
- [130] Szyrkowicz, L., Juzzolino, C., and Kaul, S. N. 2001. A Comparative study on oxidation of disperse dyes by electrochemical process, ozone, hypochlorite and fenton reagent. Water Research 35 (9): 2129-2136.
- [131] Yuan, R. X., Ramjaun, S. N., Wang, Z. H., and Liu, J. S. 2011. Effects of chloride ion on degradation of Acid Orange 7 by sulfate radical-based advanced oxidation process: Implications for formation of chlorinated aromatic compounds. Journal of Hazardous Materials 196: 173-179.
- [132] Chang, R., and Goldsby, K. A. 2013. Chemistry. 11th edition. New York: McGraw-Hill.
- [133] Silberberg, M. 2013. Principles of general chemistry. 3rd edition. New York: McGraw-Hill.
- [134] Gozmen, B., Turabik, M., and Hesenov, A. 2009. Photocatalytic degradation of Basic Red 46 and Basic Yellow 28 in single and binary mixture by UV/TiO<sub>2</sub>/periodate system. Journal of Hazardous Materials 164 (2-3): 1487-1495.
- [135] Singh, K., and Arora, S. 2011. Removal of Synthetic Textile Dyes From Wastewaters: A Critical Review on Present Treatment Technologies. Critical Reviews in Environmental Science and Technology 41 (9): 807-878.
- [136] Chen, T. Y., Kao, C. M., Hong, A., Lin, C. E., and Liang, S. H. 2009. Application of ozone on the decolorization of reactive dyes - Orange-13 and Blue-19. Desalination 249 (3): 1238-1242.

- [137] Ruan, X. C., Liu, M. Y., Zeng, Q. F., and Ding, Y. H. 2010. Degradation and decolorization of reactive red X-3B aqueous solution by ozone integrated with internal micro-electrolysis. Separation and Purification Technology 74 (2): 195-201.
- [138] Jansen, R. H. S., Zwijnenburg, A., Van Der Meer, W. G. J., and Wessling, M. 2006. Outside-in trimming of humic substances during ozonation in a membrane contactor. Environmental Science & Technology 40 (20): 6460-6465.
- [139] Razmjou, A., Arifin, E., Dong, G. X., Mansouri, J., and Chen, V. 2012. Superhydrophobic modification of TiO<sub>2</sub> nanocomposite PVDF membranes for applications in membrane distillation. Journal of Membrane Science 415: 850-863.
- [140] APHA, AWWA, and WPCF. 1998. Standard methods for the examination of water and wastewater. 20th edition. Washington D.C. USA: American Public Health Association, American Water Works Association, Water Pollution Federation.
- [141] He, Z. Q., Song, S., Zhou, H. M., Ying, H. P., and Chen, J. M. 2007. CI Reactive Black 5 decolorization by combined sonolysis and ozonation. Ultrasonics Sonochemistry 14 (3): 298-304.
- [142] Keshavarz, P., Fathikalajahi, J., and Ayatollahi, S. 2008. Mathematical modeling of the simultaneous absorption of carbon dioxide and hydrogen sulfide in a hollow fiber membrane contactor. Separation and Purification Technology 63 (1): 145-155.
- [143] Boributh, S., Assabumrungrat, S., Laosiripojana, N., and Jiraratananon, R. 2011. Effect of membrane module arrangement of gas-liquid membrane contacting process on CO<sub>2</sub> absorption performance: A modeling study. Journal of Membrane Science 372 (1-2): 75-86.
- [144] Pirgalioglu, S., and Ozbelge, T. A. 2009. Comparison of non-catalytic and catalytic ozonation processes of three different aqueous single dye solutions with respect to powder copper sulfide catalyst. Applied Catalysis a-General 363 (1-2): 157-163.

- [145] Wang, K. S., Chen, H. Y., Huang, L. C., Su, Y. C., and Chang, S. H. 2008. Degradation of Reactive Black 5 using combined electrochemical degradation-solar-light/immobilized TiO<sub>2</sub> film process and toxicity evaluation. Chemosphere 72 (2): 299-305.
- [146] Rivera, M., Pazos, M., and Sanroman, M. A. 2011. Development of an electrochemical cell for the removal of Reactive Black 5. Desalination 274 (1-3): 39-43.
- [147] Salari, D., Niaei, A., Aber, S., and Rasoulifard, M. H. 2009. The photooxidative destruction of CI Basic Yellow 2 using UV/S<sub>2</sub>O<sub>8</sub><sup>2-</sup> process in a rectangular continuous photoreactor. Journal of Hazardous Materials 166 (1): 61-66.
- [148] Wang, C. X., Yediler, A., Lienert, D., Wang, Z. J., and Kettrup, A. 2003. Ozonation of an azo dye CI Remazol Black 5 and toxicological assessment of its oxidation products. Chemosphere 52 (7): 1225-1232.
- [149] Colindres, P., Yee-Madeira, H., and Reguera, E. 2010. Removal of Reactive Black 5 from aqueous solution by ozone for water reuse in textile dyeing processes. Desalination 258 (1-3): 154-158.
- [150] Pachhade, K., Sandhya, S., and Swaminathan, K. 2009. Ozonation of reactive dye, Procion red MX-5B catalyzed by metal ions. Journal of Hazardous Materials 167 (1-3): 313-318.
- [151] Zhang, F., Yediler, A., Liang, X., and Kettrup, A. 2002. Ozonation of the purified hydrolyzed azo dye Reactive Red 120 (CI). Journal of Environmental Science and Health Part a-Toxic/Hazardous Substances & Environmental Engineering 37 (4): 707-713.
- [152] Konstantinou, I. K., and Albanis, T. A. 2004. TiO<sub>2</sub>-assisted photocatalytic degradation of azo dyes in aqueous solution: kinetic and mechanistic investigations - A review. Applied Catalysis B-Environmental 49 (1): 1-14.
- [153] Sleiman, M., Vildoza, D., Ferronato, C., and Chovelon, J. M. 2007. Photocatalytic degradation of azo dye Metanil Yellow: Optimization and kinetic modeling using a chemometric approach. Applied Catalysis B-Environmental 77 (1-2): 1-11.

- [154] Cui, Z., Drioli, E., and Lee, Y. M. 2013. Recent progress in fluoropolymers for membranes. Progress in Polymer Science  
[http://dx.doi.org/10.1016/j.progpolymsci.2013.07.008\(0\)](http://dx.doi.org/10.1016/j.progpolymsci.2013.07.008(0)).

## **APPENDICES**

**APPENDIX A**  
**Analytical method for COD and BOD**

## **A1. Closed reflux (titrimetric and colorimetric) method using COD digester**

### **Principle**

The closed reflux (titrimetric and colorimetric) method using metallic salt reagents are more economical but require homogenization of samples to obtain reproducible results. This method is conducted with ampules and culture tubes with pre-measured reagents which are available commercially. Moreover, for performing the tests, instructions furnished by the manufacturer are to be followed. Measurement of sample volume and reagent volume are critical. This method is economical in the use of metallic salt reagents and generates smaller quantity of hazardous wastes. The principle of oxidation reaction is similar to open reflux method. Volatile organic compounds are more completely oxidised in a closed system because of longer contact time with oxidants. Digestion vessels with premixed reagents are also available from commercial suppliers.

### **Reagents and standards**

Standard potassium dichromate digestion solution 0.01667M: Dissolve 4.903 g  $K_2Cr_2O_7$ , primary standard grade, previously dried at 150°C for 2 hour in 500 mL distilled water, add 167 mL conc.  $H_2SO_4$  at the rate of 5.5g  $Ag_2SO_4/kg H_2SO_4$ .

Ferriin indicator solution: Dissolve 1.485 g 1, 10-phenanthroline monohydrate and 695 mg  $FeSO_4 \cdot 7H_2O$  in distilled water and dilute to 100 mL. This indicator solution may be purchased already prepared Standard ferrous ammonium sulphates (FAS) titrant, approximately 0.1M: Dissolve 39.2g  $Fe(NH_4)_2(SO_4)_2 \cdot 6H_2O$  in distilled water. Add 20mL concentrated  $H_2SO_4$ , cool and dilute to 100 mL. Standardise this solution daily against standard  $K_2Cr_2O_7$

### **Calibration**

Dilute 5mL standard  $K_2Cr_2O_7$  digestion mixture to about 100mL. Titrate with FAS using 0.1 to 0.15mL. (2 to 3 drops) ferriin indicator.

$$\text{Normality of FAS solution} = \frac{\text{Volume of 0.01667 M } K_2Cr_2O_7 \text{ solution treated, mL}}{\text{Volume of FAS used in titration, mL}} \times 0.1$$

**Procedure**

- 1) Place sample in culture tube or ampule
- 2) Add digestion mixture
- 3) Carefully run sulphuric acid reagent down inside of vessel
- 4) Tightly cap the tubes or seal ampules. Invert several times for proper mixing
- 5) Place tubes or ampules in preheated reaction block digester
- 6) Reflux for 2h at 150°C behind a protective shield
- 7) Cool to room temperature
- 8) Titrate while stirring with FAS using 1 or 2 drops of ferrous indicator
- 9) The end points is from blue-green to reddish brown
- 10) Reflux and titrate blank in similar way with distilled water

**Calculation**

$$\text{COD as mg} \frac{\text{O}_2}{\text{L}} = \frac{(A - B) \times M \times 8000}{\text{mL sample}}$$

Where:

- |      |   |   |
|------|---|---|
| A    | = | mL FAS used for blank                         |
| B    | = | mL FAS used for sample                        |
| M    | = | molarity of FAS, and                          |
| 8000 | = | milli equivalent weight of oxygen x 1000 mL/L |



## **A2. Biological Oxygen Demand (BOD) (Titrimetric method)**

### **Principle**

This test measures the oxygen utilised for the biochemical degradation of organic material(carbonaceous demand) and oxidation of inorganic material such as sulphides and ferrous ions during a specified incubation period. It also measures the oxygen used to oxidize reduced forms of nitrogen (nitrogenous demand) unless their oxidation is prevented by an inhibitor. Temperature effects are held constant by performing a test at fixed temperature. The methodology of BOD test is to compute a difference between initial and final DO of the samples incubation. Minimum 1.5 L of sample is required for the test. DO is estimate by iodometric titration. Since the test is mainly a bio-assay procedure, it is necessary to provide standard conditions of temperature, nutrient supply, pH (6.5-7.5), adequate population of microorganisms and absence of microbial-growth-inhibiting substances. The low solubility of oxygen in water necessitates strong wastes to be diluted to ensure that the demand does not increase the available oxygen. A mixed group of microorganisms should be present in the sample; otherwise, the sample has to be seeded. Generally, temperature is controlled at 20°C and the test is conducted for 5 days, as 70 to 80% of the carbonaceous wastes are oxidized during this period. The test can be performed at any other temperature provided the correlation between BOD<sub>5</sub> 20°C is established under same experimental condition (for example BOD<sub>5</sub>, 27°C) is equivalent to BOD<sub>3</sub>, 27°C) for Indian conditions. While reporting the results, the incubation period in days and temperature in °C is essential to be mentioned.

### **Procedure**

#### **Preparation of dilution water:**

- 1) The source of dilution water may be distilled water, tap or receiving-stream water free of biodegradable organics and bioinhibitory substances such as chlorine or heavy metals.
- 2) Aerate the required volume of dilution water in a suitable bottle by bubbling clean-filtered compressed air for sufficient time to attain DO saturation at room temperature or at 20°C/27°C. Before use stabilise the water at 20°C/27°C.

- 3) Add 1 mL each of phosphate buffer, magnesium sulphate, calcium chloride and ferric chloride solutions in that order for each Litre of dilution water. Mix well. Quality of dilution water may be checked by incubating a BOD bottle full of dilution water for 5 days at 20°C for 3 days at 27°C. DO uptake of dilution water should not be more than 0.2mg/L and preferable not more than 0.1mg/L.
- 4) For wastes which are not expected to have sufficient microbial population, seed is essential. Preferred seed is effluent from a biological treatment system. Where this is not available, supernatant from domestic wastewater (domestic sewage) settled at room temperature for at least 1h but not longer than 36hours is considered sufficient in the proportion 1-2 mL/L of dilution water. Adopted microbial population can be obtained from the receiving water microbial population can be obtained from the receiving water body preferably 3-8 km below the point of discharge. In the absence of such situation, develop an adapted seed in the laboratory.
- 5) Determine BOD of the seeding material. This is seed control. From the value of seed control determine seed DO uptake. The DO uptake of seeded dilution water should be between 0.6 mg/L and 1 mg/L.

**Sample preparation:**

- 1) Neutralise the sample to pH 7, if it is highly acidic or alkaline.
- 2) Take 50mL of the sample and acidify with addition of 10mL 1 + 1 acetic acid. Add about 1g KI. Titrate with 0.025N  $\text{Na}_2\text{S}_2\text{O}_3$ , using starch indicator. Calculate the volume of  $\text{Na}_2\text{S}_2\text{O}_3$  required per Litre of the sample and accordingly add to the sample to be tested for BOD.
- 3) Certain industrial wastes contain toxic metals, e.g. plating wastes. Such samples often require special study and treatment.
- 4) Bring samples to  $20 \pm 1^\circ\text{C}$  before making dilutions.
- 5) If nitrification inhibition is desired, add 3 mg 2-chloro-6-(trichloromethyl) pyridine (TCMP) to each 300 mL bottle before capping or add sufficient amount to the dilution water to make a final concentration of 30 mg/L. Note the use of nitrogen inhibition in reporting results.

- 6) Samples having high DO contents,  $DO \geq 9$  mg/L should be treated to reduce the DO content to saturation at 20°C. Agitate or aerate with clean, filtered compressed air.

Siphon out half the required volume of seeded dilution water in a graduated cylinder or volumetric flask without entraining air. Add the desired quantity of mixed sample and dilute to the appropriate volume by siphoning dilution water. Mix well with plunger type mixing rod to avoid entraining air.

### Sample processing:

- 1) Siphon the diluted or undiluted sample in three labeled bottles and stopper immediately.
- 2) Keep 1 bottle for determination of the initial DO and incubate 2 bottles at 20°C for 5 days. See that the bottles have a water seal.
- 3) Prepare a blank in triplicate by siphoning plain dilution water (without seed) to measure the O<sub>2</sub> consumption in dilution water.
- 4) Also prepare a seed blank in triplicate to measure BOD of seed for correction of actual BOD.
- 5) Determine DO in a BOD test can in the blank on initial day and end of incubation period by Winkler method as described for DO measurement.

### Calculations

Calculate BOD of the sample as follows:

- a. When dilution water is not seeded

$$\text{BOD as O}_2\text{mg/L} = \frac{(D1 - D2) \times 100}{\% \text{ dilution}}$$

- b. When dilution is seeded

$$\text{BOD as O}_2\text{mg/L} = \frac{(D1 - D2) - (B1 - B2) \times 100}{\% \text{ dilution}}$$

- c. When material is added to sample or to seed control

$$\text{BOD as O}_2\text{mg/L} = \frac{(D1 - D2) - (B'1 - B'2) \times F \times 100}{\% \text{ dilution}}$$

Where,

D1 = DO of sample immediately after preparation, mg/L

D2 = DO of sample after incubation period, mg/L

B1 = DO of blank (seeded dilution water) before incubation, mg/L

B2 = DO of blank (seeded dilution water) after incubation, mg/L

F = ration of seed in diluted sample to seed in seed control (Vol. Of seed in diluted sample / Vol. of seed in seed control)

B'1 = DO of seed control before incubation, mg/L

B'2 = DO of seed control after incubation, mg/L

**APPENDIX B**  
**Experimental data**

**Table A1** Experimental long-term CO<sub>2</sub> chemical absorption flux data of membranes  
(Operating conditions: T = 25°C, V<sub>L</sub> = 0.1 m/s, V<sub>G</sub> = 50 ml/min, A = 0.0188 m<sup>2</sup>,  
[Taurine] = 2 mol/L)

Time (Day)	J <sub>CO2</sub> (mol/m <sup>2</sup> s)		
	Original PVDF	PVDF-PAM	PVDF-CM2
1	7.71E-03	9.53E-03	7.11E-03
3	5.86E-03	1.03E-02	6.81E-03
5	6.09E-03	9.83E-03	6.89E-03
7	5.06E-03	9.60E-03	6.39E-03
9	5.31E-03	1.01E-02	6.49E-03
11	4.12E-03	9.44E-03	7.27E-03
13	4.66E-03	9.30E-03	7.03E-03
15	3.07E-03	9.04E-03	7.60E-03

**Table A2** Experimental ozone flux data of original PVDF membrane (Operating conditions:  $T = 28^{\circ}\text{C}$ ,  $V_L = 0.62$  m/s,  $V_G = 0.12$  m/s,  $A = 0.0188$  m<sup>2</sup>,  $[\text{O}_3] = 40$  ppm,  $[\text{RB5}] = 100$  mg/L)

Time (h)	[Ozone] <sub>in</sub> (mg/L)				[Ozone] <sub>out</sub> (mg/L)				J (g/m <sup>2</sup> s)
	1	2	3	Average	1	2	3	Average	
0.25	40.97	41.06	41.17	41.07	37.00	36.90	36.95	36.95	1.23E-03
1	40.41	40.50	40.36	40.42	36.81	36.83	36.79	36.81	1.08E-03
2	40.20	40.12	40.16	40.16	36.38	37.18	37.71	37.09	9.18E-04
3	40.45	39.55	40.13	40.04	36.62	36.21	38.19	37.01	9.08E-04
4	38.55	39.18	39.10	38.94	36.13	36.33	36.00	36.15	8.34E-04
5	39.80	38.66	39.87	39.44	37.10	37.58	36.25	36.98	7.37E-04
6	40.29	40.50	40.34	40.38	36.69	38.65	37.89	37.74	7.87E-04
7	39.36	38.80	39.14	39.10	36.40	37.35	35.50	36.42	8.02E-04
8	39.97	40.30	40.20	40.16	36.97	37.50	37.88	37.45	8.09E-04
9	40.48	40.25	39.67	40.13	37.30	36.83	37.98	37.37	8.26E-04
10	40.25	40.52	40.00	40.26	37.20	38.17	37.39	37.59	7.98E-04
11	40.44	40.40	40.61	40.48	38.25	37.59	37.26	37.70	8.32E-04
12	38.70	38.90	39.44	39.01	36.92	35.64	37.10	36.55	7.35E-04
13	40.35	40.94	40.70	40.66	37.62	38.42	37.85	37.96	8.07E-04
14	41.00	41.10	41.20	41.10	38.55	37.42	39.20	38.39	8.10E-04
15	49.05	47.30	48.53	48.29	45.48	46.30	45.30	45.69	7.77E-04
16	40.38	40.90	40.30	40.53	37.59	38.40	37.66	37.88	7.90E-04
17	38.20	38.16	38.23	38.20	34.22	36.05	36.77	35.68	7.52E-04
18	41.32	40.20	40.23	40.58	38.36	37.35	38.49	38.07	7.52E-04
19	42.05	42.46	42.94	42.48	39.13	40.50	40.40	40.01	7.39E-04
20	43.60	43.28	43.22	43.37	40.90	41.54	40.10	40.85	7.53E-04

**Table A3** Experimental ozone flux data of original PVDF-PAM membrane (Operating conditions:  $T = 28^{\circ}\text{C}$ ,  $V_L = 0.62$  m/s,  $V_G = 0.12$  m/s,  $A = 0.0188$  m<sup>2</sup>,  $[\text{O}_3] = 40$  ppm,  $[\text{RB5}] = 100$  mg/L)

Time (h)	[Ozone] <sub>in</sub> (mg/L)				[Ozone] <sub>out</sub> (mg/L)				J (g/m <sup>2</sup> s)
	1	2	3	Average	1	2	3	Average	
0.25	40.68	40.78	39.80	40.42	36.94	36.43	37.09	36.82	1.08E-03
1	40.30	38.84	39.50	39.55	35.89	36.67	36.17	36.24	9.87E-04
2	39.94	40.44	39.28	39.89	36.94	36.43	37.09	36.82	9.17E-04
3	42.37	42.57	42.85	42.60	39.28	39.34	39.76	39.46	9.38E-04
4	44.05	44.70	42.63	43.79	40.70	41.38	40.55	40.88	8.72E-04
5	44.94	46.22	45.40	45.52	43.29	41.98	42.58	42.62	8.68E-04
6	45.20	45.56	45.48	45.41	42.35	42.50	42.32	42.39	9.04E-04
7	48.17	47.75	47.74	47.89	44.62	44.64	45.49	44.92	8.88E-04
8	41.32	40.58	41.72	41.21	37.50	38.25	38.60	38.12	9.24E-04
9	40.17	39.58	39.96	39.90	37.22	37.12	36.15	36.83	9.19E-04
10	41.31	41.93	42.15	41.80	38.23	39.06	39.13	38.81	8.94E-04
11	40.94	40.22	40.72	40.63	37.35	37.24	38.07	37.55	9.19E-04
12	42.92	43.64	43.82	43.46	39.83	40.26	41.60	40.56	8.66E-04
13	40.46	40.24	39.65	40.12	36.78	37.39	36.90	37.02	9.25E-04
14	39.57	39.48	39.70	39.58	35.76	36.63	36.81	36.40	9.52E-04
15	38.70	39.35	38.93	38.99	35.40	36.20	36.22	35.94	9.13E-04
16	40.70	39.90	42.50	41.03	38.08	38.01	38.13	38.07	8.85E-04
17	43.40	43.30	43.50	43.40	38.77	39.63	39.67	39.36	1.21E-03
18	39.50	39.57	39.30	39.46	36.62	36.06	36.80	36.49	8.86E-04
19	40.73	41.07	41.30	41.03	37.11	37.73	38.94	37.93	9.29E-04
20	41.87	41.30	41.06	41.41	38.56	38.02	38.91	38.50	8.71E-04

**Table A4** Experimental ozone flux data of original PTFE membrane (Operating conditions: T = 28°C, V<sub>L</sub> = 0.62 m/s, V<sub>G</sub> = 0.12 m/s, A = 0.0314 m<sup>2</sup>, [O<sub>3</sub>] = 40 ppm, [RB5] = 100 mg/L)

Time (h)	[Ozone] <sub>in</sub> (mg/L)				[Ozone] <sub>out</sub> (mg/L)				J (g/m <sup>2</sup> s)
	1	2	3	Average	1	2	3	Average	
0.25	35.71	35.83	35.61	35.72	33.51	33.48	33.45	33.48	8.67E-04



<b>1</b>	39.37	39.54	40.05	39.65	37.64	37.59	37.52	37.58	8.02E-04
<b>2</b>	39.83	39.57	39.92	39.77	37.64	37.76	37.69	37.70	8.05E-04
<b>3</b>	40.23	40.64	40.72	40.53	38.39	38.51	38.31	38.40	8.24E-04
<b>4</b>	40.68	41.49	41.46	41.21	39.20	38.89	39.19	39.09	8.20E-04
<b>5</b>	41.84	41.87	41.74	41.82	39.48	39.67	39.97	39.71	8.18E-04
<b>6</b>	41.91	41.85	41.79	41.85	39.89	39.32	40.15	39.79	8.00E-04
<b>8</b>	43.61	43.90	42.56	43.36	41.31	41.17	41.30	41.26	8.13E-04
<b>10</b>	40.46	40.43	40.45	40.45	38.18	38.39	38.20	38.26	8.48E-04
<b>12</b>	40.62	40.68	40.66	40.65	38.63	38.59	38.33	38.52	8.28E-04
<b>14</b>	40.50	40.33	40.37	40.40	38.59	38.39	37.85	38.28	8.23E-04
<b>16</b>	40.74	40.51	40.37	40.54	38.21	38.56	38.47	38.41	8.24E-04
<b>18</b>	41.47	41.38	40.79	41.21	39.13	39.27	38.86	39.09	8.24E-04
<b>20</b>	42.52	43.12	43.31	42.98	40.86	40.89	40.86	40.87	8.19E-04

---

**Table A5** Experimental decolorization data of RB5 (Operating conditions: T = 28°C, V<sub>L</sub> = 0.62 m/s, V<sub>G</sub> = 0.12 m/s, [O<sub>3</sub>] = 40 ppm, [RB5] = 100 mg/L)

Membrane	Time	C/C <sub>0</sub>				pH	Conductivity (μS/cm)
		RB5	COD	BOD <sub>5</sub> /COD	TOC		
Original PVDF	0	1.00	1.00	-	-	5.86	-
	5	0.72	0.89	-	-	3.55	-
	10	0.58	0.80	-	-	3.14	-
	20	0.34	0.72	-	-	2.94	-
	40	0.09	0.72	-	-	2.81	-
	60	0.03	0.55	-	-	2.87	-
PVDF-PAM	0	1.00	1.00	1.00	1.00	5.60	234
	5	0.76	0.75	-	0.94	4.24	237
	10	0.62	0.72	-	0.95	3.41	291
	20	0.37	0.65	0.73	0.91	3.17	368
	40	0.10	0.54	0.78	0.82	2.94	485
	60	0.00	0.44	1.12	0.80	2.84	540
PTFE	0	1.00	1.00	-	-	6.09	-
	5	0.59	0.84	-	-	3.61	-
	10	0.35	0.80	-	-	3.24	-
	20	0.07	0.58	-	-	3.04	-
	40	0.00	0.57	-	-	2.96	-
	60	0.00	0.48	-	-	2.96	-

**Table A6** Experimental decolorization data of BY28 (Operating conditions: T = 28°C,  $V_L = 0.62$  m/s,  $V_G = 0.12$  m/s,  $[O_3] = 40$  ppm,  $[BY28] = 100$  mg/L)

Membrane	Time	Color	C/C <sub>0</sub>			pH	Conductivity ( $\mu$ S/cm)
			COD	BOD <sub>5</sub> /COD	TOC		
Original PVDF	0	1.00	1.00	-	-	6.58	-
	5	0.72	0.97	-	-	4.89	-
	10	0.61	0.84	-	-	3.84	-
	20	0.35	0.78	-	-	3.35	-
	40	0.20	0.77	-	-	3.24	-
	60	0.08	0.62	-	-	3.19	-
PVDF-PAM	0	1.00	1.00	0.08	1.00	6.56	210
	5	0.72	0.91	-	0.94	4.87	207
	10	0.62	0.90	-	0.93	3.88	223
	20	0.34	0.85	0.13	0.92	3.45	263
	40	0.17	0.67	0.15	0.87	3.33	319
	60	0.10	0.60	0.15	0.86	3.29	336
PTFE	0	1.00	1.00	-	-	6.55	-
	5	0.64	0.97	-	-	4.37	-
	10	0.50	0.88	-	-	3.58	-
	20	0.33	0.71	-	-	3.39	-
	40	0.07	0.65	-	-	3.24	-
	60	0.02	0.57	-	-	3.25	-

## VITAE

### NAME

Mr. Sermpong Sairiam

### DATE OF BIRTH

21 July 1984

### EDUCATIONAL RECORD

#### BACHELOR'S DEGREE

Bachelor's degree of Science, Chulalongkorn University, 2007

#### MASTER'S DEGREE

Master's degree of Science (Environmental Management), Chulalongkorn University, 2009

#### DOCTORAL'S DEGREE

Doctoral of Philosophy (Environmental Management) Chulalongkorn University, 2013

### SCHOLARSHIP

- The Commission of Higher Education
- Center of Excellence on Hazardous Substance Management Program (HSM)

### PUBLICATIONS

- Sermpong Sairiam, Loh Chun Heng, Wang Rong, and Ratana Jiraratananon. 2013. Surface modification of PVDF hollow fiber membrane to enhance hydrophobicity using organosilanes. Journal of Applied Polymer Science 130 (1): 610-621.
- Sermpong Sairiam, Wang Rong, and Ratana Jiraratananon. Durability and stability of modified PVDF membranes exposed to ozone and application in membrane contactor for dye solution treatment. (Status: Under reviewed)

### CONFERENCES

- Sermpong Sairiam, Loh Chun Heng, Wang Rong, and Ratana Jiraratananon. 2011. Ozonation of dye wastewater by membrane contacting process using modified PVDF membrane. Commission on Higher Education Congress IV: University Staff Development Consortium, 14-16 September 2011, Chonburi, Thailand.
- Sermpong Sairiam, Loh Chun Heng, Wang Rong, and Ratana Jiraratananon. 2012. Enhancing hydrophobicity of PVDF hollow fiber membrane by surface modification using organosilanes. The 10<sup>th</sup> International Conference on Membrane Science & Technology (MST2012): Sustainable Energy and Environment, 22-24 August 2012, Bangkok, Thailand.